

Collective patterns of pedestrians interacting with attractions

Jaeyoung Kwak

arXiv:1711.07833v1 [physics.soc-ph] 21 Nov 2017

Collective patterns of pedestrians interacting with attractions

Jaeyoung Kwak

A doctoral dissertation completed for the degree of Doctor of Science (Technology) to be defended, with the permission of the Aalto University School of Engineering, at a public examination held at the lecture hall M1 (room M232), Otakaari 1, Espoo on December 1, 2017 at 12 noon.

**Aalto University
School of Engineering
Department of Built Environment
Spatial Planning and Transportation Engineering**

Supervising professors

Professor Tapio Luttinen
Aalto University, Finland

Thesis advisors

Dr. Hang-Hyun Jo

Asia Pacific Center for Theoretical Physics (APCTP), Republic of Korea
Pohang University of Science and Technology, Republic of Korea
Aalto University, Finland

Dr. Iisakki Kosonen

Aalto University, Finland

Preliminary examiners

Professor Majid Sarvi

The University of Melbourne, Australia

Associate Professor Daichi Yanagisawa

The University of Tokyo, Japan

Opponents

Associate Professor Winnie Daamen

Delft University of Technology, The Netherlands

Aalto University publication series

DOCTORAL DISSERTATIONS 203/2017

© 2017 Jaeyoung Kwak

ISBN 978-952-60-7674-4 (printed)

ISBN 978-952-60-7673-7 (pdf)

ISSN-L 1799-4934

ISSN 1799-4934 (printed)

ISSN 1799-4942 (pdf)

<http://urn.fi/URN:ISBN:978-952-60-7673-7>

Unigrafia Oy

Helsinki 2017

Finland



Author

Jaeyoung Kwak

Name of the doctoral dissertation

Collective patterns of pedestrians interacting with attractions

Publisher School of Engineering**Unit** Department of Built Environment**Series** Aalto University publication series DOCTORAL DISSERTATIONS 203/2017**Field of research** Spatial Planning and Transportation Engineering**Manuscript submitted** 1 June 2017**Date of the defence** 1 December 2017**Permission to publish granted (date)** 21 August 2017**Language** English **Monograph** **Article dissertation** **Essay dissertation****Abstract**

Walking is a fundamental activity of a human life, not only for moving between places but also for interacting with surrounding environments. While walking to destinations, pedestrians may acquaint themselves with attractions such as artworks, shop displays, and public events. If such attractions are tempting enough, pedestrians opt to stop walking to join the attractions. Although the existence of attractions may considerably affect the pedestrian flow patterns, little attention has been paid to the interactions between pedestrians and attractions, and their impacts on pedestrian traffic.

This dissertation developed two microscopic models of pedestrian flow interacting with attractions. In numerical simulations, the presented models were examined by systematically controlling model parameters. After performing the numerical simulations, various collective patterns were identified and summarized in phase diagrams based on macroscopic measures. By doing so, this dissertation investigated the dynamics of pedestrian flow interacting with attractions from the perspective of attracted pedestrians and passersby.

The first model represents the attractive force towards the attractions in line with the social force models. The first model predicted various collective behaviors of attracted pedestrians, such as forming stable clusters around the attractions and rushing into the attractions. To understand collective patterns of pedestrians' visiting behavior, the second model was formulated as a function of the social influence and the average duration of visiting an attraction. The second model suggested that increasing the social influence and the average duration of visiting an attraction tended to attract more visitors to the attraction, but the increment was effective for a certain range of the parameters. Based on the second model, jamming transitions in pedestrian flow interacting with an attraction were also studied. It was found that an attendee cluster can trigger jamming transitions by increasing conflicts among pedestrians near the attraction.

This dissertation contributes to the current body of knowledge on the collective behavior of pedestrian motions. This is achieved by modeling pedestrian dynamics interacting with attractions and providing possible explanations of the collective patterns. The presented models and their applications enable one to understand various collective patterns of pedestrians interacting with attractions. The findings presented in this dissertation can provide an insight into pedestrian flow patterns in stores and improve the understanding of collective phenomena relevant to pedestrian facility management.

Keywords collective dynamics, pedestrian, attraction, social force models, numerical simulation**ISBN (printed)** 978-952-60-7674-4**ISBN (pdf)** 978-952-60-7673-7**ISSN-L** 1799-4934**ISSN (printed)** 1799-4934**ISSN (pdf)** 1799-4942**Location of publisher** Helsinki**Location of printing** Helsinki**Year** 2017**Pages** 120**urn** <http://urn.fi/URN:ISBN:978-952-60-7673-7>

Preface

During my years at Aalto University, I have an enjoyable period of learning not only in the research arena but also on a personal level. Numerous individuals helped my learning both in– and outside the academic sphere. I greatly appreciate their kind support. Without their support, this dissertation would not have come into existence. I would like to offer my special thanks to the people who supported and helped me so much throughout this period.

I would like to express my very great appreciation to my supervisor Professor Tapio Luttinen for patiently guiding this work and offering the freedom to explore the unknowns in the area of pedestrian flow dynamics. I wish to acknowledge the help provided by my thesis advisors Drs. Hang-Hyun Jo and Iisakki Kosonen. I am particularly grateful to Dr. Jo for helping me go through the research problems. I appreciate Dr. Kosonen for his commentary role in this work.

I would also like to thank preliminary examiners Professors Majid Sarvi and Daichi Yanagisawa for giving me valuable comments that helped me to improve this dissertation. Additionally, I would like to express my gratitude towards Professor Winne Daamen for being my opponent.

I would like to acknowledge financial support from Aalto University 4D–Space MIDE project, School of Engineering Doctoral Program, and Energy Efficiency Research Program. CSC-IT Center for Science, Finland provided me computational resources.

Finally, I would like to thank my family for their unconditional love and support over the years.

Helsinki, November 6, 2018,

Jaeyoung Kwak

Contents

Preface	5
Contents	7
List of Publications	9
Author's Contribution	11
1. Introduction	17
1.1 Background	17
1.2 Research Questions	19
1.3 Research Approach	21
1.4 Dissertation Outline	21
2. Related Work	23
2.1 Modeling Approaches	23
2.1.1 Macroscopic Models	23
2.1.2 Cellular Automata	25
2.1.3 Velocity-based Models	27
2.1.4 Force-based Models	29
2.1.5 Remarks	34
2.2 The Concept of Phases	38
3. Numerical Simulation Models	41
3.1 Study I: Attractive Force Model	43
3.2 Study II: Joining Behavior Model	45
3.3 Study III: Modeling Pedestrian Flow near an Attendee Cluster	48
4. Results	53
4.1 Study I: Collective Dynamics of Attracted Pedestrians	53
4.2 Study II: Visiting Behavior	56

4.3	Study III: Jamming Transitions Induced by an Attraction	58
4.3.1	Unidirectional Flow	60
4.3.2	Bidirectional Flow	61
4.3.3	Microscopic Understanding of Jamming Transitions	63
4.3.4	Attendee Cluster as a Dynamic Bottleneck	65
5.	Conclusions and Discussions	67
5.1	Summary	67
5.2	Contributions	69
5.3	Limitations	70
5.4	Future Work	71
	References	75
	Publications	87

List of Publications

This thesis consists of an overview and of the following publications which are referred to in the text by their Roman numerals.

- I** Kwak, J., Jo, H-H., Luttimen, T., and Kosonen, I. Collective dynamics of pedestrians interacting with attractions. *Physical Review E*, Volume 88, 6, 062810, December 2013.
- II** Kwak, J., Jo, H-H., Luttimen, T., and Kosonen, I. Effects of switching behavior for the attraction on pedestrian dynamics. *PLOS ONE*, Volume 10, 7, e0133668, July 2015.
- III** Kwak, J., Jo, H-H., Luttimen, T., and Kosonen, I. Jamming transitions induced by an attraction in pedestrian flow. *Physical Review E*, Volume 96, 2, 022319, August 2017.

Author's Contribution

Publication I: “Collective dynamics of pedestrians interacting with attractions”

Jaeyoung Kwak is the first/corresponding author of Publication I. He was responsible for conducting all the research work including development of research ideas/questions, formulation and implementation of the presented model, and analysis of the numerical simulation results. The manuscript was mainly written by Kwak. Dr. Jo actively advised Kwak on writing the manuscript including the manuscript structure and style, and preparing figures and tables. Prof. Luttinen and Dr. Kosonen were in a commentary role.

Publication II: “Effects of switching behavior for the attraction on pedestrian dynamics”

Jaeyoung Kwak is the first/corresponding author of Publication II. He was responsible for conducting all the research work. Kwak conceived the research ideas/questions, designed and performed the numerical simulations, and analyzed the simulation results. Dr. Jo actively advised Kwak on developing the research ideas/questions, designing the numerical experiments, and analyzing the results. The manuscript was mainly written by Kwak, and other authors (Dr. Jo, Prof. Luttinen, and Dr. Kosonen) provided feedback for the manuscript.

Publication III: “Jamming transitions induced by an attraction in pedestrian flow”

Jaeyoung Kwak is the first/corresponding author of Publication III. He was responsible for conducting all the research work. He conceived the research ideas and developed the research questions. Kwak formulated the presented model, performed the numerical simulations, and interpreted the results. The manuscript was mainly written by Kwak, and other authors (Dr. Jo, Prof. Luttinen, and Dr. Kosonen) were in a commentary role.

List of Frequently Used Symbols

This section shows frequently used symbols in this dissertation, especially for developing numerical simulation models and interpreting their results in Chapters 3 and 4.

Social Force Model

Δt	Simulation time step
Δt_s	Stride time
λ_{ij}	Pedestrian i 's minimum anisotropic strength against pedestrian j
ϕ_{ij}	Angle between pedestrian i 's velocity vector and relative location of pedestrian j with respect to pedestrian i
τ	Pedestrian relaxation time
\vec{d}_{ij}	Distance vector pointing from pedestrian j to pedestrian i , i.e., $\vec{d}_{ij} \equiv \vec{x}_i - \vec{x}_j$
\vec{e}_i	Unit vector pointing desired walking direction of pedestrian i
$\vec{e}_{i,0}$	Unit vector pointing initial desired walking direction of pedestrian i
\vec{e}_{iA}	Unit vector pointing from attraction A to pedestrian i
\vec{e}_{iB}	Unit vector pointing from boundary B to pedestrian i
\vec{e}_{ij}	Unit vector pointing from pedestrian j to pedestrian i
$\vec{f}_{i,d}$	Driving force of pedestrian i
\vec{f}_{iA}	Attractive force between pedestrian i and attraction A

\vec{f}_{iB}	Repulsive force between pedestrian i and boundary B
\vec{f}_{ij}	Repulsive force between pedestrian i and pedestrian j
\vec{g}_{ij}	Interpersonal elastic force between pedestrian i and pedestrian j
\vec{t}_{ij}	Unit vector in shearing direction; perpendicular to \vec{e}_{ij}
\vec{v}_i	Velocity of pedestrian i
\vec{v}_j	Velocity of pedestrian j
b_{ij}	Effective distance between pedestrian i and pedestrian j
C	Relative attraction strength, i.e., $C = C_a/C_r$
C_x	Social force interaction strength; $x = p, b, r, s$ (p : interpersonal repulsion, b : boundary repulsion, r : repulsive interaction from attraction, a : attractive interaction from attraction)
d_{iA}	Distance between pedestrian i and attraction A
d_{iB}	Distance between pedestrian i and boundary B
d_{ij}	Distance between pedestrian i and pedestrian j , i.e., $d_{ij} = \ \vec{d}_{ij}\ $
$h(\cdot)$	Ramp function; $h(x)$ yields x if $x > 0$, otherwise 0
k_x	Elastic constants; $x = n, t$ (n : normal, t : tangential)
l_x	Social force interaction range; $x = p, b, r, s$ (p : interpersonal repulsion, b : boundary repulsion, r : repulsive interaction from attraction, a : attractive interaction from attraction)
r_i	Radius of pedestrian i
v_d	Pedestrian desired speed
v_i	Speed of pedestrian i
v_j	Speed of pedestrian j
v_{\max}	Pedestrian maximum speed
w_{ij}	Anisotropic function defined between pedestrian i and pedestrian j
y_{ij}	Relative displacement of pedestrian i and pedestrian j

Joining Behavior Model

K_x	Baseline values; $x = 0, a$ (0: for N_0 , a : for N_a)
N_0	The number of pedestrians who have not joined the attraction yet
N_a	The number of pedestrians who have already joined the attraction
P_a	Joining probability
R_a	The range of perception
s	Social influence parameter
t_d	Average duration of visiting an attraction

Modeling Pedestrian Flow near an Attraction

ψ	Streamline function of passerby flow
$r_c(t)$	Attendee cluster size at time t , i.e., $r_c = r_c(t)$
T_c	Time-to-collision

Collective Behavior Measures

E	Efficiency of motion
$E(x)$	Stationary state average of local efficiency in a 1 m long segment x , i.e., $E(x) = \langle E(x, t) \rangle$
$E(x, t)$	Local efficiency of motion in a 1 m long segment x at time t
E_a	Minimum value of $E(x)$ near the attraction
E_i	Pedestrian i 's efficiency of motion
E_{up}	Minimum value of $E(x)$ upstream of the attraction
K	Normalized kinetic energy
$n_c(t)$	Conflict index at time t
N_p	The number of pedestrians near the attraction, i.e., within a range of R_a from the attraction
$N_p(A, t)$	The set of passersby in a section of $25 \text{ m} \leq x \leq 35 \text{ m}$ at time t

$N_p(x, t)$ The set of passersby in a 1 m long segment x at time t

N_v The number of pedestrians near the attraction who have visited the attraction

$N_{c,i}(t)$ The number of conflicts experienced by passerby i at time t

P_f Freezing probability

Other Symbols

L Corridor length

Q Pedestrian influx

W Corridor width

1. Introduction

1.1 Background

Collective dynamics of many-body systems has attracted much attention to traffic and related systems, such as granular particles [103, 118], vehicles [15, 35, 80], pedestrians [37, 41], and animals [19, 52, 105]. This subject has been studied by developing a set of individual behavioral rules in order to quantify emergent collective patterns from interactions among individuals. The beginning of such a bottom-up approach can be traced to the work of Maxwell and Boltzmann [4, 13, 92]. Maxwell suggested the concept of the ideal gas in which every gas particle is subject to the same equation of motion. He developed a macroscopic description of gases based on microscopic descriptions of particle behavior. Later, Boltzmann proposed the law of increasing entropy by extending Maxwell's approach of gas dynamics. He stated that the entropy of a system, a macrostate often interpreted as a degree of disorder in a system of particles, grows as the number of possible microstates increases. Here, a microstate represents a configuration of an individual atom or molecule such as position and velocity. A macrostate is defined as an observable quantity of the system, for instance, the temperature or the number of gas particles in a container. The work of Maxwell and Boltzmann demonstrated how one can explain an observed macroscopic pattern in terms of individual particle behaviors. Still today, the line of thoughts presented by them is highly relevant to understand collective patterns of motions.

Based on the bottom-up approach, various interesting collective behaviors have been identified in traffic flow studies. For example, Nagel and Schreckenberg explained traffic jam patterns based on their particle hopping model [81, 82]. In the model, a highway section is represented as a

one-dimensional array of multiple cells and each cell either can be occupied by one vehicle or can be empty. The velocity of a vehicle is expressed in the number of cells hopping forward at the next time step. All the vehicles update their position based on four update rules: acceleration, slowing down, randomization, and car motion rules. According to the acceleration rule, a vehicle can proceed one more cell at the next time step if the distance to the vehicle ahead is large enough. The slowing down rule states that the vehicle reduces the number of cells hopping forward at the next time step based on the distance to the vehicle ahead. The randomization rule represents fluctuations in the vehicle motions by reducing the number of cells hopping forward at the next time step by one with a certain probability. After these three rules are applied to all vehicles, according to the car motion rule, the vehicles move ahead with the updated velocity. Nagel and Schreckenberg explained complex traffic flow patterns with a set of rules describing individual vehicle motions.

Examples of the bottom-up approach can be also found in pedestrian flow studies. For instance, Helbing and his colleagues studied the formation of pedestrian trail systems based on an active walker model [41, 43]. Their active walker model includes three sets of equations for pedestrian motion, ground condition, and pedestrian orientation. The equation of motion describes position and velocity of individual pedestrians. The equation of ground condition reflects creation and destruction of footprints. The equation of pedestrian orientation evaluates pedestrians' desired walking direction based on the ground condition. Their model explained how different topological structures of human trail systems form. It was demonstrated that formations of such trail systems can be described as self-organization phenomena. The self-organization phenomena have been one of the current central topics in pedestrian studies.

A considerable amount of literature has reported various interesting collective patterns of pedestrian motions such as lane formation [12, 42, 111], faster-is-slower effect [37], and turbulent movement [40, 70, 76]. These collective patterns arise from repulsive interactions among pedestrians which can be observed when they are moving from one place to another.

Not only moving between places, pedestrians are also interacting with surrounding environment especially attractions such as shop displays and public events. It has been well recognized that existence of such attractions can influence pedestrian flow patterns. For instance, Goffman [30] described that window shoppers act like obstructions to passersby on the

streets when they stop to check store displays. Those shoppers can further interfere with other pedestrians when the shoppers enter and leave the stores. In another study, Helbing and Molnár [42] stated that attracted pedestrians form groups near attractions because of attractive interactions. Furthermore, one can infer that existence of the attractions in stores might be relevant to extreme pedestrian behaviors observed during shopping holidays such as Black Friday in the United States ¹. Despite its relevance to pedestrian behavior, up to now, far too little attention has been paid to the collective dynamics of the attractive interactions between pedestrians and attractions. The effects of such attractive interactions will be the topic of this dissertation.

1.2 Research Questions

This dissertation aims at investigating collective patterns of pedestrians interacting with attractions by developing numerical simulation models. Three research questions are developed in order to address the effect of attractive interactions mentioned in Section 1.1, such as pedestrian groups near attractions and their impact on pedestrian flow.

The first research question is formulated as, **(RQ1) how do collective patterns of pedestrian motions emerge from the attractive interactions between pedestrians and attractions?** This research question is inspired by the impulse stops [11, 102]. The impulse stop is a behavior of visiting an attraction without planning to do so in advance. An attraction is a place or an object that might be interesting for pedestrians, such as shop displays and public events. Understanding such impulse stops can support effective design and management of pedestrian facilities, for instance, placing merchandise in stores in order to encourage consumers to stop to buy [49]. However, little attention has been paid to the attractive interactions between pedestrians and attractions.

It is widely believed that individual choice behavior of joining an attraction can be influenced not only by the attractiveness of the attractions

¹Over 20 video clips are available on YouTube.com showing people fighting over merchandise and many news articles have reported about Black Friday incidents. Examples include <http://www.youtube.com/watch?v=K3RDTxVCKC4>, <http://www.independent.co.uk/news/world/americas/death-counter-records-number-of-people-killed-or-injured-on-black-friday-a6731766.html>, and <http://www.forbes.com/sites/adriankingsleyhughes/2012/11/24/black-friday-2012-shoppers-fight-over-cheap-deals>

but also by social influence from other individuals. For instance, previous studies on stimulus crowd effects reported that a pedestrian is more likely to shift one's attention towards the crowd as its size grows [27, 72]. This belief is also generally accepted in the marketing area, which can be interpreted that having more visitors in a store can attract more pedestrians to the store [6, 14]. Based on that belief, marketing strategies have focused on increasing the duration of visiting a store and the strength of social interactions [53]. Although the understanding of such a social influence on joining behavior has been widely accepted and practiced, the idea has not been incorporated into microscopic pedestrian behavior models. Therefore, the second research question is formulated as **(RQ2) how can social influence on one's choice behavior shape the collective patterns of pedestrians' visiting behavior?**

RQ1 and **RQ2** focus on modeling the attractive interactions between pedestrians and attractions. Based on **RQ1** and **RQ2**, Studies I and II have reported various collective patterns emerging from the attractive interactions. Nevertheless, little is known about their influence on passerby traffic. Pedestrians facilities are usually designed not only for accommodating pedestrians who are interested in shopping and attending social occasions, but also for passersby who regularly commute and walk through the facilities. It is apparent that if a large attendee cluster exists near an attraction, passersby are forced to walk through the reduced available space. Consequently, the attendee cluster is acting as a pedestrian bottleneck for passersby. The flow through the bottleneck can show transitions from the free flow state to the jamming state and may end in gridlock. Up to now, most of the pedestrian bottleneck studies have been performed for static bottlenecks, meaning that the bottlenecks are at fixed locations and their size does not change over time [44, 97]. One might think that assuming an attendee cluster as a static bottleneck is enough to understand the jamming transitions induced by an attraction. However, the assumption of the static bottleneck cannot reflect the interactions among the attraction, attracted pedestrians, and passersby contributing to the onset of jamming transitions. Accordingly, the third research question is formulated as **(RQ3) how can pedestrian flow interacting with an attraction result in pedestrian jams?** An attendee cluster is conceptualized as a dynamic bottleneck in the sense that its size changes over time according to the joining behavior of attracted pedestrians.

1.3 Research Approach

In order to address research questions discussed in Section 1.2, I have extended microscopic pedestrian models for the attractive interactions between pedestrians and attractions. In Study I, the attractive force is appended to the social force model in order to incorporate the attractive interactions between pedestrians and attractions. In Study II, I introduce a joining probability model which can reflect social influence from other pedestrians. In Study III, the presented models are further extended for simulating jamming patterns of pedestrians interacting with an attraction.

The presented models are then examined by means of numerical simulations. Simulation parameters are systematically controlled in order to observe various collective patterns arising from interactions between pedestrians and attractions. I devise macroscopic measures in order to quantify various collective patterns and then summarize the results in phase diagrams. In Study I, the macroscopic measures are introduced to quantify various attendee cluster formations. In Study II, pedestrian visiting patterns are distinguished. In Study III, different jam patterns near an attraction are identified. By doing so, this dissertation investigates the dynamics of pedestrian flow interacting with attractions from the perspective of the activity needs for attracted pedestrians and the mobility needs for passersby.

1.4 Dissertation Outline

This dissertation is organized as follows. Chapter 2 provides a review of existing literature that is closely linked with the topic of this dissertation. Chapter 3 describes presented numerical simulation models and their setups. The results of numerical simulations are presented in Chapter 4. Finally, Chapter 5 summarizes the main findings, discusses limitations, and suggests future research directions.

2. Related Work

This chapter provides a review of existing literature that is closely linked with the topic of this dissertation. In Section 2.1, I provide an overview of the existing pedestrian models on microscopic and macroscopic scales. First, I describe macroscopic pedestrian flow models which have been developed based on fluid dynamic equations (Section 2.1.1). In macroscopic models, pedestrian streams are considered similar to fluid streams, so the large-scale pedestrian motion is the major interest. Then, I present microscopic pedestrian flow models including cellular automata (Section 2.1.2), velocity-based models (Section 2.1.3), and force-based models (Section 2.1.4). In microscopic models, each pedestrian is treated like an individual particle, thus the modeling effort is focusing on developing mathematic expressions of individual motions. Section 2.1.5 summarizes the presented modeling approaches and identifies research directions. Section 2.2 discusses the concept of phases in pedestrian flow, which is important to quantify numerical simulation results presented in this dissertation.

2.1 Modeling Approaches

2.1.1 Macroscopic Models

Continuity equation in fluid mechanics states that the mass within a finite control volume remains constant because of the rates of mass inflow and outflow balance out through the control volume [1, 5, 78]. The differential form of the continuity equation is

$$\frac{\partial \rho}{\partial t} + \nabla \rho \vec{v} = 0, \quad (2.1)$$

where ρ is density and \vec{v} is velocity vector of a fluid stream.

Hughes models

Hughes [48] developed a macroscopic pedestrian flow model analogous to Lighthill–Whitham–Richard (LWR) macroscopic modeling approach in vehicular traffic flow studies [68, 91]. First, he formulated that walking direction of a pedestrian stream is perpendicular to the potential Φ :

$$\begin{aligned}\hat{\Phi}_x &= -\frac{\partial\Phi/\partial x}{\sqrt{(\partial\Phi/\partial x)^2 + (\partial\Phi/\partial y)^2}} \\ \hat{\Phi}_y &= -\frac{\partial\Phi/\partial y}{\sqrt{(\partial\Phi/\partial x)^2 + (\partial\Phi/\partial y)^2}}.\end{aligned}\quad (2.2)$$

Here, $\hat{\Phi}_x$ and $\hat{\Phi}_y$ indicate directional cosines of pedestrian stream motion. Second, he represented the velocity of a pedestrian stream $\vec{v} = (v_x, v_y)$ with speed function $f = f(\rho)$ and directional cosines $\hat{\Phi}_x$ and $\hat{\Phi}_y$,

$$\begin{aligned}v_x &= f(\rho)\hat{\Phi}_x \\ v_y &= f(\rho)\hat{\Phi}_y.\end{aligned}\quad (2.3)$$

Third, he also took into account that pedestrians tend to minimize their travel time while avoiding extremely high-density areas. He introduced walking strategy function,

$$\frac{1}{\sqrt{(\partial\Phi/\partial x)^2 + (\partial\Phi/\partial y)^2}} = g(\rho)\sqrt{v_x^2 + v_y^2}, \quad (2.4)$$

where $g(\rho)$ is a discomfort function. Hughes [48] set the value of $g(\rho)$ as 1 for most density levels but increased it for high pedestrian density situations. Based on the continuity equation in Equation (2.1) and Equations (2.2) to (2.4), Hughes presented the governing equations for pedestrian flow:

$$-\frac{\partial\rho}{\partial t} + \frac{\partial}{\partial x}\left(\rho g(\rho)f^2(\rho)\frac{\partial\Phi}{\partial x}\right) + \frac{\partial}{\partial y}\left(\rho g(\rho)f^2(\rho)\frac{\partial\Phi}{\partial y}\right) = 0 \quad (2.5)$$

and

$$\frac{1}{\sqrt{(\partial\Phi/\partial x)^2 + (\partial\Phi/\partial y)^2}} = g(\rho)f(\rho). \quad (2.6)$$

Later, Huang *et al.* [47] interpreted the potential function $\Phi(x, y)$ as a walking cost potential. They assumed that a pedestrian stream follows a path minimizing walking cost according to a generalized cost function $C = C(\rho, x, y, t)$. In line with Eikonal equation [50, 95, 116, 117], they reformulated a walking strategy function of Hughes's model [Equation (2.4)]:

$$C\frac{\vec{q}}{\|\vec{q}\|} + \nabla\Phi = 0, \quad (2.7)$$

where, the flow \vec{q} is defined as a product of density and velocity, i.e., $\vec{q} = \rho\vec{v}$.

2.1.2 Cellular Automata

In cellular automata (CA), pedestrian walking space is divided into uniform grids (or cells) and pedestrian movements are updated at discrete time step. Each pedestrian occupies a particular cell and moves between cells according to the prescribed rules. A pedestrian can move to a neighboring cell and the set of neighboring cells can be defined in two ways: von Neumann neighborhood and Moore neighborhood. In a rectangular grid, the von Neumann neighborhood includes a central cell and its four adjacent cells neighboring by edges of the central cell. The Moore neighborhood consists of a central cell and the eight cells surrounding the central one, adding diagonal connectivity to the von Neumann neighborhood. The CA-based approaches have been one of the popular pedestrian flow models because the approaches offer simple and efficient computation.

Gipps-Marksjö model

Gipps and Marksjö [29] proposed the gain-cost model in which the walking space is discretized into $0.5 \text{ m} \times 0.5 \text{ m}$ square cells. Each cell can be occupied by no more than one pedestrian. They modeled that a pedestrian in cell i moves to cell j which maximizes the benefit of his movement. Similar to the Moore neighborhood, a set of available cells includes cell i occupied by the pedestrian and eight neighboring cells. The benefit B_j for cell j is calculated by subtracting cost score S_j from gain function value $P(\sigma_j)$, i.e.,

$$B_j = P(\sigma_j) - S_j. \quad (2.8)$$

The cost score S_j represents the repulsion effects from nearby pedestrians and obstacles assigned to the cell j . The gain function $P(\sigma_j)$ reflects the distance to the destination d . The cost score function S_j is given as

$$S_j = \frac{1}{(\Delta - \alpha)^2 + \beta}, \quad (2.9)$$

where Δ is the distance between cell j and a cell i in which the pedestrian is standing. Here, $\alpha = 0.4$ is a constant which is slightly smaller than the size of a pedestrian ($= 0.5 \text{ m}$), and $\beta = 0.015$ is an arbitrary constant which moderates fluctuation in the cost score function S_j . The gain function $P(\sigma_j)$ is given as

$$P(\sigma_j) = K |\cos \sigma_j| \cos \sigma_j, \quad (2.10)$$

where K is gain function constant and σ_j is the angle between a vector pointing from current position to a destination and a vector pointing to

cell j where the pedestrian plans to move. If the pedestrian is not going to move, $P(\sigma_j)$ becomes zero. According to the definition of a dot product between two vectors, $\cos \sigma_j$ is calculated as

$$\cos \sigma_j = \frac{(\vec{x}_j - \vec{x}_i) \cdot (\vec{x}_d - \vec{x}_i)}{|\vec{x}_j - \vec{x}_i| |\vec{x}_d - \vec{x}_i|}, \quad (2.11)$$

where \vec{x}_j , \vec{x}_i , and \vec{x}_d are the location of cell j , cell i , and the destination d , respectively.

Blue-Adler model

Similar to the particle hopping model of Nagel and Schreckenberg [81, 82], Blue and Alder [8, 9, 10] suggested an alternative formulation of cellular automata for pedestrian motions based on three sets of behavioral rules including sidestepping, forward movement, and conflict mitigation. Sidestepping rules describe lateral movements of pedestrians: move to left or right lanes, or stay in the same lane. Forward movement rules decide the desired speed and available gap ahead. Conflict mitigations enable pedestrians to avoid a head-on collision between approaching pedestrians from opposite directions. Pedestrian movements are updated with the probability of movement related to the behavioral rules.

Floor field model

Burstedde *et al.* [12] and Kirchner and Schadschneider [61] introduced the floor field model. In the floor field model, pedestrians are walking on a floor field which is represented as a superposition of a static floor field and a dynamic floor field. The static floor field indicates quantities fixed over time, such as the shortest distance to an exit. The dynamics field represents virtual traces created by pedestrians who passed a certain area. The concept of dynamic floor field is analogous to chemotaxis of ants. In ant traffic systems, leading ants secrete pheromones when they march towards a food source, so following ants can reach the source by chemotaxis. The concept of floor field has been applied to develop pedestrian navigation models, such as in studies performed by Asano *et al.* [2], Hartmann [34], and Kneidl *et al.* [62].

The floor field model describes pedestrian movements by means of a transition probability. The transition probability p_{ij} for moving to a neighboring cell (i, j) is

$$p_{ij} = N \exp(k_D D_{ij} + k_S S_{ij}) (1 - n_{ij}) \xi_{ij}, \quad (2.12)$$

where D_{ij} and S_{ij} are strength of dynamic and static fields at cell (i, j) ,

and k_D and k_S are sensitivity parameters of D_{ij} and S_{ij} , respectively. Occupation number n_{ij} is 1 if cell (i, j) is occupied by a pedestrian, 0 for otherwise. Obstacle number ξ_{ij} becomes 0 for a cell obstacles or walls, while it is 1 for cells where pedestrians can move to. Normalization factor N is given as

$$N = \frac{1}{\sum_{(i,j)} \exp(k_D D_{ij} + k_S S_{ij})(1 - n_{ij})\xi_{ij}}. \quad (2.13)$$

After calculating the transition probability p_{ij} , each pedestrian decides where he or she will move and then updates one's position.

2.1.3 Velocity-based Models

In velocity-based models, pedestrian motions are described by a first-order ordinary differential equation,

$$\frac{d\vec{x}_i(t)}{dt} = \vec{v}_i(t). \quad (2.14)$$

Here, $\vec{x}_i(t)$ is the position of pedestrian i at time t and $\vec{v}_i(t)$ is his velocity at time t . In contrast to CA-based approaches, the velocity-based models can express pedestrian position and speed as continuous variables. The velocity-based models can simulate pedestrian movements without calculating force terms, so inertia effects do not occur. Thus, the implementation is easier than force-based models which are described by a second-order ordinary differential equation (see Section 2.1.4). Different velocity-based models have been proposed by introducing various formulations of $\vec{v}_i(t)$.

Contractile particle model

Baglietto and Parisi [3] presented the contractile particle model in which pedestrians are represented as circles with variable radii. Velocity of pedestrian i is described with desired velocity $\vec{v}_{i,d}$ and escape velocity $\vec{v}_{i,e}$.

$$\vec{v}_i(t) = \begin{cases} \vec{v}_{i,d} & \text{if pedestrian } i \text{ is free of contact,} \\ \vec{v}_{i,e} & \text{otherwise,} \end{cases} \quad (2.15)$$

where $\vec{v}_{i,d}$ is the desired velocity pointing destination from current position \vec{x}_i , and $\vec{v}_{i,e}$ is the escape velocity from the boundary of obstacles or other pedestrians in contact. The desired velocity $\vec{v}_{i,d}$ is

$$\vec{v}_{i,d} = v_{i,d}\vec{e}_i, \quad (2.16)$$

where $v_{i,d}$ is the desired speed and \vec{e}_i is a unit vector in the desired direction. The desired speed is formulated as

$$v_{i,d} = v_{d,\max} \left(\frac{r_i - r_{\min}}{r_{\max} - r_{\min}} \right)^\beta, \quad (2.17)$$

where $v_{d,\max}$ is the maximum desired speed which a pedestrian can attain if his movement is not restricted by other pedestrians or obstacles. The pedestrian radius r_i varies between the maximum radius r_{\max} and the minimum radius r_{\min} . The exponent β controls the shape of desired speed function in Equation (2.17).

The escape velocity $\vec{v}_{i,e}$ is given as

$$\vec{v}_{i,e} = v_e \frac{\sum_j \vec{e}_{ij}}{\left\| \sum_j \vec{e}_{ij} \right\|}, \quad (2.18)$$

where v_e is the escape speed and \vec{e}_{ij} is a unit vector pointing from pedestrian j to i . The escape speed v_e set to be the same as the maximum value of desired speed, i.e., $v_e = v_{d,\max}$.

Gradient navigation model

Dietrich and Köster [21] introduced the gradient navigation model. In the model, pedestrian motions are described with relaxed speed $w_i(t)$ and navigation function $\vec{N}(\vec{x}_i, t)$:

$$\frac{d\vec{x}_i(t)}{dt} = w_i(t) \vec{N}(\vec{x}_i, t) \quad (2.19)$$

Here, the navigation function $\vec{N}(\vec{x}_i, t)$ represents desired walking direction. The relaxed speed $w_i(t)$ is given as

$$\frac{dw_i(t)}{dt} = \frac{1}{\tau} \left[v_d \left\| \vec{N}(\vec{x}_i, t) \right\| - w_i(t) \right], \quad (2.20)$$

where τ is relaxation constant, and v_d is the desired speed of pedestrian i which is determined based on the local crowd density $\rho(x_i)$. The navigation function \vec{N} is given as a superposition of navigation vectors \vec{N}_T and \vec{N}_P , and these navigation vectors are given as gradient of distance functions. i.e.,

$$\vec{N}(\vec{x}_i, t) = g(g(\vec{N}_T) + g(\vec{N}_P)), \quad (2.21)$$

where, $g(\vec{x})$ is a scaling function normalizing a vector \vec{x} to a length in $[0, 1]$. Here, \vec{N}_T is desired walking direction vector which minimizes walking time to destination σ ,

$$\vec{N}_T = -\nabla\sigma. \quad (2.22)$$

Repulsion effects from other pedestrians and obstacles are represented by \vec{N}_P ,

$$\vec{N}_P = - \left(\sum_{j \neq i} \nabla P_{i,j} + \sum_B \nabla P_{i,B} \right), \quad (2.23)$$

where $P_{i,j}$ and $P_{i,B}$ are functions of distance to other pedestrian j and obstacle B , respectively. See Dietrich and Köster [21] for further details of the model.

2.1.4 Force-based Models

While velocity-based models are formulated based on a first-order ordinary differential equation, force-based models predict pedestrian motions with a second-order ordinary differential equation, i.e.,

$$\frac{d^2 \vec{x}_i(t)}{dt^2} = \vec{f}_i(t). \quad (2.24)$$

Here, $\vec{f}_i(t)$ is the force acting on pedestrian i at time t . The force-based models represent interactions among pedestrians with virtual forces and can consider physical contacts among pedestrians similar to the case of granular flows [24]. Different force-based models have been proposed based on analogies with various forces in Newtonian mechanics. The force-based models have been developed in order to describe pedestrian behaviors in detail, especially for the case of high pedestrian density.

Magnetic force model

By the analogy with Coulomb's law, Okazaki [86] proposed the magnetic force model. In the model, each pedestrian is modeled as a positively charged particle, and similarly, obstacles such as walls and columns are also modeled as positive poles. In contrast, the destination points are represented as negative poles. According to the magnetic force model, pedestrian i walking towards his destination is described as a positively charged particle attracted by a negative pole. Avoiding other pedestrians and obstacles are described by repulsive accelerations acting on pedestrian i from positively charged particles and poles. The magnetic force $\vec{F}_{i,m}$ exerts on pedestrian i from a negative pole is given as

$$\vec{F}_{i,m} = \frac{kq_1q_2\vec{r}}{r^3}, \quad (2.25)$$

where k is magnetic force constant. The intensity of positively charged particle (i.e., pedestrian) is indicated by q_1 , and that of negative pole (i.e., destination) is denoted by q_2 . The distance vector from pedestrian i to a

destination is denoted by \vec{r} and r is its magnitude. The repulsive acceleration acting on pedestrian i from pedestrian j is given as

$$\vec{a}_{ij} = \vec{v}_i \cos(\alpha) \tan(\beta), \quad (2.26)$$

where \vec{v}_i is the velocity of pedestrian i . The angle α is defined between v_i and v_{ij} . The angle β is defined between v_{ij} and a tangential line to the circumference of pedestrian j from the position of pedestrian i . Here, v_{ij} is the relative velocity of pedestrian i to pedestrian j . Note that, the tangential line is crossing the velocity vector of pedestrian j .

Social force models

Although the magnetic force model is considered as the first force-based model, the model has not been widely applied. This seems to be because the formulation and implementation of the magnetic force model are complicated and not straightforward. Helbing and Molnár [42] proposed the social force model, analogously to self-propelled particle models [22, 74, 98, 105]. The social force model [42] describes the pedestrian movements as a superposition of driving, repulsive, and attractive force terms. Each pedestrian i is modeled as a circle with radius r_i in a two-dimensional space. The position and velocity of each pedestrian i at time t , denoted by $\vec{x}_i(t)$ and $\vec{v}_i(t)$, evolve according to the following equations:

$$\frac{d\vec{x}_i(t)}{dt} = \vec{v}_i(t) \quad (2.27)$$

and

$$\frac{d\vec{v}_i(t)}{dt} = \vec{f}_{i,d} + \sum_{j \neq i} \vec{f}_{ij} + \sum_B \vec{f}_{iB} + \sum_A \vec{f}_{iA}. \quad (2.28)$$

Here, the driving force $\vec{f}_{i,d}$ describes the pedestrian i accelerating to reach its destination. The repulsive force between pedestrians i and j , \vec{f}_{ij} , denotes the tendency of pedestrians to keep a certain distance from each other. The repulsive force from boundary B , \vec{f}_{iB} , shows the interaction between pedestrian i and boundary B (i.e., walls and obstacles). The attractive force \vec{f}_{iA} indicates pedestrian movements toward attractive stimuli. The attractive stimuli can be, for instance, attractive interactions among pedestrian group members or between pedestrians and attractions such as shop displays and museum exhibits.

The driving force $\vec{f}_{i,d}$ is given as

$$\vec{f}_{i,d} = \frac{v_d \vec{e}_i - \vec{v}_i(t)}{\tau}, \quad (2.29)$$

where v_d is the desired speed and \vec{e}_i is a unit vector in the desired direction, independent of the position of the pedestrian i . The relaxation time τ controls how fast the pedestrian i adapts its velocity to the desired velocity.

The repulsive force between pedestrians i and j , denoted by \vec{f}_{ij} , is the sum of the gradient of repulsive potential,

$$\vec{f}_{ij} = -\nabla_{\vec{d}_{ij}} V(b_{ij}). \quad (2.30)$$

Here, the repulsion potential represents the level of interpersonal repulsion associated with the relative positions of pedestrians i and j . Similar to the relationship between force and potential energy in physics, the interpersonal repulsive force can be expressed as the negative of the derivate of the potential function. The repulsive potential is given as

$$V(d_{ij}) = C_p l_p \exp\left(-\frac{b_{ij}}{l_p}\right). \quad (2.31)$$

Here, C_p and l_p denote the strength and the range of repulsive interaction between pedestrians, and b_{ij} is the effective distance between pedestrians i and j . The social force models can be categorized according to the formulation of the effective distance b_{ij} .

Circular specification (CS) [35] is the most simplistic form of the repulsive interaction, assuming that b_{ij} is as a function of d_{ij} , the distance between pedestrians i and j ,

$$b_{ij} = d_{ij} - (r_i + r_j). \quad (2.32)$$

The explicit form of f_{ij} can be written as

$$\vec{f}_{ij} = C_p \exp\left(\frac{r_i + r_j - d_{ij}}{l_p}\right) \vec{e}_{ij}, \quad (2.33)$$

where $\vec{e}_{ij} = \vec{d}_{ij}/d_{ij}$ is a unit vector pointing from pedestrian j to pedestrian i , and $\vec{d}_{ij} \equiv \vec{x}_i - \vec{x}_j$ is the distance vector pointing from pedestrian j to pedestrian i . Due to its simplicity, CS has been widely applied for agent-based modeling [37, 87, 89] and multiscale modeling [18, 46, 45]. Although CS describes the pedestrian motion with a minimal number of parameters, it has limitation on reflecting the influence of relative velocity.

Helbing and Molnár [42] introduced Elliptical specification (ES-1), considering pedestrian j 's stride, $\vec{y}_{ij} \equiv \vec{v}_j \Delta t_s$ with the stride time Δt_s . The effective distance b_{ij} is given as

$$\begin{aligned} b_{ij} &= \frac{1}{2} \sqrt{(\|\vec{d}_{ij}\| + \|\vec{d}_{ij} - \vec{v}_j \Delta t_s\|)^2 - \|\vec{v}_j \Delta t_s\|^2} \\ &= \frac{1}{2} \sqrt{(\|\vec{d}_{ij}\| + \|\vec{d}_{ij} - \vec{y}_{ij}\|)^2 - \|\vec{y}_{ij}\|^2}. \end{aligned} \quad (2.34)$$

Based on Equation (2.34), the explicit form of \vec{f}_{ij} is given as

$$\vec{f}_{ij} = C_p \exp\left(-\frac{b_{ij}}{l_p}\right) \frac{\|\vec{d}_{ij}\| + \|\vec{d}_{ij} - \vec{y}_{ij}\|}{4b_{ij}} \left(\frac{\vec{d}_{ij}}{\|\vec{d}_{ij}\|} + \frac{\vec{d}_{ij} - \vec{y}_{ij}}{\|\vec{d}_{ij} - \vec{y}_{ij}\|} \right). \quad (2.35)$$

Later, Johansson *et al.* [51] introduced ES-2, an improved version of the ES-1, by revising b_{ij} with relative displacement of pedestrians i and j , $\vec{y}_{ij} \equiv (\vec{v}_j - \vec{v}_i)\Delta t_s$.

$$\begin{aligned} b_{ij} &= \frac{1}{2} \sqrt{(\|\vec{d}_{ij}\| + \|\vec{d}_{ij} - (\vec{v}_j - \vec{v}_i)\Delta t_s\|)^2 - \|(\vec{v}_j - \vec{v}_i)\Delta t_s\|^2} \\ &= \frac{1}{2} \sqrt{(\|\vec{d}_{ij}\| + \|\vec{d}_{ij} - \vec{y}_{ij}\|)^2 - \|\vec{y}_{ij}\|^2}, \end{aligned} \quad (2.36)$$

The interpersonal elastic force \vec{g}_{ij} can be added to the interpersonal repulsion force term \vec{f}_{ij} when the distance d_{ij} is smaller than the sum $r_{ij} = r_i + r_j$ of their radii r_i and r_j . Similar to the case of granular particles [24], Helbing [35] suggested the interpersonal elastic force as:

$$\vec{g}_{ij} = h(r_{ij} - d_{ij}) \{k_n \vec{e}_{ij} + k_t [(\vec{v}_j - \vec{v}_i) \cdot \vec{t}_{ij}] \vec{t}_{ij}\}, \quad (2.37)$$

where k_n and k_t are the normal and tangential elastic constants. A unit vector \vec{e}_{ij} is pointing from pedestrian j to pedestrian i , and \vec{t}_{ij} is a unit vector perpendicular to \vec{e}_{ij} . The function $h(x)$ yields x if $x > 0$, while it gives 0 if $x \leq 0$. Later, Moussaïd *et al.* [76] presented a simpler form of the interpersonal compression mainly considering normal elastic force:

$$\vec{g}_{ij} = k_n h(r_{ij} - d_{ij}) \vec{e}_{ij}. \quad (2.38)$$

The repulsive force from boundaries is

$$\vec{f}_{iB} = C_b \exp\left(-\frac{d_{iB}}{l_b}\right) \vec{e}_{iB}, \quad (2.39)$$

where d_{iB} is the perpendicular distance between pedestrian i and wall, and \vec{e}_{iB} is the unit vector pointing from the wall B to the pedestrian i . The strength and the range of repulsive interaction from boundaries are denoted by C_b and l_b .

In addition to the repulsive interactions, Helbing and Molnár [42] introduced the attractive force term, indicating attractive interactions between pedestrian group members and with attractions such as shop displays and museum exhibits. Later, Xu and Duh [109] formulated the interaction between group members i and k , \vec{f}_{ik} , as a summation of a bonding and a repulsive force between the members:

$$\vec{f}_{ik} = \left[-C_b \exp\left(\frac{d_{ik} - r_{ik}}{l_b}\right) + \frac{C_p}{2} \exp\left(\frac{r_{ik} - d_{ik}}{l_p}\right) \right] \vec{e}_{ik}. \quad (2.40)$$

The first term on the right-hand side indicates the bonding effect between pedestrian i and group member k , while the second term indicates the repulsive interaction between the members. The strength and the range of bonding force between pedestrians are denoted by C_b and l_b , respectively. Note that C_p is the strength of interpersonal repulsion between individual pedestrians who are not in the same pedestrian group. Here, \vec{e}_{ik} is the unit vector pointing from group member k to the pedestrian i . Xu and Duh [109] set the strength of repulsive force between group members as $C_p/2$, indicating that the repulsive force strength between same group members is half of that among individuals who are not in the same group.

In another study, Moussaïd *et al.* [77] suggested a model of attractive interaction among pedestrian group members,

$$\vec{f}_{iG} = -\beta_1 \alpha_i \vec{v}_i + q_A \beta_2 \vec{e}_{Gi} + \sum_{k \neq i} q_R \beta_3 \vec{e}_{ki}. \quad (2.41)$$

The first term on the right-hand side reflects the gazing behavior of a group member i . The second term indicates the attractive force between group member i and the center of the pedestrian group G . The third term shows the repulsive force between pedestrian i group member k . Here, β_1 and β_2 are the strength of the attractive interactions between group members and for pedestrian i and the group center G , respectively. The repulsive force strength β_3 is defined between pedestrian i and group member k . Unit vectors \vec{e}_{Gi} and e_{ki} are pointing from pedestrian i to the group center G and pointing from pedestrian i to group member k , respectively. The head rotation angle is denoted by α_1 . In addition, q_A and q_R are relevant to threshold distance between pedestrian i and the group center G , and between pedestrian i to group member k . If $q_A = 1$ and $q_R = 1$, the corresponding distance is smaller than the threshold values, otherwise 0.

Centrifugal force models

Yu *et al.* [111] proposed the centrifugal force model in which the repulsive force term is analogous to centrifugal force in mechanics. In the social force models, the repulsive force term is formulated as a derivative of repulsive potential. Although the social force models have been extended in order to incorporate relative velocity, the relative velocity is only associated with the interpersonal distance but not explicitly with the repulsive force term. In the centrifugal force model, the repulsive force term is formulated as a function of the relative velocity.

$$\vec{f}_{ij} = -K_{ij} \frac{v_{ij}^2}{d_{ij}} \vec{e}_{ij}, \quad (2.42)$$

where v_{ij} is the projection of the relative velocity of pedestrians i and j in the direction \vec{e}_{ij} ,

$$\vec{v}_{ij} = \frac{1}{2} [(\vec{v}_i - \vec{v}_j) \cdot \vec{e}_{ij} + \|(\vec{v}_i - \vec{v}_j) \cdot \vec{e}_{ij}\|]. \quad (2.43)$$

An anisotropic effect factor K_{ij} reflects that pedestrians react to others in front of them within their angle of view 180° ,

$$K_{ij} = \frac{1}{2} \left[\frac{\vec{v}_i \cdot \vec{e}_{ij} + \|\vec{v}_i \cdot \vec{e}_{ij}\|}{\|\vec{v}_i\|} \right]. \quad (2.44)$$

Likewise, the boundary repulsive force is given in the centrifugal force model as

$$\vec{f}_{iB} = -K_{iB} \left(\frac{v_{iB}^2}{d_{ij}} \right) \vec{e}_{iB} \quad (2.45)$$

with

$$K_{iB} = \frac{1}{2} \left[\frac{\vec{v}_i \cdot \vec{e}_{iB} + \|\vec{v}_i \cdot \vec{e}_{iB}\|}{\|\vec{v}_i\|} \right]. \quad (2.46)$$

Later, Chraibi *et al.* [17] introduced the generalized centrifugal force model with consideration of desired speed for the repulsive force terms. The interpersonal repulsive force term \vec{f}_{ij} is given as

$$\vec{f}_{ij} = -K_{ij} \frac{(\eta v_d + v_{ij})^2}{d_{ij} - r_i(v_i) - r_j(v_j)} \vec{e}_{ij}. \quad (2.47)$$

Here, η is the repulsive force strength parameter and r_i is required space for pedestrian i 's motion. They suggested the required space for stride r_i as a function of torso size and pedestrian i 's velocity,

$$r_i(v_i) = r_0 + v_i \Delta t_s, \quad (2.48)$$

where r_0 is torso size and Δt_s is stride time. Similar to Equation (2.47), the boundary repulsive force is given as

$$\vec{f}_{iB} = -K_{iB} \frac{(\eta v_d + v_{ij})^2}{d_{iB} - r_i(v_i)} \vec{e}_{iB}, \quad (2.49)$$

where b_{iB} is the distance between boundary B and pedestrian i .

2.1.5 Remarks

Summary

In Section 2.1, I have reviewed modeling approaches including macroscopic and microscopic approaches. From a viewpoint of fluid dynamics, macroscopic models treat pedestrians motions similar to fluid streams [47,

48]. This type of approach can directly estimate pedestrian flow characteristics such as pedestrian density and flow over a large area. However, due to its modeling approach, macroscopic models do not explicitly reflect interactions among pedestrians. Thus, macroscopic models are often limited to aggregated descriptions of pedestrian flow.

On the other hand, microscopic models view pedestrians as self-driven particles. Numerous approaches have been proposed such as cellular automata (CA) [10, 12, 29], velocity-based models [3, 21], and force-based models [42, 86, 111]. In CA-based approaches, space is discretized into two-dimensional lattices where each cell can have at most one pedestrian. Pedestrians move between cells according to the probability of movement. The CA-based approaches offer simple and efficient computation but yield limited accuracy on describing pedestrian movements due to the nature of discretized time and space.

Velocity-based models predict pedestrian movements based on a first-order ordinary differential equation. The velocity-based models can simulate pedestrian movements without calculating force terms, so inertia effects do not occur. However, the velocity-based models provide a limited representation of high-density situations when physical interactions among pedestrians become critical.

Force-based models describe pedestrian motions as a combination of force terms that can be expressed as a second-order ordinary differential equation. Internal motivation and external stimuli are modeled as force terms, and pedestrian trajectories are calculated by summing these force terms in continuous space. Although force-based models can describe pedestrian behaviors in detail, they are computationally expensive. Due to the existence of under-damped solutions in second-order ordinary differential equations, sometimes force-based models can produce unrealistic inertia effects such as oscillatory behavior in pedestrian trajectories [17, 63, 64].

Table 2.1 classifies pedestrian models discussed in this section and Table 2.2 summarizes advantages and limitations of different modeling approaches. Interested readers can find extensive reviews of pedestrian flow models presented by Bellomo and Dogbe [7], Duives *et al.* [23], Papadimitriou *et al.* [88], and Templeton *et al.* [101]. Bellomo and Dogbe [7] summarized different mathematical models of crowd behaviors and discussed issues on representation scales of the models. They pointed out challenges on developing macroscopic descriptions of collective phenomena

Table 2.1. Classification of pedestrian models.

Macroscopic Models	Hughes models [47, 48]
Cellular Automata	Gipps-Marksjö model [29] Blue-Adler model [10] Floor field model [12, 61]
Velocity-based Models	Contractile particle model [3] Gradient navigation model [21]
Force-based Models	Magnetic force model [86] Social force models [35, 42, 51] Centrifugal force models [17, 111]

Table 2.2. Advantages and limitations of different modeling approaches.

Modeling Approaches	Advantages	Limitations
Macroscopic Models	computationally cheap	aggregated descriptions
Cellular Automata	simple efficient computing	limited accuracy
Velocity-based Models	no inertia effect	lack of physical interactions
Force-based Models	detailed presentations	computationally expensive inertia effect

based on microscopic models of individual behaviors. Duives *et al.* [23] compared crowd simulation models and assessed the models' capability for predicting self-organized phenomena in various geometries of indoor space. Papadimitriou *et al.* [88] reviewed pedestrian movement models and crossing behavior studies in urban environments. They emphasized the importance of integrating pedestrian movement models with decision-making models such as crossing behavior models. Templeton *et al.* [101] examined the underlying assumptions of various crowd behavior models and reported that the majority of crowd behavior models fails to replicate realistic large-scale collective behaviors that have been observed in the previous empirical studies.

This dissertation has investigated collective patterns of pedestrian flow emerging from interactions between pedestrians and attractions. In order to incorporate behavioral aspects of individuals, the microscopic modeling approach was employed. Among various microscopic models, the social force models have been widely applied, for instance, in agent-based modeling [37, 87, 89] and multiscale modeling [18, 46, 45], due to their simplicity. The repulsive force terms in the models are given as natural exponential functions that are easy to integrate and differentiate. The social force models have produced promising results in that the model embodies behavioral elements and physical forces. The original model and its variants have successfully demonstrated various interesting phenomena such as lane formation [42], bottleneck oscillation [42], and turbulent movement [110]. Accordingly, the social force model was selected for this dissertation.

Gaps in the existing social force models

Different specifications of repulsive force terms have been proposed for the social force models, such as circular specification (CS) [35], elliptical specification (ES-1) [42], an improved version of the ES-1 (ES-2) introduced by Johansson *et al.* [51]. Furthermore, improved numerical implementations of the models have been suggested in order to suppress oscillatory behavior in pedestrian trajectories [63, 64]. In addition to the repulsive interactions, the effect of attractive interactions also has been investigated, first introduced by Helbing and Molnár [42]. For example, Xu and Duh [109] simulated bonding effects of pedestrian groups and evaluated their impacts on pedestrian flows. In another study, Moussaïd *et al.* [77] analyzed attractive interactions among pedestrian group members and their spa-

tial patterns. However, little attention has been paid to the attractive interactions between pedestrians and attractions.

Based on the review of existing social force models, it is identified that relatively little is known about the effect of attractive interactions between pedestrians and attractions. Therefore, this dissertation aims at proposing numerical simulation models to study the attractive interactions between pedestrians and attractions.

2.2 The Concept of Phases

Phase is one of the fundamental concepts in thermodynamics and statistical physics [94, 96]. In these areas, phases indicate different forms of a material or a system of particles. For instance, H_2O is in ice, liquid water, or vapor phases depending on temperature and pressure. If a material is in a certain phase, it means that the physical properties of the material are homogeneous even if there are small changes in external conditions. For instance, the specific heat capacity of water is virtually constant if it is in a phase such as water, ice, or vapor. A phase transition can be defined when one can observe a qualitative change from one phase to another by controlling an independent variable. As an example, boiling water shows a phase transition from liquid water to vapor as temperature increases. A phase diagram depicts different phases in a graph as a function of control variables.

The term “phase” often indicates different jam patterns in freeway traffic studies. In two-phase traffic theory [79, 104, 106], traffic flow patterns can be classified into either free flow phase or jammed phase. In the free flow phase, the vehicle density is not high and vehicles can keep large enough distance among them. Although interactions among vehicles exist, the interactions do not significantly reduce the speed of freeway traffic. In the jammed phase, on the other hand, interactions among vehicles come into effect, so movements of a vehicle can be restricted by other vehicles. Consequently, the vehicle speed is decreasing as the vehicle density is growing. Speed drop and stop-and-go patterns can be observed when the freeway traffic turns into the congested phase. According to three-phase traffic theory [55, 57], the traffic flow patterns are categorized into three phases: free flow, synchronized flow, and wide moving jam phases. In the synchronized flow phase, average speed becomes significantly lower than in the free flow phase, but stopping behavior is not notable yet. The

speed drop is often observed at a fixed location and usually does not move upstream. In the wide moving jam phase, however, a congested area propagates upstream and it can move through an area in any state of free or synchronized free phases. In this case, one can observe a coexisting of wide moving jam and either free or synchronized free phases. Stop-and-go patterns can be observed in that vehicles have to stop when they approach the congested area and then speed up when they leave the areas. Furthermore, various jam patterns can be further categorized in terms of multi-phases according to spatio-temporal patterns of the congested area [39, 93].

In pedestrian flow studies, growing body of literature has mainly focused on jamming transitions, thus the concept of phases is frequently utilized similar to the case of vehicular traffic studies. For example, Ezaki *et al.* [25] and Suzuno *et al.* [100] summarized their study results by presenting jammed phase. Nowak and Schadschneider [85] studied lane formation in bidirectional flow and suggested four phases including free flow, disorder, lanes, and gridlock phases. Although moving between places is not the only purpose of pedestrian walking, many of pedestrian flow studies have only focused on pedestrian jams in line with pedestrian mobility. Consequently, there remains a need for further research to quantify various patterns or phases in pedestrian motions.

In self-propelled particle studies, the concept of phases has been applied for representing various patterns of collective motions. For instance, D'Orsogna *et al.* [22] summarized the collective patterns of self-propelled particles based on configurational patterns, such as clumps, ring clumping, and rings. Similar to self-propelled particles, pedestrians can freely move in a two-dimensional space, and their motion shows different patterns not only when they travel but also when they form groups and gather around near an attraction. Therefore, the concept of phases can be applied to explain various patterns of pedestrian motions. In this dissertation, macroscopic measures are introduced to characterize different phases of collective pedestrian behaviors.

3. Numerical Simulation Models

In this chapter, I explain numerical simulation models developed in this dissertation. First, I present a numerical simulation model of attractive interactions between pedestrians and attractions. Analogously to self-propelled particle models [22, 74], the attractive interactions between pedestrians and attractions are expressed as a superposition of attractive and repulsive force terms. For simplicity, all the pedestrians are subject to the same attractive interactions. The attractive force term makes the pedestrians approach the attractions. The repulsive force term keeps the pedestrians a certain distance from the attractions. Like other social force terms, the attractive force and repulsive force terms in the attractive interaction model are given in an exponential form with the strength and range parameters. Development of the model is described in Section 3.1.

Second, I show a joining behavior model which is inspired by the stimulus crowd effect studied by Milgram *et al.* [72] and Gallup *et al.* [27]. Their studies reported that more passersby adapted the behavior of stimulus group as the group size grows. The group members were asked to look up an object on a busy city street for a short time, raising the awareness of the object. Based on their findings, it was assumed that the probability of joining an attraction increases according to the number of pedestrians attending the attraction. If an individual joins an attraction, then he or she stays there for a certain length of time. After the individual leaves the attraction, he or she is not going to visit there anymore. Pedestrian motions were numerically described with the social force model and the joining behavior model. Formulation of the model is presented in Section 3.2.

Third, I describe the setup of numerical simulations on pedestrian flow near an attendee cluster. The pedestrians were categorized into two types: attracted pedestrians and passersby. The attracted pedestrians decided to join an attraction according to the joining behavior model presented

in Section 3.2. The passersby are the pedestrians who are not interested in the attraction, thus they do not visit the attraction. It was assumed that they aimed at smoothly bypassing obstacles while walking towards their destination. The concept of attainable speed was implemented by which each pedestrian adjusted his desired walking speed depending on available space in front of him. Introducing attainable speed of pedestrian motion prevented excessive overlaps among pedestrians. Consequently, it provided a better representation of pedestrian stopping behavior. Details of the numerical simulation model are explained in Section 3.3.

Numerical simulations have been performed for a straight corridor of length L along x -axis and width W along y -axis. It has been assumed that a straight corridor is a basic element of pedestrian facilities, and the pedestrian facilities can be modeled as a combination of such straight corridors. In this dissertation, the corridor length L is considerably larger than the corridor width W in order to make sure that all the pedestrians can see attractions on lower or upper boundaries of the corridor. The study of pedestrian jams induced by an attraction can be performed by setting W small. A long straight corridor provides enough space for a pedestrian queue formed upstream of an attraction. For the straight corridor, bidirectional pedestrian flow was mainly considered. That is, one half of the population is walking towards the right boundary of the corridor from the left, and the opposite direction for the other half. Pedestrians were represented as circles with radius r_i . They moved with desired speed $v_d = 1.2$ m/s and with relaxation time $\tau = 0.5$ s, and their speed was limited to $v_{\max} = 2.0$ m/s. Here, the desired speed is defined as a speed at which a pedestrian would like to walk if one's walking is not hindered by other pedestrians. The relaxation time controls how fast the pedestrian adapts current speed to desired speed. Pedestrian trajectories were updated with the social force model in Section 2.1.4 for each simulation time step $\Delta t = 0.05$ s. Relevant equations for updating pedestrian motions are presented as

$$\frac{d\vec{v}_i(t)}{dt} = \vec{f}_{i,d} + \sum_{j \neq i} \vec{f}_{ij} + \sum_B \vec{f}_{iB}, \quad (3.1)$$

with

$$\begin{aligned}
 \vec{f}_{i,d} &= \frac{v_d \vec{e}_i - \vec{v}_i(t)}{\tau}, \\
 \vec{f}_{ij} &= C_p \exp\left(-\frac{b_{ij}}{l_p}\right) \frac{\|\vec{d}_{ij}\| + \|\vec{d}_{ij} - \vec{y}_{ij}\|}{4b_{ij}} \left(\frac{\vec{d}_{ij}}{\|\vec{d}_{ij}\|} + \frac{\vec{d}_{ij} - \vec{y}_{ij}}{\|\vec{d}_{ij} - \vec{y}_{ij}\|} \right) + \vec{g}_{ij}, \\
 b_{ij} &= \frac{1}{2} \sqrt{(\|\vec{d}_{ij}\| + \|\vec{d}_{ij} - \vec{y}_{ij}\|)^2 - \|\vec{y}_{ij}\|^2}, \\
 \vec{y}_{ij} &= (\vec{v}_j - \vec{v}_i) \Delta t_s, \\
 \vec{f}_{iB} &= C_b \exp\left(-\frac{d_{iB}}{l_b}\right) \vec{e}_{iB}.
 \end{aligned} \tag{3.2}$$

Following previous studies [109, 112, 114], the first-order Euler method was employed for a numerical integration of Equation (3.1). The numerical integration of Equation (3.1) was discretized as

$$\begin{aligned}
 \vec{v}_i(t + \Delta t) &= \vec{v}_i(t) + \vec{a}_i(t) \Delta t, \\
 \vec{x}_i(t + \Delta t) &= \vec{x}_i(t) + \vec{v}_i(t + \Delta t) \Delta t.
 \end{aligned} \tag{3.3}$$

Here, $\vec{a}_i(t)$ is the acceleration of pedestrian i at time t and the velocity of pedestrian i at time t is given as $\vec{v}_i(t)$. The position of pedestrian i at time t is denoted by $\vec{x}_i(t)$.

Specific setups of each study are further explained in the following sections.

3.1 Study I: Attractive Force Model

In Study I, the collective effects of attractive interactions between pedestrians and attractions were numerically studied by devising an attractive force term \vec{f}_{iA} . The attractive force term \vec{f}_{iA} indicates pedestrian movements toward attractive stimuli, for instance, shop displays and museum exhibits. The attractive force toward attractions was modeled similarly to the interaction between pedestrians and the wall, but in terms of both attractive and repulsive interactions. The repulsive effect of attractions is necessary so that pedestrians can keep a certain distance from attractions.

Mogilner *et al.* [74] suggested that attractive interactions among individuals can be modeled by adding repulsion and attraction terms, i.e.,

$$F = C_r \exp\left(-\frac{d_{ij}}{l_r}\right) - C_a \exp\left(-\frac{d_{ij}}{l_a}\right), \tag{3.4}$$

where F is the magnitude of the attractive force between a pair of individuals. The distance between two individuals i and j are represented

by d_{ij} . Repulsion and attraction strength parameters are indicated by C_r and C_a , respectively. Range parameters are denoted by l_r for repulsion and l_a for attraction. They also noted that short-range strong repulsive and long-range weak attractive interactions are needed to make the individuals keep a certain distance between them while forming a stable group. Mogilner *et al.* [74] and D'Orsogna *et al.* [22] demonstrated that the pairwise attractive and repulsive forces in Equation (3.4) can reproduce various formations of swarm particles.

Analogously to self-propelled particle models [22, 74], the strength and range of attractive force were modeled as

$$\vec{f}_{iA} = \left[C_r \exp\left(\frac{r_i - d_{iA}}{l_r}\right) - C_a \exp\left(\frac{r_i - d_{iA}}{l_a}\right) \right] \vec{e}_{iA}. \quad (3.5)$$

The distance between pedestrian i and attraction A is indicated by d_{iA} , and \vec{e}_{iA} is the unit vector pointing from attraction A to pedestrian i . Here, C_a and l_a denote the strength and the range of attractive interaction toward attractions, respectively. Similarly, C_r and l_r denote the strength and the range of repulsive interaction from attractions. As in Reference [74], the strength and range parameters were set to be $C_r > C_a$ and $l_a > l_r$. By these conditions, the attractions attract distant pedestrians but not too close to the attractions. Pedestrian radius r_i is incorporated with the model to consider the effect of pedestrian size on effective distance between pedestrian i and attraction A .

The presented model in Equation (3.5) was coupled with the social force model presented in Equation (3.1). Accordingly, the social force model was given as

$$\frac{d\vec{v}_i(t)}{dt} = \vec{f}_{i,d} + \sum_{j \neq i} \vec{f}_{ij} + \sum_B \vec{f}_{iB} + \sum_A \vec{f}_{iA}. \quad (3.6)$$

The interpersonal elastic force \vec{g}_{ij} in Equation (3.2) was given as

$$\vec{g}_{ij} = h(r_{ij} - d_{ij}) \{ k_n \vec{e}_{ij} + k_t [(\vec{v}_j - \vec{v}_i) \cdot \vec{t}_{ij}] \vec{t}_{ij} \}. \quad (3.7)$$

Other force terms in the implementation were same as in Equation (3.2).

In numerical simulations, the corridor dimensions were set as $L = 25$ m and $W = 4$ m, with periodic boundary condition in the direction of x -axis. According to the periodic boundary condition, pedestrians walk into the corridor through one side when they have left through the opposite side. Periodic boundary condition was used in order to keep the number of pedestrians constant over the corridor during the numerical simulations. Five attractions were placed for every 5 m on both upper and lower walls

of the corridor. To consider the dimension of attractions, each attraction was modeled as three point masses: one point at the center, the other two points at the distance of 0.5 m from the center. The parameters of the repulsive force terms were given based on previous works: $C_p = 3$, $l_p = 0.2$, $\Delta t_s = 0.5$, $k_n = 25$, $k_t = 12.5$, $C_b = 10$, and $l_b = 0.2$ [36, 42, 51, 76]. Here, the values of C_r and l_r were set to be the same as C_b and l_b . In Study I, short-range strong repulsive and long-range weak attractive interactions were considered, thus the values of C_a and l_a were chosen such that $l_a > l_r$ and $C_a < C_r$. Accordingly, the value of l_a were set to be 1. The effect of attractive interaction toward attractions can be studied by controlling the ratio of C_a to C_r , defining the relative attraction strength $C = C_a/C_r$ with $C_r = 10$. The pedestrian density $\rho = N/A$ was also controlled for the corridor area $A = 100 \text{ m}^2$. At the initial time $t = 0$, pedestrian positions were randomly generated with uniform distribution over the whole corridor without overlapping.

3.2 Study II: Joining Behavior Model

Study I examined attractive interactions between pedestrians and attractions by appending the attractive force toward the attractions as shown in Equation (3.5). Although the extended social force model can produce various collective patterns of pedestrian movements, Study I did not explicitly take into account selective attention. The selective attention is a widely recognized behavioral mechanism by which people can focus on tempting stimuli and disregard uninteresting ones [31, 108].

Furthermore, it has been widely believed that individual choice behavior can be influenced by social influence from other individuals. For instance, previous studies on stimulus crowd effects reported that a passerby is more likely to shift his attention towards the crowd as its size grows [27, 72]. This belief is generally accepted in the marketing area, which can be interpreted that having more visitors in a store can attract more passersby to the store [6, 14]. It was also suggested that the sensitivity to others' choice is different for different places, time-of-day, and visitors' motivation [27, 53]. In addition, the social influence is also relevant to understand individual choice behavior in emergency evacuations. Helbing *et al.* [37] suggested that pedestrians in evacuation scenarios were likely to follow the movement of the majority group due to the lack of information. Kinateder *et al.* [59] discovered that evacuees tended to follow the

routes taken by others in virtual reality (VR) experiments of tunnel fires. Based on laboratory experiments of simulated evacuations, Haghani and Sarvi [33] confirmed that evacuees preferred an exit having more crowds to other exits when the evacuees were unaware of situations of every exit.

Based on the idea of selective attention [31, 108] and social influence [6, 14, 27, 53, 72], it was assumed that an individual decided whether he or she was going to visit an attraction based on the number of pedestrians attending the attraction. This is also known as a preferential attachment which can be observed in scientific paper citation [90], network growth [83, 99], and animal group size dynamics [84, 99]. According to Gallup *et al.* [27], the preferential attachment model can be written as

$$P(N_i) = \frac{N_i^k}{N_i^k + N_j^k}, \quad (3.8)$$

where $P(N_i)$ is the probability of attachment. The number of pedestrians in groups i and j are denoted by N_i and N_j , respectively. The exponent k controls the probability function shape. For $k = 1$, the probability function increases as the group size grows and then saturates when the group size is large enough. If $k \geq 2$, the probability function sharply increases before it reaches a particular value, showing a quorum response [99]. Similar to the studies of Milgram *et al.* [72] and Gallup *et al.* [27], the exponent k was set to be 1. For the case of joining behavior, the subscript i can be replaced by a indicating pedestrians already joined an attraction. Likewise, the subscript j can be replaced by 0 denoting pedestrians who are not stopping by the attraction. In other words, N_a and N_0 are the number of pedestrians who have already joined and for the pedestrians who have not joined the attraction yet, respectively. In addition, N_a was multiplied by social influence parameter s in order to reflect the sensitivity to others' choice.

$$P_a = \frac{sN_a}{N_0 + sN_a}, \quad (3.9)$$

where the social influence parameter $s > 0$ can be also understood as pedestrians' awareness of the attraction. The above equation shows that the choice probability increases when s or N_a grows. However, the choice probability cannot be estimated if there is nobody within the range of perception. In order to avoid such indeterminate case, K_0 and K_a were introduced as baseline values of N_a and N_0 , respectively, i.e.,

$$P_a = \frac{s(N_a + K_a)}{(N_0 + K_0) + s(N_a + K_a)}. \quad (3.10)$$

According to previous studies [27, 53, 72], it was assumed that the strength of social influence can be different for different situations and can be controlled in Equation (3.10). When there is nobody near the attraction (i.e., N_a and N_0 are 0), the joining probability becomes $P_a = sK_a/(K_0 + sK_a)$. In this case, the joining probability depends on the values of K_0 and K_a , meaning that an individual is more likely join the attraction as the value of K_a increases.

When an individual can see an attraction in the perception range $R_i = 10$ m, the individual evaluates the joining probability in Equation (3.10). If the individual decides to join the attraction, then he or she shifts desired direction vector \vec{e}_i toward the attraction. Once an individual has joined an attraction, he or she will stay near the attraction for an exponentially distributed time with an average duration of visiting an attraction t_d [27, 42, 67]. After a lapse of t_d , the individual leaves the attraction and continues walking towards initial destination, not visiting the attraction again. While t_d was observed on the order of a second in References [27, 72], t_d was a control variable in Study II ranging up to 300 s in order to consider different types of attractions in terms of t_d .

Pedestrian motions were updated with the social force model presented in Equation (3.1). Comparing to the setup of Study I, a simpler form of interpersonal elastic force \vec{g}_{ij} in Equation (3.2) was given as in Reference [76], i.e.,

$$\vec{g}_{ij} = k_n h(r_{ij} - d_{ij}) \vec{e}_{ij}. \quad (3.11)$$

Other force terms in the implementation are same as in Equation (3.2).

In numerical simulations, the corridor dimensions were set as $L = 30$ m and $W = 6$ m, with periodic boundary condition in the direction of x -axis. An attraction was placed at the center of the lower wall, i.e., at the distance of 15 m from the left boundary of the corridor. The number of pedestrians in the corridor, N , was given as 100. As in Study I, pedestrian positions were randomly generated with a uniform distribution over the whole corridor without overlapping. The parameters of the repulsive force terms were given based on previous works: $C_p = 3$, $l_p = 0.2$, $\Delta t_s = 0.5$, $k = 62.5$, $C_b = 10$, and $l_b = 0.2$ [42, 51, 66, 76]. For simplicity, K_a and K_0 were set to be 1, meaning that both options are equally attractive when the individual would see nobody within his perception range. An individual was counted as an attending pedestrian if his efficiency of motion $E_i = (\vec{v}_i \cdot \vec{e}_i)/v_d$ was lower than 0.05 within a range of 3 m from the center of the attraction after he decided to join there. The efficiency of motion indicates

how much the driving force contributes to the progress of pedestrian i towards his destination with a range from 0 to 1 [38, 66]. Here, $E_i = 1$ implies that the individual is walking towards his destination with the desired velocity while lower E_i indicates that an individual is distracted from his initial destination because of the attraction.

3.3 Study III: Modeling Pedestrian Flow near an Attendee Cluster

In Study III, the corridor dimensions were set as $L = 60$ m and $W = 4$ m, with an open boundary condition in the direction of x -axis. An attraction was placed at the center of the lower wall, i.e., at the distance of 30 m from the left boundary of the corridor. An open boundary condition was employed in order to continuously supply passersby to the corridor. By doing so, pedestrians can enter the corridor regardless of the number of leaving pedestrians. On the other hand, if the number of pedestrians in the corridor is fixed by periodic boundary condition, the number of passersby tends to decrease as the number of attracted pedestrians increases.

The number of pedestrians in the corridor was associated with the pedestrian influx Q , i.e., the arrival rate of pedestrians entering the corridor. The unit of Q is indicated by P/s, which stands for pedestrians per second. Based on previous studies [69, 71], the pedestrian inter-arrival time was assumed to follow a shifted exponential distribution. That is, pedestrians were entering the corridor independently and their arrival pattern was not influenced by that of others. The minimum headway was set to 0.4 s between successive pedestrians entering the corridor, which is large enough to prevent overlaps between arriving pedestrians.

Pedestrians were entering the corridor through the left and the right boundaries in case of bidirectional flow scenario. The corridor boundaries were sliced into inlets with a width of 0.5 m which is slightly larger than pedestrian size (i.e., $2r_i = 0.4$ m), so there are 8 inlets on each boundary. In each inlet, pedestrians were entering the corridor unassociated with entering pedestrians in the neighboring inlets. For each entering pedestrian, the vertical position was randomly generated based on uniform distribution within the entering inlet without overlapping with other nearby pedestrians and boundaries. In effect, pedestrians were inserted at random places on either side.

In addition to bidirectional flow scenario, unidirectional flow was also considered because one can observe different collective patterns of passersby

that were not observed in the bidirectional flow. In unidirectional flow scenario, all the pedestrians were entering the corridor through the left boundary and walking towards the right.

Similar to Study II, pedestrian motions were updated with the social force model in Equation (3.1). However, the formulation of desired speed v_d in driving force term $f_{i,d}$ was modified in order to provide a better representation of pedestrian stopping behavior. Inspired by the previous studies [16, 89], it was assumed that the desired speed v_d is an attainable speed of pedestrian i depending on the available walking space in front of the pedestrian,

$$v_d = \min\{v_0, d_{ij}/T_c\}, \quad (3.12)$$

where v_0 is a comfortable walking speed and d_{ij} is the distance between pedestrian i and the first pedestrian j encountering with pedestrian i in the course of \vec{v}_i . Time-to-collision T_c represents how much time remains for a collision of two pedestrians i and j . In line with previous studies [54, 76], time-to-collision T_c was estimated by extending current velocities of pedestrians i and j , v_i and v_j , from their current positions, x_i and x_j :

$$T_c = \frac{\beta - \sqrt{\beta^2 - \alpha\gamma}}{\alpha}, \quad (3.13)$$

where $\alpha = \|\vec{v}_i - \vec{v}_j\|^2$, $\beta = (\vec{x}_i - \vec{x}_j) \cdot (\vec{v}_i - \vec{v}_j)$, and $\gamma = \|\vec{x}_i - \vec{x}_j\|^2 - (r_i + r_j)^2$. Note that T_c is valid for $T_c > 0$, meaning that pedestrians i and j are in a course of collision, whereas $T_c < 0$ implies the opposite case. If $T_c = 0$, disks of pedestrians i and j are in contact.

It was assumed that passersby aim at smoothly bypassing obstacles while walking towards their destination. Note that passersby in Study III are the pedestrians who are not interested in the attraction, thus they do not visit the attraction. Analogously to the potential flow in fluid dynamics [1, 5] and in pedestrian stream model [48], the streamline function was employed to steer passersby between boundaries of the corridor. The streamlines represent plausible trajectories of particles smoothly bypassing obstacles, and the partial derivatives of the streamlines can express the flow velocity components in x- and y-directions for a location $z = (x, y)$. For passerby flow moving near an attraction, an attendee cluster can act as an obstacle. It was assumed that passersby set their initial desired walking direction $\vec{e}_{i,0}$ along the streamlines. As reported in a previous study [67], the shape of an attendee cluster near an attraction can be approximated as a semicircle. By doing so, one can set the streamline

function ψ for passerby traffic similar to the case of fluid flow around a circular cylinder in a two dimensional space [1, 5]:

$$\psi = v_0 d_{zA} \sin(\theta_z) \left(1 - \frac{r_c}{d_{zA}}\right), \quad (3.14)$$

where v_0 is the comfortable walking speed and d_{zA} is the distance between the center of the semicircle A and location $z = (x, y)$. The angle θ_z was measured between $y = 0$ m and \vec{d}_{zA} . The attendee cluster size at time t is denoted by $r_c = r_c(t)$. To measure r_c , the walking area near the attraction was sliced into thin layers with the width of a pedestrian size (i.e., $2r_i = 0.4$ m) in the horizontal direction. From the bottom layer to the top layer, one can count the number of layers consecutively occupied by attendees. The attendee cluster size r_c was then obtained by multiplying the number of consecutive layers by the layer width 0.4 m. The initial desired walking direction $\vec{e}_{i,0}$ can be obtained as

$$\vec{e}_{i,0} = \left(\frac{\partial \psi}{\partial y}, -\frac{\partial \psi}{\partial x} \right). \quad (3.15)$$

Note that passersby pursue their initial destination, thus their desired walking direction \vec{e}_i is identical to $\vec{e}_{i,0}$ given in Equation (3.15), i.e, $\vec{e}_i = \vec{e}_{i,0}$.

The repulsive force \vec{f}_{ij} was also modified to simulate the motions of attracted pedestrians near an attraction and passersby who do not visit the attraction. The anisotropic function ω_{ij} was included in \vec{f}_{ij} in order to represents pedestrian i 's directional sensitivity to pedestrian j [51]. The modified repulsive force \vec{f}_{ij} is given as

$$\vec{f}_{ij} = \omega_{ij} C_p \exp\left(-\frac{b_{ij}}{l_p}\right) \frac{\|\vec{d}_{ij}\| + \|\vec{d}_{ij} - \vec{y}_{ij}\|}{4b_{ij}} \left(\frac{\vec{d}_{ij}}{\|\vec{d}_{ij}\|} + \frac{\vec{d}_{ij} - \vec{y}_{ij}}{\|\vec{d}_{ij} - \vec{y}_{ij}\|} \right) \quad (3.16)$$

with

$$\omega_{ij} = \lambda_{ij} + (1 - \lambda_{ij}) \frac{1 + \cos \phi_{ij}}{2}. \quad (3.17)$$

Here, $0 \leq \lambda_{ij} \leq 1$ is pedestrian i 's minimum anisotropic strength against pedestrian j . The angle ϕ_{ij} was measured between velocity vector of pedestrian i , \vec{v}_i , and relative location of pedestrian j with respect to pedestrian i , $\vec{d}_{ji} = \vec{x}_j - \vec{x}_i$. In Study III, pedestrians were represented as non-elastic solid discs in order to mimic pedestrian stopping behavior. Thus, interpersonal elastic force \vec{g}_{ij} compression among pedestrians was not modeled.

The parameters of the repulsive force terms were given based on previous works: $C_p = 3$, $l_p = 0.3$, $\Delta t_s = 2.5$, $C_b = 6$, and $l_b = 0.3$ [42, 51, 66, 67,

113]. The minimum anisotropic strength λ_{ij} was set to 0.25 for attendees near the attraction and 0.5 for others, yielding that the attendees exert smaller repulsive force on others than passersby do. Consequently, the attendees can stay closer to the attraction while being less disturbed by the passersby.

As in Study II, an individual evaluates the joining probability when the attraction can be seen by the individual 10 m ahead. The joining behavior model was implemented as in Study II, but the average duration of visiting an attraction t_d was set to be 30 s. While the influence of t_d on pedestrian visiting behavior was one of the main interests in Study II, Study III focused on the impact of Q and s on passerby traffic flow near an attraction. Setting up the value of t_d as 30 s enables one to observe enough number of passersby and attendees near the attraction. If t_d is too small, an attendee cluster might not be observed. On the other hand, if t_d is too large, passerby flow might not exist because large t_d tends to produce a large attendee cluster which can block the corridor.

4. Results

4.1 Study I: Collective Dynamics of Attracted Pedestrians

To study collective dynamics of attractive interactions between pedestrians and attractions, the attractive force model presented in Section 3.1 was implemented and examined in Study I. Extensive numerical simulations were performed by controlling relative attraction strength C and pedestrian density ρ .

One can predict four representative patterns depending on C and ρ . When ρ is low, three different phases are observed. For small C , pedestrians walk to their destinations without being influenced by attractions, which shows a free flow phase (see Figure 4.1(a)). For intermediate values of C , the attractive interactions lead to an agglomerate phase where pedestrians form stable clusters around attractions, as shown in Figure 4.1(b). When C is strong, one can observe a competitive phase characterized by pedestrians rushing into attractions and pushing others; see Figure 4.1(c). If ρ is high, the agglomerate phase is not observed anymore. Instead, the free moving and competitive phases coexist only for the intermediate attractive interaction (see Figure 4.1(d)).

These collective patterns of pedestrian movements or phases were characterized by introducing the efficiency of motion E and the normalized kinetic energy K [38] as following:

$$E = \left\langle \frac{1}{N} \sum_{i=1}^N \frac{\vec{v}_i \cdot \vec{e}_i}{v_d} \right\rangle \quad (4.1)$$

and

$$K = \left\langle \frac{1}{N} \sum_{i=1}^N \frac{\|\vec{v}_i\|^2}{v_d^2} \right\rangle. \quad (4.2)$$

Here $\langle \cdot \rangle$ represents an average over 60 independent simulation runs after

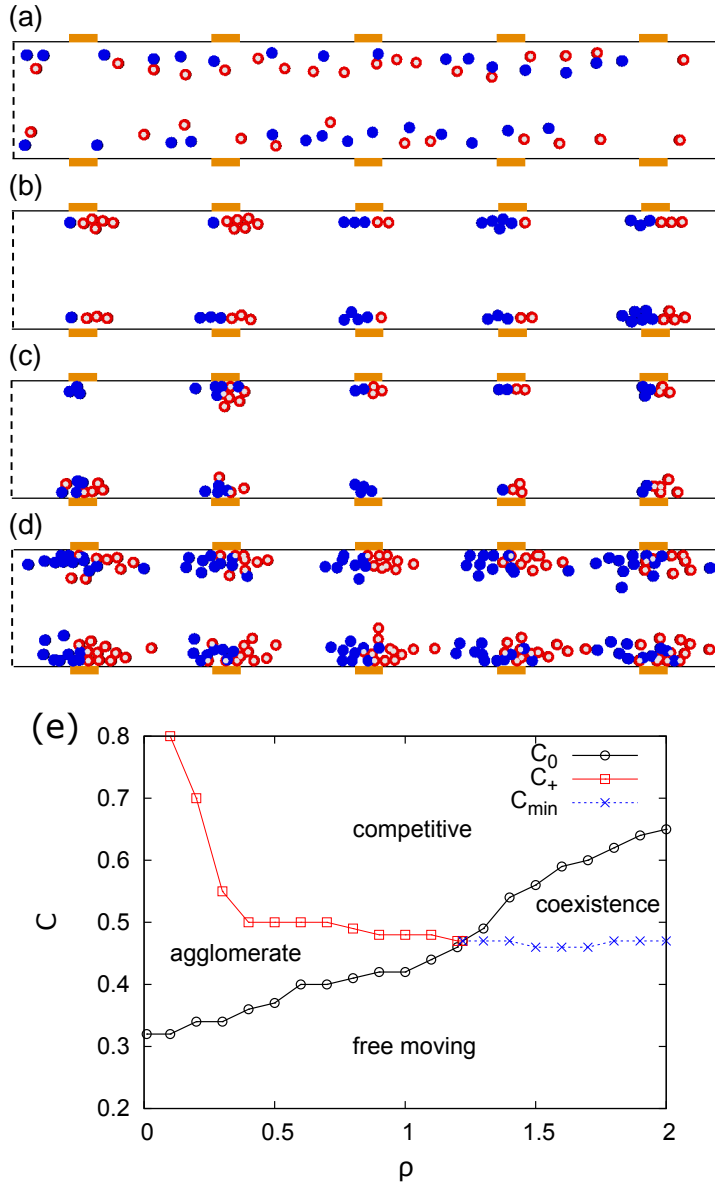


Figure 4.1. (color online) Snapshots of numerical simulations for various collective patterns: (a) free moving, (b) agglomerate, (c) competitive phase, and (d) coexistence subphase. The attractions, depicted by rectangles, are located on the walls of the corridor with periodic boundary conditions in the horizontal direction. Blue and red circles depict the pedestrians with desired directions to the left and to the right, respectively. (e) Phase diagram summarizing the numerical results. The parameter space of the pedestrian density ρ and the relative attraction strength C is divided into four regions by means of C_0 (\circ), C_+ (\square), and C_{\min} (\times). Here, C_0 shows the critical point at which the efficiency of motion E becomes zero. C_+ denotes parameter combination (ρ, C) at which the normalized kinetic energy K begins to grow from 0 while $E = 0$. C_{\min} indicates parameter combination (ρ, C) at which $\partial K / \partial C > 0$ while $E > 0$.

reaching the stationary state. The efficiency reflects the contribution of the driving force in the pedestrian motion. If all the pedestrians walk with their desired velocity, the efficiency becomes 1. On the other hand, the zero efficiency can be obtained if pedestrians do not move in their desired directions and form clusters at attractions. The normalized kinetic energy

has the value of 0 if all the pedestrians do not move, otherwise it has a positive value.

Based on those macroscopic measures, different phases were identified. For a given ρ , E decreased according to C , meaning that pedestrians are more distracted from their desired velocity due to the larger strength of attractions. Interestingly, E became 0 at a finite value of $C = C_0(\rho)$, indicating the transition from the free moving phase to the agglomerate phase for low ρ or to the competitive phase for high ρ . As C increased, K turned to be 0 at the same critical point of $C = C_0$, and then gradually increased from 0 at $C = C_+(\rho)$ with $C_+ \geq C_0$. The boundaries among different phases were characterized in terms of C_0 and C_+ . For low values of ρ , the free moving phase for $C < C_0$ was characterized by

$$E > 0 \text{ and } K > 0, \quad (4.3)$$

indicating that kinetic energy of pedestrian motion is mostly used for progressing towards their destinations. The upper boundary of free flow phase was identified by $C = C_0(\rho)$ at which E becomes 0. For $C_0 < C < C_+$, the agglomerate phase was characterized by

$$E = K = 0, \quad (4.4)$$

showing that pedestrians came to a standstill. When $C > C_+$, the competitive phase by

$$E = 0 \text{ and } K > 0, \quad (4.5)$$

reflecting that pedestrians do not walk in their desired directions but still moving near the attractions. For high values of ρ , however, K decreased and then increased according to C but without becoming zero. The striking difference from the case with low ρ is the existence of parameter region characterized by both

$$E > 0 \text{ and } \frac{\partial K}{\partial C} > 0. \quad (4.6)$$

This implies that some pedestrians rush into attractions as in the competitive phase (i.e., $\partial K/\partial C > 0$), while other pedestrians move in their desired directions as in the free moving phase (i.e., $E > 0$). The moving pedestrians are also attracted by attractions but cannot stay around them because of interpersonal repulsion effect by other pedestrians closer to attractions. Thus, this parameter region was characterized as a coexistence subphase. The coexistence subphase belongs to the free moving phase in the sense that the coexistence subphase was also characterized by $E > 0$ and $K > 0$. However, one can identify the lower boundary of coexistence

subphase by determining C_{\min} that minimizes K . The upper boundary to the competitive phase was determined by the critical point C_0 . It was found that $C_0(\rho)$ is an increasing function of ρ because stronger attractions are needed to entice more pedestrians. Different phases characterizing different collective patterns of pedestrians and transitions among them were summarized in the phase diagram of Figure 4.1(e).

The appearance of various phases in Study I can be explained by the interplay between attraction strength and interpersonal repulsion effect. If the pedestrian density is low, one can observe the transition from the free phase to the agglomerate phase and finally to the competitive phase. As C increases, pedestrians tend to be more distracted from their velocity due to the larger strength of attractions, yielding to the appearance of the agglomerate phase. After the agglomerate phase emerges, further increasing C leads to competitive phase. In this phase, attracted pedestrians jostle each other because of the interpersonal repulsion effect. As C increases, their jostling behavior becomes more severe because higher C increases the desire to reaching the attractions, leading to smaller interpersonal distance. Consequently, the interpersonal repulsion effect becomes critical. For high pedestrian density, the agglomerate phase does not appear and the coexistence subphase emerges. The moving pedestrians are also attracted by the attractions but cannot stay around the attractions. This is due to the interpersonal repulsion effect by other pedestrians closer to the attractions.

4.2 Study II: Visiting Behavior

In Study II, the pedestrian joining behavior model in Section 3.2 was implemented and numerically studied in order to understand the collective patterns of pedestrians' visiting behavior. Note that while pedestrians in Study I were subject to the same equation of motion, the joining behavior model in Study II enabled pedestrians to make decisions between walking in the desired direction and stopping by an attraction. The numerical simulation results showed different patterns of pedestrian movements depending on the social influence strength s and the average duration of visiting an attraction t_d . If s is weak, one can define an unsaturated phase where some pedestrians move towards the attraction while others walk in their desired directions; see Figure 4.2(a). For large values of s , a saturated phase can be defined, in which every pedestrian near the attraction

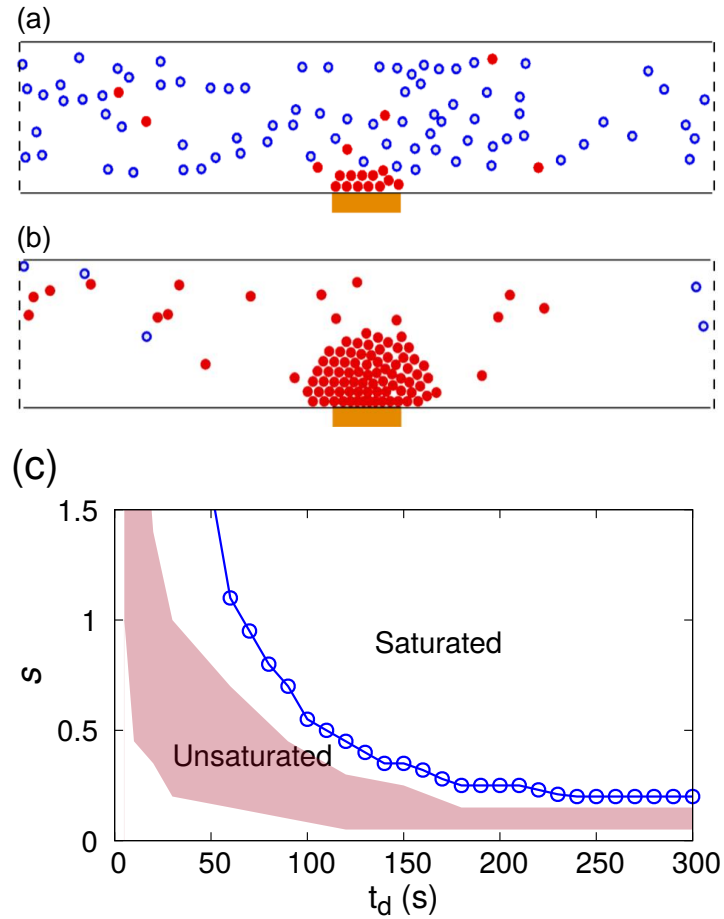


Figure 4.2. (color online) Snapshots of numerical simulations for different collective patterns: (a) unsaturated phase and (b) saturated phase. The attraction, depicted by an orange rectangle, is located at the center of the lower wall. Filled red and hollow blue circles depict the pedestrians who have and have not visited the attraction, respectively. (c) A feasibility zone of effective improvements and an envelope of the saturated phase. The red shaded area depicts a feasibility zone of the effective improvements characterized in terms of the marginal benefits. The blue solid line with circle symbols represents the envelope of the saturated phase.

is joining or has visited the attraction, as shown in Figure 4.2(b). These different patterns were characterized by comparing N_p and N_v . One can define N_p as the number of pedestrians near the attraction, i.e., within a range of $R_a = 10$ m from the center of the attraction, and N_v as the number of pedestrians near the attraction who have visited the attraction. Here, a pedestrian is considered as “having visited an attraction” if one is joining there or one has left the attraction after having stayed there for t_d . The saturated phase was characterized by

$$N_v = N_p, \quad (4.7)$$

indicating that all the pedestrians near the attraction have visited the attraction. On the other hand, the unsaturated phase was characterized

by

$$N_v < N_p, \quad (4.8)$$

where some pedestrians have visited the attraction while others walk in their desired directions.

In addition to describing observed visiting patterns, two marginal benefits of facility improvements were also evaluated to reflect the change in N_v . It was assumed that facility improvements can be achieved by either increasing the social influence strength s or the average duration of visiting an attraction t_d . Accordingly, the marginal benefits were calculated as the first derivate of N_v with respect to s and t_d , respectively. If the marginal benefits are significant, the corresponding parameter region of s and t_d is denoted by a feasibility zone of the effective improvements. That is, higher increase of N_v is expected with smaller increase of s and t_d . Other than the feasibility zone, the impact of changing these variables are insignificant. Figure 4.2(c) summarizes the finding in Study II.

As can be seen from Figure 4.2(c), the parameter space of s and t_d was divided into two regions according to the value of N_v . For each value of $t_d > 43$ s, N_v increases as s increases, and then finally reaches N_p at a critical value of s , i.e., s_c . This indicates the transition from the unsaturated phase to the saturated phase. For the region of $t_d < 43$ s, N_v increases as s grows but does not reach to its maximum allowed value even for the large values of s . The average duration of visiting an attraction t_d is not long enough, so it fails to obtain sufficient amount of visitors. One can also observe that s_c substantially decreases for $t_d \leq 120$ s and appears to stay around 0.2 when t_d is larger than 180 s. It is reasonable to suppose that the departure rate of attending pedestrians is positively associated with the reciprocal of t_d while the arrival rate of joining pedestrians is linked to s . Accordingly, one can infer that the impact of the departure rate on N_v is dominated by that of the arrival rate when t_d is large, so the marginal impact of increasing t_d becomes less notable for larger t_d .

4.3 Study III: Jamming Transitions Induced by an Attraction

Study III investigated jamming transitions in pedestrian flow interacting with an attraction by means of numerical simulations. Similar to Study II, the simulation model was mainly based on the social force model presented in Chapter 3 for pedestrian motions and the probability of joining an attraction presented. In order to provide a better representation

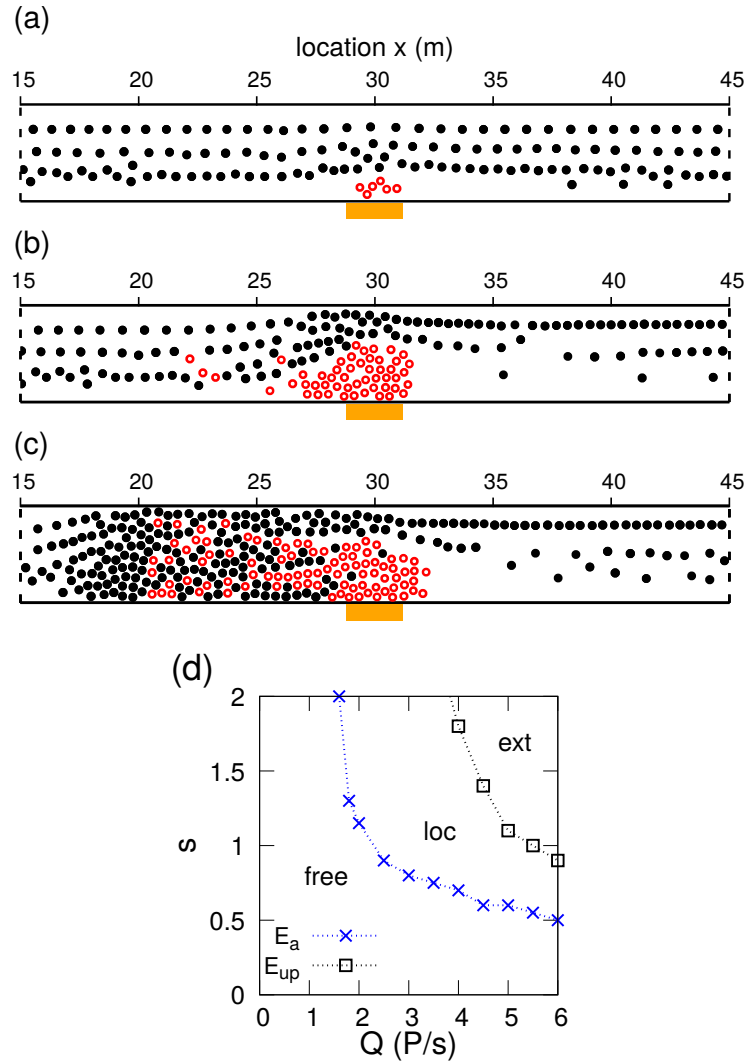


Figure 4.3. (color online) Representative snapshots of different passerby flow patterns in unidirectional flow: (a) free flow phase, (b) localized jam phase, and (c) extended jam phase. The attraction, depicted by an orange rectangle, is located at the center of the lower wall with open boundary conditions in the horizontal direction. Passersby walking from the left to the right are indicated by filled black circles. Hollow red circles depict pedestrians attracted by the attraction. (d) Phase diagram summarizing the numerical results of unidirectional flow. Here, ‘free’, ‘loc’, and ‘ext’ indicate the free flow phase, the localized jam phase, and the extended jam phase, respectively. Note that P/s stands for pedestrians per second, being the unit of pedestrian flux Q .

of pedestrian stopping behavior, formulations of the desired speed v_d and desired walking direction vector e_i were further improved as presented in Section 3.3. By controlling pedestrian influx Q and the social influence parameter s , various pedestrian flow patterns were observed in unidirectional and bidirectional flow scenarios. Again, note that the unit of Q is indicated by P/s, which stands for pedestrians per second.

4.3.1 Unidirectional Flow

In unidirectional flow, a free flow phase was defined for small Q and s , see Figure 4.3(a). A localized jam phase appeared in the vicinity of the attraction for medium and high Q with the intermediate range of s , as can be seen from Figure 4.3(b). Passersby walked slowly near the attraction because of the reduced walking area, and then they recovered their speed after they walked away from the attraction. One can observe that pedestrians walking away from the attraction tend to form lanes. This is possible because the standard deviation of speed among the walking away pedestrians is not significant after the pedestrians recover their speed. According to the study of Moussaïd *et al.* [75], the formation of pedestrian lanes is stable when pedestrians are walking at nearly the same speed. Once the walking away pedestrians form lanes, the lanes are not likely to collapse. An extended jam phase was observed when both Q and s were large. In the extended jam phase, the pedestrian queue was growing towards the left boundary and the queue was persisting for a long period of time; see Figure 4.3(c). The attendee cluster did not maintain its semi-circular shape anymore. This seems to be because passersby seized up the attracted pedestrians. Meanwhile, pedestrians in the queue still could slowly walk towards the right side of the corridor as they initially intended. When Q and s were very large, the extended jam phase could end up in a freezing phenomenon with a certain probability, indicating that passersby could not proceed beyond the attraction due to the clogging effect. Some passersby were pushed out towards the attraction by the attracted pedestrians and inevitably they prevented attracted pedestrians from joining the attraction. Consequently, the attracted pedestrians could not approach the boundary of the attendee cluster although they kept their walking direction towards the attraction. Simultaneously, the passersby near the attraction attempted to walk away from the attraction, but they could not because they were blocked by the attracted pedestrians. Eventually, the pedestrian movements near the attraction came to a halt.

Based on observations presented in Figures 4.3(a) to 4.3(c), different passerby flow patterns were characterized in terms of stationary state average of local efficiency, $E(x)$:

$$E(x) = \langle E(x, t) \rangle = \left\langle \frac{1}{|N_p(x, t)|} \sum_{i \in N_p(x, t)} E_i \right\rangle, \quad (4.9)$$

where $\langle \cdot \rangle$ represents the average obtained from 50 independent simulation runs after reaching the stationary state. The individual efficiency of motion $E_i = (\vec{v}_i \cdot \vec{e}_{i,0})/v_0$ can be understood as a normalized speed of pedestrian i in the horizontal direction. The local efficiency $E(x, t)$ indicates how fast passersby in segment x progress towards their destination at time t . The set $N_p(x, t)$ is the collection of passersby in a 1 m long segment x at time t , and $|N_p(x, t)|$ is the cardinality of the set $N_p(x, t)$. If $|N_p(x, t)| = 0$, $E(x, t)$ was set to be 1 inferring that a passerby can walk with comfortable speed v_0 if the passerby is in the segment x at time t . When $E(x) = 1$, the passersby can freely walk without reducing their speed. In contrast, $E(x) = 0$ implies that the passersby have reached a standstill.

A section of $27 \text{ m} \leq x \leq 33 \text{ m}$ was selected to evaluate the stationary state average value in the vicinity of the attraction, and the minimum value of $E(x)$ was denoted by E_a . Likewise, a section of $12 \text{ m} \leq x \leq 18 \text{ m}$ was selected for upstream of the attraction, and the minimum value of $E(x)$ in the section was indicated by E_{up} . For small values of s , the free flow phase was characterized by

$$E_a \approx 1 \text{ and } E_{up} \approx 1. \quad (4.10)$$

Likewise, the localized jam phase was characterized by

$$0 < E_a < 1 \text{ and } E_{up} \approx 1. \quad (4.11)$$

When Q and s were large, the extended jam phase was characterized by

$$0 \leq E_a < 1 \text{ and } 0 \leq E_{up} < 1. \quad (4.12)$$

Figure 4.3(d) summarizes numerical results by dividing the parameter space of Q and s into different phases. Note that, in extended jam phase, one can observe the freezing phenomena with a certain probability.

4.3.2 Bidirectional Flow

In bidirectional flow, the free flow phase appeared when Q was small with weak s , similar to the case of the unidirectional flow scenario. From Figure 4.4(a), one can observe that passersby walk towards their destinations without being interrupted by the cluster of attracted pedestrians. Passersby walking to the right formed lines in the lower part of the corridor while the upper part of the corridor was occupied by passersby walking to the left. This spatial segregation appeared as a result of lane formation process which has been reported in previous studies [26, 42, 65, 115].

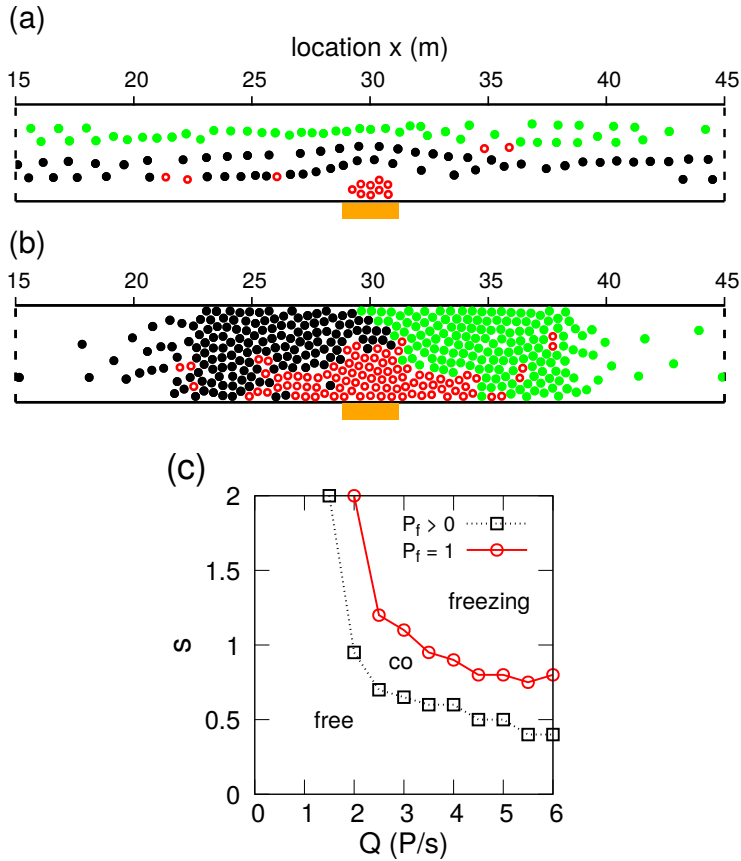


Figure 4.4. (color online) Representative snapshots of different passerby flow patterns in bidirectional flow: (a) free flow phase and (b) freezing phase. The attraction, depicted by an orange rectangle, is located at the center of the lower wall with open boundary conditions in the horizontal direction. Filled black and green circles indicate passersby walking to the right and to the left, respectively. Hollow red circles depict pedestrians attracted by the attraction. (c) Phase diagram summarizing the numerical results of bidirectional flow. Here, ‘free’, ‘freezing’, and ‘co’ indicate the free flow phase, the freezing phase, and the coexisting phase, respectively.

At the same time, the attracted pedestrians formed a cluster in a semi-circular shape near the attraction. If Q and s were large, a freezing phase was observed. In the freezing phase, oppositely walking pedestrians reached a complete stop because they blocked each other, as shown in Figure 4.4(b).

One can identify the freezing phase by means of cumulative throughput at $x = 30$ m, according to Reference [20]. The cumulative throughput at time t is calculated by summing the number of passersby walking through $x = 30$ m from the beginning of the numerical simulation to time t . If the cumulative throughput does not change for 120 s, it infers the appearance of the freezing phenomenon. The freezing probability P_f was obtained by counting the occurrence of freezing phenomena over 50 independent simulation runs for each parameter combination (Q, s) . For small value of $Q \leq 1.4$ P/s, P_f is zero up to $s = 2$, indicating that the freez-

ing phenomenon is not observable. Parameter combinations of (Q, s) was categorized as the free flow phase if

$$P_f = 0, \quad (4.13)$$

yielding $E_a \approx 1$. The freezing phase was characterized by

$$P_f = 1 \quad (4.14)$$

always showing $E_a = 0$. In addition, one can define a coexisting phase for parameter space between envelopes of $P_f = 0$ and $P_f = 1$. In the coexisting phase, either free flow or freezing phenomena can be observed depending on random seeds in the numerical simulations. That was characterized by

$$0 < P_f < 1. \quad (4.15)$$

Figure 4.4(c) summarizes numerical results of bidirectional flow. In the coexisting phase, one can observe freezing phenomena with a certain probability.

4.3.3 Microscopic Understanding of Jamming Transitions

While previous subsections focused on describing collective patterns of various jam patterns, this subsection presents the appearance of such different patterns at the individual level in a unified way. The conflicts among pedestrians were closely looked into in order to understand the individual level behavior. Similar to previous studies [60, 85], a conflict index was employed to measure the average number of conflicts per passerby. When two pedestrians are in contact and hinder each other, this situation is called a conflict. The number of conflicts $N_{c,i}(t)$ was evaluated by counting the number of pedestrians who hinder the progress of passerby i at time t . In numerical simulations of Study III, most conflicts appeared near the attraction; therefore, one can calculate the conflict index for pedestrians in location x such that $25 \text{ m} \leq x \leq 35 \text{ m}$. The conflict index was measured as

$$n_c(t) = \frac{1}{|N_p(A, t)|} \sum_{i \in N_p(A, t)} N_{c,i}(t), \quad (4.16)$$

where $N_p(A, t)$ is the set of passersby in the section of $25 \text{ m} \leq x \leq 35 \text{ m}$ at time t and $|N_p(A, t)|$ is the cardinality of the set $N_p(A, t)$.

The representative time series of conflict index $n_c(t)$ is presented in Figure 4.5. As can be seen from Figure 4.5(a), a sharp increase of the conflict

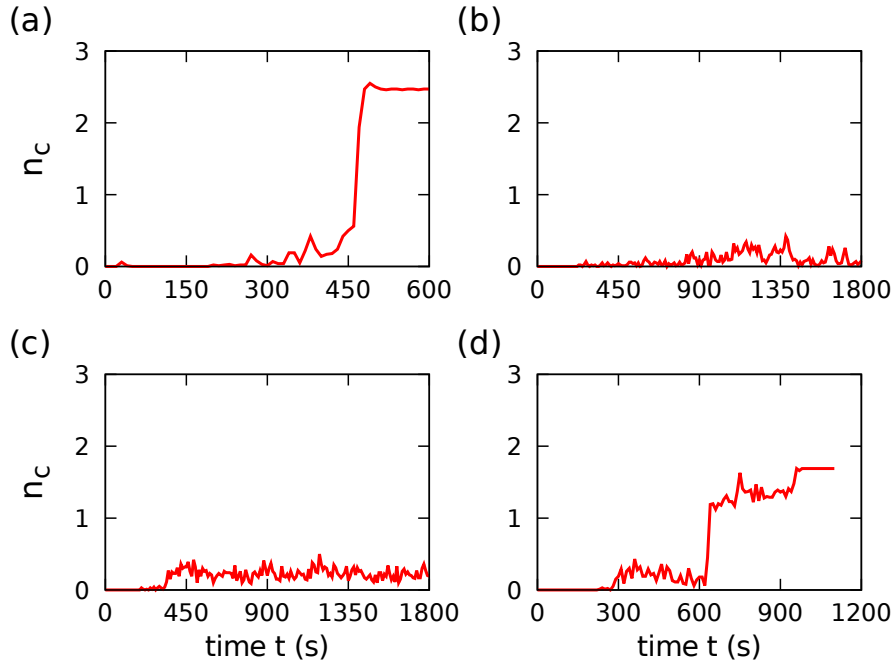


Figure 4.5. (Color online) Representative time series of conflict index $n_c(t)$ (a) freezing phase in bidirectional flow with $Q = 4$ P/s and $s = 1$. (b) localized jam phase in unidirectional flow with $Q = 5$ P/s and $s = 1$. (c) extended jam phase in unidirectional flow with $Q = 5$ P/s and $s = 1.8$. (d) same parameter combination (Q, s) as (c), but with a different set of random seeds.

index indicates the appearance of the freezing phenomenon, which leads the pedestrian flow into the freezing phase. In Figure 4.5(b), the conflict index increases and then decreases in the course of time. One can observe the localized jam phase in which the jam near the attraction does not further grow upstream. Figures 4.5(c) and 4.5(d) were generated with the same parameter combination $(Q, s) = (5, 1.8)$ in unidirectional flow but with different sets of random seeds. As shown in Figure 4.5(c), in the extended jam phase, the conflict index $n_c(t)$ is maintained near a certain level after reaching the stationary state, indicating the persistent jam in the corridor. In Figure 4.5(d), the behavior of $n_c(t)$ curve is similar to that of the extended jam phase in the beginning, but the curve abruptly increases at near $t = 600$ s. That is, the pedestrian flow eventually ends up in a freezing phenomenon in that conflicting pedestrians fail to coordinate their movements.

In both bidirectional and unidirectional flows, attracted pedestrians often trigger conflicts among pedestrians. When the attracted pedestrians are walking towards the attraction, sometimes they cross the paths of passersby and hinder their walking. Furthermore, such crossing behavior of attracted pedestrians makes others change their walking directions due to the interpersonal repulsion, possibly giving rise to conflicts among

the others. Once a couple of pedestrians hinder each other, they need some time and space to resolve the conflict by adjusting their walking directions. If there is not enough space for the pedestrian movement, the conflict situation cannot be resolved and it turns into a blockage in the pedestrian flow. Under higher pedestrian flux Q , conflicting pedestrians likely have less time for resolving the conflict while additional pedestrians arrive behind the blockage. Once the arriving pedestrians stand behind the blockage, the number of conflicts among pedestrians is rapidly increasing as indicated in Figures 4.5(a) and 4.5(d). In the case of the bidirectional flow, this freezing phenomenon is similar to the freezing-by-heating phenomenon [38]. However, note that the freezing phenomenon in the numerical simulations is caused by attracted pedestrians without noise terms in the equation of motion.

4.3.4 Attendee Cluster as a Dynamic Bottleneck

As presented in previous subsections, the attendee cluster is acting as a pedestrian bottleneck for passersby. This finding is consistent with the description suggested by Goffman [30]. The flow through the bottleneck can show transitions from the free flow state to the jamming state and may end in gridlock. In the bidirectional flow, the free flow phase can turn into the freezing phase if Q and s are large. Jamming transitions in the unidirectional flow are different from those of the bidirectional flow: from the free flow phase to the localized jam phase, and then to the extended jam phase. In addition, it is possible that the extended jam phase ends up in freezing phenomena for large Q and s . Although different jamming transitions were observed for uni- and bi-directional flow scenarios, an attendee cluster can be conceptualized as a dynamic bottleneck in the sense that its size changes over time according to the joining behavior of attracted pedestrians. One might assume that an attendee cluster can be approximated as a static bottleneck which is at a fixed location and whose size does not change over time. Readers can find representative studies on static bottlenecks from Hoogendoorn and Daamen [44] and Seyfried *et al.* [97]. However, the assumption of the static bottleneck cannot reflect the fluctuating attendee cluster size, which arises from the interactions among the attraction, attracted pedestrians, and passersby.

In order to understand the influence of the attendee cluster size on jamming transitions, numerical simulations were performed with a static bottleneck. In this case, all the pedestrians were modeled as passersby. In

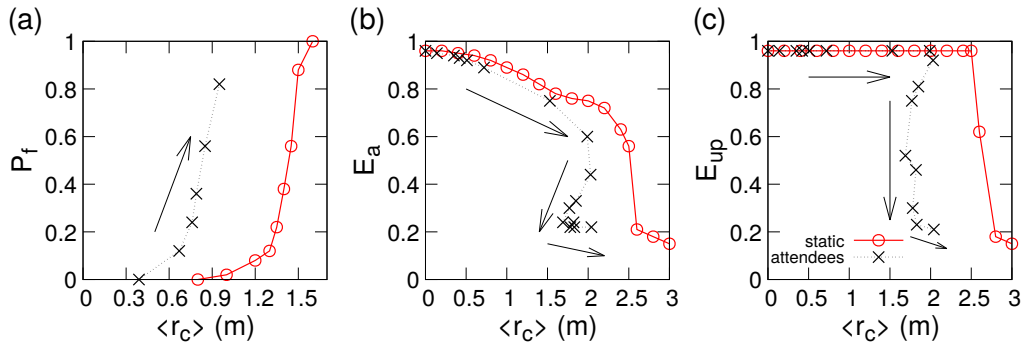


Figure 4.6. (Color online) Dependence of various measures on a stationary state average of cluster size $\langle r_c \rangle$ for pedestrian influx $Q = 5$ P/s. The results of a static bottleneck and an attendee cluster are denoted by \circ and \times , respectively. Arrows indicate the direction of increasing s , for the results of the attendee cluster. (a) Freezing probability P_f for bidirectional flow indicating the appearance of freezing phase (b) local efficiency near the attraction E_a for unidirectional flow reflecting the onset of localized jam phase, and (c) local efficiency upstream E_{up} for unidirectional flow, which is relevant to extended jam phase.

doing so, one can exclude the interactions among passersby and attendees, thereby focusing on the influence of reduced available space. For the comparison, a stationary state average of cluster size $\langle r_c \rangle$ was used because the attendee cluster size changes in the course of time but the size of the static bottleneck is constant. In the case of a static bottleneck, the notation of $\langle r_c \rangle$ was also used for convenience. A semicircle with radius $\langle r_c \rangle$ was placed at the center of the lower corridor boundary, acting as a static bottleneck. By changing $\langle r_c \rangle$, one can observe the behavior of various measures including P_f , E_a , and E_{up} (see Figure 4.6).

It was obvious that larger $\langle r_c \rangle$ led to higher freezing probability P_f for the bidirectional flow, as shown in Figure 4.6(a). However, P_f of the attendee cluster case was higher than that of the static bottleneck for a given value of $\langle r_c \rangle$. While E_a and E_{up} curves obtained from the static bottleneck case showed a clear dependence on $\langle r_c \rangle$, those from attendee cluster did not show clear tendency when $\langle r_c \rangle > 1.5$ m (see Figures 4.6(b) and 4.6(c)). Although increasing $\langle r_c \rangle$ evidently led to a localized jam transition, it can be suggested that conflicts among pedestrians play an important role in jamming transitions if $\langle r_c \rangle$ is large enough. It can, therefore, be said that the attendee cluster acts as a dynamic bottleneck that behaves qualitatively different than the static bottleneck in terms of jamming transitions.

5. Conclusions and Discussions

5.1 Summary

This dissertation aimed at studying collective dynamics of pedestrians interacting with attractions. The dissertation topic was investigated based on three research questions presented in Section 1.2:

(RQ1) how do collective patterns of pedestrian motions emerge from the attractive interactions between pedestrians and attractions?

(RQ2) how can social influence on one's choice behavior shape the collective patterns of pedestrians' visiting behavior?

(RQ3) how can pedestrian flow interacting with an attraction result in pedestrian jams?

In other words, **RQ1** mainly focused on the formation of attendees near attractions, and **RQ2** paid particular attention to collective visiting patterns when individual choice behavior is likely influenced by others. **RQ3** devoted to pedestrian jamming transitions induced by an attraction.

In order to address the research questions, microscopic pedestrian models were extended by incorporating the attractive interactions between pedestrians and attractions, and implemented in numerical simulations. After performing the numerical simulations, various collective patterns were identified and summarized in phase diagrams based on macroscopic measures. By doing so, this dissertation investigated the dynamics of pedestrian flow interacting with attractions from the perspective of attracted pedestrians and passersby.

In line with **RQ1**, Study I addressed collective effects of attractive interactions between pedestrians and attractions by means of numerical simulations. In order to do that, the attractive interactions were modeled [see Equation (3.5)] and appended to the social force model [see Equa-

tion (3.6)]. By means of numerical simulations, the attractive interactions were examined by controlling the attractive interaction strength and the pedestrian density. The interactions led pedestrians to form stable clusters around attractions, or even to rush into attractions if the interaction becomes stronger. In this case, the attracted pedestrians tended to push each other because of the interpersonal repulsion effect. It was also found that for high pedestrian density and intermediate interaction strength, some pedestrians rush into attractions while others move to neighboring attractions. The moving pedestrians were also attracted by the attractions but cannot stay around the attraction. This is due to the interpersonal repulsion effect by other pedestrians closer to the attractions. These collective patterns of pedestrian movements or phases and transitions between them were systematically presented in a phase diagram, see Figure 4.1(e).

With reference to **RQ2**, Study II investigated the social influence on collective visiting behavior by developing a joining probability model as shown in Equation (3.10). The joining probability was formulated as a function of social influence from others, reflecting that individual choice behavior is likely influenced by others. Numerical simulations produced different patterns of pedestrian behavior depending on the strength of the social influence and the average duration of visiting an attraction. When the social influence was strong along with a long duration of visiting an attraction, the saturated phase was defined at which all the pedestrians have visited the attraction. If the social influence was not strong enough, the unsaturated phase appeared where one can observe that some pedestrians head for the attraction while others walk in their desired direction. These collective patterns of pedestrian behavior were summarized in a phase diagram [see Figure 4.2(c)] by comparing the number of pedestrians who have visited the attraction to the number of pedestrians near the attraction. One can identify under what conditions enhancing the social influence strength and the average duration of visiting an attraction would be effective by measuring the marginal benefits with respect to those parameters.

Motivated by **RQ3**, Study III numerically studied jamming transitions in pedestrian flow interacting with an attraction, mostly based on the social force model for pedestrians who can join the attraction. Various pedestrian flow patterns were observed by controlling pedestrian influx and the social influence parameter. For bidirectional flow scenario, one

could observe a transition from the free flow phase to the freezing phase in which oppositely walking pedestrians reach a complete stop and block each other. On the other hand, a different transition behavior appeared in the unidirectional flow scenario, i.e., from the free flow phase to the localized jam phase, and then to the extended jam phase. It was also observed that the extended jam phase could end up in freezing phenomena with a certain probability when pedestrian flux was high with strong social influence. Study III highlighted that attractive interactions between pedestrians and an attraction could lead to jamming transitions due to the conflicts among pedestrians near the attraction.

5.2 Contributions

This dissertation contributes to the current body of knowledge on the collective behavior of pedestrian motions. This is achieved by modeling their dynamics interacting with attractions and providing possible explanations of the collective patterns. The contributions of this dissertation are further stated in three folds.

In Study I, the attractive force model was developed based on the idea of “short-range strong repulsive and long-range weak attractive interactions [22, 74].” While previous studies [22, 74] developed attractive interaction models for interacting self-propelled particles, Study I presented an attractive interaction model for pedestrians interacting with attractions. The presented model demonstrated that the social force models can be extended to predict various collective behaviors associated with attractions. The appearance of various collective patterns was explained by the interplay between attraction strength and interpersonal repulsion effect. Interestingly, despite its simple formulation, the presented model can provide a plausible explanation of extreme pedestrian behavior in stores, such as Black Friday incidents in the United States.

In Study II, the joining probability model was developed in line with selective attention [31, 108] and social influence [6, 14, 27, 53, 72]. Previous studies [27, 72] reported that the joining probability increases as the stimulus group size grows. The presented joining probability model in Study II was developed by incorporating with social influence parameter and duration of visiting an attraction that were not considered in the previous studies. The numerical simulation results showed different patterns of collective visiting behavior: unsaturated and saturated phases.

The appearance of the saturated phase was explained by an interplay between social influence strength and the average duration of visiting an attraction.

Study III characterized the dynamics of pedestrian jams induced by the attraction. By describing pedestrian conflicts at a microscopic level, it was highlighted that attractive interactions between pedestrians and an attraction could trigger jamming transitions by increasing the number of conflicts among pedestrians near the attraction. Therefore, it is suggested that existence of an attraction acts similar to a noise term in an equation of particle motions [38], which leads to freezing phenomena in the pedestrian flow. Furthermore, an attendee cluster near an attraction was conceptualized as a dynamic bottleneck and identified that a dynamic bottleneck behaves qualitatively different than the static bottleneck in terms of jamming transitions.

The findings presented in this dissertation can provide an insight into pedestrian flow patterns in stores and pedestrian facility management strategies. Numerical simulation results imply that safe and efficient use of pedestrian facilities can be achieved by moderating the control variables. For instance, findings from Study II suggest that increasing social influence strength s and the average duration of visiting an attraction t_d is not effective all the time, especially when these variables are already high enough. Increasing relative attraction strength C and pedestrian density ρ can even lead to extreme and dangerous situations such as the competitive phase in Study I. Likewise, increasing pedestrian influx Q and social influence strength s yields undesirable situations, like freezing phenomena in Study III, in terms of pedestrian safety and efficiency.

5.3 Limitations

Although the presented models were developed based on analogies with self-propelled particles [74, 105] and findings in behavioral science studies [27, 72], numerical simulation results were not compared against field observations yet. For the place where impulse stops are significant, the presented model in Study I can be tested and parameters in the attractive force model (i.e., C_a , C_r , l_a , and l_r) need to be measured from field observations. For the joining behavior model in Studies II and III, the average duration of visiting an attraction t_d can be measured for attendees near an attraction and then social influence parameter s can be predicted based

on the number of pedestrians having visited the attraction. The predicted value of s can be utilized to test various scenarios.

In this dissertation, simple scenarios of pedestrian flow in a straight corridor have been focused in order to study essential features of collective pedestrian dynamics interacting with attractions. Although a straight corridor can be assumed as a basic element of pedestrian facilities, some pedestrian flow scenarios such as crossings at intersections and multi-directional flows in open space cannot be covered by the presented results of the numerical simulations. Therefore, suitable modifications and extensions are required to apply the presented models to real world examples.

For simplicity, it was assumed that the pedestrians in numerical simulations did not change their decision after they decided what they were going to do. However, pedestrians in the real world can change their decision as a response to the situations around them. A pedestrian, who decides to join an attraction, can change one's mind after realizing that there are too many attendees near the attraction. Modeling and implementing such decision changing behavior can be an important extension of the presented models.

5.4 Future Work

The presented models can be further improved and extended. The attractive force model in Study I was developed in line with the social force model and predicted various collective patterns arising from the attractive interactions between pedestrians and attractions. However, the presented model appears to be valid only for the social force model. Although the social force model and other force-based models have well explained various collective patterns, it has been pointed out that the force-based models are complicated and a careful implementation is required in order to avoid the pitfalls [17, 63, 64]. Chraibi *et al.* [16] remarked that velocity-based models are gaining more attention among researchers because of their simplicity. Developing attractive interaction model for velocity-based models can be a topic for future work.

The collective phenomena predicted in Study I can be compared against field observations. In Study I, it was assumed that all the pedestrians were subject to the same attractive interactions. A future study might explore trajectory data of pedestrians fighting over merchandise during shopping holidays like Black Friday. In that case, pedestrians are likely

to behave in the same way near an attraction, similar to the setup of numerical simulations in Study I. However, one can easily observe that an attraction is not always attractive for everyone. For instance, in a museum, some visitors are watching a portrait because they are interested in it while others pass by it and see other artworks. Consequently, verification of Study I can be performed for pedestrians attracted by attractions, inferring that those pedestrians are subject to the same attractive interaction. Attracted pedestrian behavior near artworks in museums and shop displays in shopping malls can be studied based on observed trajectories and velocity field. Note that the presented model in Study I predicts pedestrian behavior under the influence of attractions for a short period, mainly focusing on momentary response to the attractions.

The joining behavior model in Study II can be formulated in different forms. The presented joining behavior model was developed based on the idea of behavioral contagion, inferring that an individual tends to follow what others do [27, 72]. Although the assumption of behavioral contagion has been widely applied especially in pedestrian evacuation studies [37], the assumption has been questioned. Haghani and Sarvi [32] reported that evacuees showed congestion avoidance behavior in emergency evacuations especially when evacuees were well aware of the situations near exits. That is, the behavioral contagion is not always useful for explaining pedestrian joining behavior. If there are too many attendees near an attraction, the attraction is not necessarily attractive for every pedestrian near the attraction. For some pedestrians, seeing too many attendees can decrease the probability of joining the attraction. In future studies, the congestion avoidance behavior can be incorporated in the joining behavior model. In addition, the joining behavior model can be extended in order to take into account various characteristics of pedestrians and attractions by adding additional behavioral features, such as the explicit representation of group behaviors [114] and interest function [58]. One can postulate that pedestrians have time budget, so they evaluate the attractiveness and the cost of time due to joining the attractions. Heterogeneous properties of pedestrian joining behavior can be considered in terms of the congestion avoidance behavior, group behaviors, interest functions, and the cost of time.

In future studies, the presented joining behavior model can be verified against empirical observations. It was assumed that the joining probability grew as the number of attendees increased and the pedestrians de-

cided to join the attraction 10 m ahead of it. In order to obtain naturalistic movement of pedestrians near attractions, it is desirable to obtain video recordings of public areas like shopping malls. Pedestrian trajectories need to be extracted from the video recordings. The extracted trajectories can be used for estimating the distance between pedestrians and attractions, and for identifying decision moments at which pedestrians suddenly change their walking direction. Based on the decision moments, one can understand when and where pedestrians decide to join the attraction. From the video recordings, the number of attendees near attractions and passersby can be counted and the joining probability can be measured for different attendee size at various places and time. One can discover the relationship between the joining probability and the number of attendees near the attractions. If the joining probability increases as the number of attendees grows, one can say that the assumption of behavioral contagion is observable. On the other hand, if a decreasing trend of joining probability against the number of attendees is observed, the congestion avoidance behavior might exist. In addition, the duration of visiting an attraction was assumed to follow an exponential distribution. The duration of visiting each attraction can be measured for each attendee, so its distribution can be identified. The evacuation exit choice models [32, 107] can be extended and modified for verifying assumptions of the presented joining probability model.

A natural progression of Study III is to analyze the numerical simulation results from the perspective of capacity estimation. Capacity estimation can focus on the optimal capacity, balancing the mobility needs for passersby and the activity needs for attracted pedestrians. One can explicitly consider the capacity of the attractions, meaning that only a certain number of attendees can stay near the attractions. The concept of stochastic capacity [28, 56, 73] can also be studied based on the findings of Study III. In Study III, for some parameter values, speed breakdown is observed depending on random seeds, inferring that capacity might follow a probability distribution.

Future extensions of Study III can be planned from the perspective of pedestrian flow experiments. Although the joining behavior presented in this study might not be controlled in experimental studies, the experiments can be performed for different levels of pedestrian flux and joining probability. The number of passersby and pedestrians joining the attraction, and their trajectories with velocity vectors need to be collected from

future pedestrian experiments. For various experiment configurations, the number of conflicts among pedestrians can be measured and the influence of the conflicts on pedestrian jams can be analyzed.

In this dissertation, the parameter values used in numerical simulations were in a limited range. Although the selected parameter values produced interesting collective phenomena, performing additional numerical simulations with a larger set of their values might yield more findings that are interesting. It is noted that the shape of phase diagrams presented in the dissertation can be changed for different parameter values and numerical simulation settings such as corridor width and the number of attractions. Changing numerical simulation parameters might show the appearance of different collective patterns of pedestrian motions.

References

- [1] J. D. Anderson. *Fundamentals of aerodynamics*. McGraw-Hill Education, New York, NY, 5th edition, 2010.
- [2] M. Asano, T. Iryo, and M. Kuwahara. Microscopic pedestrian simulation model combined with a tactical model for route choice behaviour. *Transportation Research Part C: Emerging Technologies*, 18:842–855, 2010.
- [3] G. Baglietto and D. R. Parisi. Continuous-space automaton model for pedestrian dynamics. *Physical Review E*, 83:056117+, 2011.
- [4] P. Ball. *Critical mass: How one thing leads to another*. Farrar, Straus and Giroux, New York, NY, 2006.
- [5] G. K. Batchelor. *An introduction to fluid dynamics*. Cambridge University Press, Cambridge, UK, 2000.
- [6] W. O. Bearden, R. G. Netemeyer, and J. E. Teel. Measurement of consumer susceptibility to interpersonal influence. *Journal of Consumer Research*, 15:473–481, 1989.
- [7] N. Bellomo and C. Dogbe. On the modeling of traffic and crowds: A survey of models, speculations, and perspectives. *SIAM Review*, 53:409–463, 2011.
- [8] V. Blue and J. Adler. Emergent fundamental pedestrian flows from cellular automata microsimulation. *Transportation Research Record: Journal of the Transportation Research Board*, pages 29–36, 1998.
- [9] V. Blue and J. Adler. Cellular automata microsimulation of bidirectional pedestrian flows. *Transportation Research Record: Journal of the Transportation Research Board*, 1678:135–141, 1999.

- [10] V. J. Blue and J. L. Adler. Cellular automata microsimulation for modeling bi-directional pedestrian walkways. *Transportation Research Part B: Methodological*, 35:293–312, 2001.
- [11] A. Borgers and H. Timmermans. A model of pedestrian route choice and demand for retail facilities within inner-city shopping areas. *Geographical Analysis*, 18:115–128, 1986.
- [12] C. Burstedde, K. Klauck, A. Schadschneider, and J. Zittartz. Simulation of pedestrian dynamics using a two-dimensional cellular automaton. *Physica A: Statistical Mechanics and its Applications*, 295:507–525, 2001.
- [13] C. Cercignani. *Ludwig Boltzmann: The man who trusted atoms*. Oxford University Press, New York, NY, 1998.
- [14] T. L. Childers and A. R. Rao. The influence of familial and peer-based reference groups on consumer decisions. *Journal of Consumer Research*, 19:198–211, 1992.
- [15] D. Chowdhury, L. Santen, and A. Schadschneider. Statistical physics of vehicular traffic and some related systems. *Physics Reports*, 329:199–329, 2000.
- [16] M. Chraïbi, T. Ezaki, A. Tordeux, K. Nishinari, A. Schadschneider, and A. Seyfried. Jamming transitions in force-based models for pedestrian dynamics. *Physical Review E*, 92:042809+, 2015.
- [17] M. Chraïbi, A. Seyfried, and A. Schadschneider. Generalized centrifugal force model for pedestrian dynamics. *Physical Review E*, 82:046111+, 2010.
- [18] A. Corbetta. *Multiscale crowd dynamics: physical analysis, modeling and applications*. PhD thesis, Eindhoven University of Technology, 2016.
- [19] I. D. Couzin and N. R. Franks. Self-organized lane formation and optimized traffic flow in army ants. *Proceedings of the Royal Society of London B: Biological Sciences*, 270:139–146, 2002.
- [20] C. F. Daganzo. *Fundamentals of transportation and traffic operations*. Pergamon, Oxford, UK, 1997.
- [21] F. Dietrich and G. Köster. Gradient navigation model for pedestrian dynamics. *Physical Review E*, 89:062801+, 2014.

- [22] M. R. D’Orsogna, Y. L. Chuang, A. L. Bertozzi, and L. S. Chayes. Self-propelled particles with soft-core interactions: Patterns, stability, and collapse. *Physical Review Letters*, 96:104302+, 2006.
- [23] D. C. Duives, W. Daamen, and S. P. Hoogendoorn. State-of-the-art crowd motion simulation models. *Transportation Research Part C: Emerging Technologies*, 37:193–209, 2013.
- [24] J. Duran. *Sands, powders, and grains: an introduction to the physics of granular materials*. Springer, New York, NY, 1999.
- [25] T. Ezaki, D. Yanagisawa, and K. Nishinari. Pedestrian flow through multiple bottlenecks. *Physical Review E*, 86:026118+, 2012.
- [26] C. Feliciani and K. Nishinari. Empirical analysis of the lane formation process in bidirectional pedestrian flow. *Physical Review E*, 94:032304+, 2016.
- [27] A. C. Gallup, J. J. Hale, D. J. T. Sumpter, S. Garnier, A. Kacelnik, J. R. Krebs, and I. D. Couzin. Visual attention and the acquisition of information in human crowds. *Proceedings of the National Academy of Sciences*, 109:7245–7250, 2012.
- [28] J. Geistefeldt and W. Brilon. A comparative assessment of stochastic capacity estimation methods. In *Transportation and Traffic Theory 2009*, New York. Springer.
- [29] P. G. Gipps and B. Marksjö. A micro-simulation model for pedestrian flows. *Mathematics and Computers in Simulation*, 27:95–105, 1985.
- [30] E. Goffman. *Relations in public: Microstudies of the public order*. Basic Books, New York, 1971.
- [31] E. B. Goldstein. *Sensation and perception*. Thomson Wadsworth, 7th edition, 2007.
- [32] M. Haghani and M. Sarvi. Following the crowd or avoiding it? Empirical investigation of imitative behaviour in emergency escape of human crowds. *Animal Behaviour*, 124:47–56, 2017.
- [33] M. Haghani and M. Sarvi. Social dynamics in emergency evacuations: Disentangling crowd’s attraction and repulsion effects. *Physica A: Statistical Mechanics and its Applications*, 475:24–34, 2017.

- [34] D. Hartmann. Adaptive pedestrian dynamics based on geodesics. *New Journal of Physics*, 12:043032+, 2010.
- [35] D. Helbing. Traffic and related self-driven many-particle systems. *Reviews of Modern Physics*, 73:1067–1141, 2001.
- [36] D. Helbing, L. Buzna, A. Johansson, and T. Werner. Self-organized pedestrian crowd dynamics: Experiments, simulations, and design solutions. *Transportation Science*, 39:1–24, 2005.
- [37] D. Helbing, I. Farkas, and T. Vicsek. Simulating dynamical features of escape panic. *Nature*, 407:487–490, 2000.
- [38] D. Helbing, I. J. Farkas, and T. Vicsek. Freezing by heating in a driven mesoscopic system. *Physical Review Letters*, 84:1240–1243, 2000.
- [39] D. Helbing, A. Hennecke, and M. Treiber. Phase diagram of traffic states in the presence of inhomogeneities. *Physical Review Letters*, 82:4360–4363, 1999.
- [40] D. Helbing, A. Johansson, and H. Z. Al-Abideen. Dynamics of crowd disasters: An empirical study. *Physical Review E*, 75:046109+, 2007.
- [41] D. Helbing, J. Keltsch, and P. Molnar. Modelling the evolution of human trail systems. *Nature*, 388:47–50, 1997.
- [42] D. Helbing and P. Molnár. Social force model for pedestrian dynamics. *Physical Review E*, 51:4282–4286, 1995.
- [43] D. Helbing, F. Schweitzer, J. Keltsch, and P. Molnár. Active walker model for the formation of human and animal trail systems. *Physical Review E*, 56:2527–2539, 1997.
- [44] S. P. Hoogendoorn and W. Daamen. Pedestrian behavior at bottlenecks. *Transportation Science*, 39:147–159, 2005.
- [45] S. P. Hoogendoorn, F. L. M. van Wageningen-Kessels, W. Daamen, and D. C. Duives. Continuum modelling of pedestrian flows: From microscopic principles to self-organised macroscopic phenomena. *Physica A*, 416:684–694, 2014.
- [46] S. P. Hoogendoorn, F. L. M. van Wageningen-Kessels, W. Daamen, D. C. Duives, and M. Sarvi. Continuum theory for pedestrian traffic

- flow: Local route choicemodelling and its implications. *Transportation Research Part C: Emerging Technologies*, 59:183–397, 2015.
- [47] L. Huang, S. C. Wong, M. Zhang, C. W. Shu, and W. H. Lam. Revisiting Hughes’ dynamic continuum model for pedestrian flow and the development of an efficient solution algorithm. *Transportation Research Part B: Methodological*, 43:127–141, 2009.
- [48] R. Hughes. A continuum theory for the flow of pedestrians. *Transportation Research Part B: Methodological*, 36:507–535, 2002.
- [49] S. K. Hui, J. J. Inman, Y. Huang, and J. A. Suher. The effect of in-store travel distance on unplanned spending: Applications to mobile promotion strategies. *Journal of Marketing Research*, 77:1–16, 2013.
- [50] W. K. Jeong and R. T. Whitaker. A fast iterative method for eikonal equations. *SIAM Journal on Scientific Computing*, 30:2512–2534, 2008.
- [51] A. Johansson, D. Helbing, and P. Shukla. Specification of the social force pedestrian model by evolutionary adjustment to video tracking data. *Advances in Complex Systems*, 10:271–288, 2007.
- [52] A. John, A. Schadschneider, D. Chowdhury, and K. Nishinari. Trafficlike collective movement of ants on trails: Absence of a jammed phase. *Physical Review Letters*, 102:108001+, 2009.
- [53] V. D. Kaltcheva and B. A. Weitz. When should a retailer create an exciting store environment? *Journal of Marketing*, 70:107–118, 2006.
- [54] I. Karamouzas, B. Skinner, and S. J. Guy. Universal power law governing pedestrian interactions. *Physical Review Letters*, 113:238701+, 2014.
- [55] B. S. Kerner. *The physics of traffic: empirical freeway pattern features, engineering applications, and theory*. Springer, 2004.
- [56] B. S. Kerner, S. L. Klenov, and M. Schreckenberg. Probabilistic physical characteristics of phase transitions at highway bottlenecks: incommensurability of three-phase and two-phase traffic-flow theories. *Physical Review E*, 89:052807+, 2014.

- [57] B. S. Kerner and H. Rehborn. Experimental properties of phase transitions in traffic flow. *Physical Review Letters*, 79:4030+, 1997.
- [58] P. M. Kielar and A. Borrmann. Modeling pedestrians' interest in locations: A concept to improve simulations of pedestrian destination choice. *Simulation Modelling Practice and Theory*, 61:47–62, 2016.
- [59] M. Kinaterer, E. Ronchi, D. Gromer, M. Müller, M. Jost, M. Nehfischer, A. Mühlberger, and P. Pauli. Social influence on route choice in a virtual reality tunnel fire. *Transportation research part F: traffic psychology and behaviour*, 26:116–125, 2014.
- [60] A. Kirchner, K. Nishinari, and A. Schadschneider. Friction effects and clogging in a cellular automaton model for pedestrian dynamics. *Physical Review E*, 67:056122+, 2003.
- [61] A. Kirchner and A. Schadschneider. Simulation of evacuation processes using a bionics-inspired cellular automaton model for pedestrian dynamics. *Physica A: Statistical Mechanics and its Applications*, 312:260–276, 2002.
- [62] A. Kneidl, D. Hartmann, and A. Borrmann. A hybrid multi-scale approach for simulation of pedestrian dynamics. *Transportation Research Part C: Emerging Technologies*, 37:223–237, 2013.
- [63] G. Köster, F. Tremml, and M. Gödel. Avoiding numerical pitfalls in social force models. *Physical Review E*, 87:063305+, 2013.
- [64] T. Kretz. On oscillations in the Social Force Model. *Physica A: Statistical Mechanics and its Applications*, 438:272–285, 2015.
- [65] T. Kretz, A. Grünebohm, M. Kaufman, F. Mazur, and M. Schreckenberg. Experimental study of pedestrian counterflow in a corridor. *Journal of Statistical Mechanics: Theory and Experiment*, 2006:P10001+, 2006.
- [66] J. Kwak, H. H. Jo, T. Luttinen, and I. Kosonen. Collective dynamics of pedestrians interacting with attractions. *Physical Review E*, 88:062810+, 2013.
- [67] J. Kwak, H. H. Jo, T. Luttinen, and I. Kosonen. Effects of switching behavior for the attraction on pedestrian dynamics. *PLOS ONE*, 10:e0133668+, 2015.

- [68] M. J. Lighthill and G. B. Whitham. On kinetic wave II: a theory of traffic flow on crowded roads. *Proceedings of the Royal Society of London A: Mathematical, Physical and Engineering Sciences*, 229:317–345, 1955.
- [69] T. Luttinen. Properties of Cowan’s M3 headway distribution. *Transportation Research Record: Journal of the Transportation Research Board*, 1678:189–196, 1999.
- [70] J. Ma, W. G. Song, S. M. Lo, and Z. M. Fang. New insights into turbulent pedestrian movement pattern in crowd-quakes. *Journal of Statistical Mechanics: Theory and Experiment*, 2013:P02028+, 2013.
- [71] A. D. May. *Traffic flow fundamentals*. Prentice Hall, Englewood Cliffs, NJ, 1990.
- [72] S. Milgram, L. Bickman, and L. Berkowitz. Note on the drawing power of crowds of different size. *Journal of Personality and Social Psychology*, 13:79–82, 1969.
- [73] M. Minderhoud, H. Botma, and P. Bovy. Assessment of roadway capacity estimation methods. *Transportation Research Record: Journal of the Transportation Research Board*, 1572:59–67, 1997.
- [74] A. Mogilner, L. Edelstein-Keshet, L. Bent, and A. Spiros. Mutual interactions, potentials, and individual distance in a social aggregation. *Journal of Mathematical Biology*, 47:353–389, 2003.
- [75] M. Moussaïd, E. G. Guilloit, M. Moreau, J. Fehrenbach, O. Chabiron, S. Lemerrier, J. Pettré, C. Appert-Rolland, P. Degond, and G. Theraulaz. Traffic instabilities in self-organized pedestrian crowds. *PLOS Computational Biology*, 8:e1002442+, 2012.
- [76] M. Moussaïd, D. Helbing, and G. Theraulaz. How simple rules determine pedestrian behavior and crowd disasters. *Proceedings of the National Academy of Sciences*, 108:6884–6888, 2011.
- [77] M. Moussaïd, N. Perozo, S. Garnier, D. Helbing, and G. Theraulaz. The walking behaviour of pedestrian social groups and its impact on crowd dynamics. *PLOS ONE*, 5:e10047+, 2010.

- [78] B. R. Munson, T. H. Okiishi, W. W. Huebsch, and A. P. Rothmayer. *Fundamentals of fluid mechanics*. John Wiley & Sons, Hoboken, NJ, 7th edition, 2013.
- [79] R. Nagai, T. Nagatani, and A. Yamada. Phase diagram in multi-phase traffic model. *Physica A: Statistical Mechanics and its Applications*, 355:530–550, 2005.
- [80] T. Nagatani. The physics of traffic jams. *Reports on Progress in Physics*, 65:1331–1386, 2002.
- [81] K. Nagel. Particle hopping models and traffic flow theory. *Physical Review E*, 53:4655–4672, 1996.
- [82] K. Nagel and M. Schreckenberg. A cellular automaton model for freeway traffic. *Journal de Physique I*, 2:2221–2229, 1992.
- [83] M. E. J. Newman. The structure and function of complex networks. *SIAM review*, 45:167–256, 2003.
- [84] S. Nicolis, J. Fernández, C. Pérez-Penichet, C. Noda, F. Tejera, O. Ramos, D. J. T. Sumpter, and E. Altshuler. Foraging at the edge of chaos: Internal clock versus external forcing. *Physical Review Letters*, 110:268104+, 2013.
- [85] S. Nowak and A. Schadschneider. Quantitative analysis of pedestrian counterflow in a cellular automaton model. *Physical Review E*, 85:066128+, 2012.
- [86] S. Okazaki. A study of pedestrian movement in architectural space. Part 1: pedestrian movement by the application of magnetic models. *Transactions of Architectural Institute of Japan*, 283:111–119, 1979.
- [87] C. L. N. Oliveira, A. P. Vieira, D. Helbing, J. S. Andrade, and H. J. Herrmann. Keep-left behavior induced by asymmetrically profiled walls. *Physical Review X*, 6:011003+, 2016.
- [88] E. Papadimitriou, G. Yannis, and J. Golias. A critical assessment of pedestrian behaviour models. *Transportation research part F: traffic psychology and behaviour*, 12:242–255, 2009.
- [89] D. R. Parisi, M. Gilman, and H. Moldovan. A modification of the Social Force Model can reproduce experimental data of pedestrian flows in normal conditions. *Physica A: Statistical Mechanics and its Applications*, 388:3600–3608, 2009.

- [90] D. D. S. Price. A general theory of bibliometric and other cumulative advantage processes. *Journal of the American Society for Information Science*, 27:292–306, 1976.
- [91] P. I. Richards. Shock waves on the highway. *Operations Research*, 4:42–51, 1956.
- [92] C. Ruhla. *The physics of chance: from Blaise Pascal to Niels Bohr*. Oxford University Press, New York, NY, 1992.
- [93] M. Schönhof and D. Helbing. Empirical features of congested traffic states and their implications for traffic modeling. *Transportation Science*, 41:135–166, 2007.
- [94] D. V. Schroeder. *An introduction to thermal physics*. Addison-Wesley, San Francisco, CA, 2000.
- [95] J. A. Sethian. Fast marching methods. *SIAM review*, 41:199–235, 1999.
- [96] J. Sethna. *Statistical mechanics : entropy, order parameters, and complexity*. Oxford University Press, New York, NY, 2006.
- [97] A. Seyfried, O. Passon, B. Steffen, M. Boltes, T. Rupprecht, and W. Klingsch. New insights into pedestrian flow through bottlenecks. *Transportation Science*, 43:395–406, 2009.
- [98] J. L. Silverberg, M. Bierbaum, J. P. Sethna, and I. Cohen. Collective motion of humans in mosh and circle pits at heavy metal concerts. *Physical Review Letters*, 110:228701+, 2013.
- [99] D. J. T. Sumpter. *Collective animal behavior*. Princeton University Press, Princeton, NJ, 2010.
- [100] K. Suzuno, A. Tomoeda, and D. Ueyama. Analytical investigation of the faster-is-slower effect with a simplified phenomenological model. *Physical Review E*, 88:052813+, 2013.
- [101] A. Templeton, J. Drury, and A. Philippides. From mindless masses to small groups: Conceptualizing collective behavior in crowd modeling. *Review of General Psychology*, 19:215–229, 2015.
- [102] H. Timmermans, X. van der Hagen, and A. Borgers. Transportation systems, retail environments and pedestrian trip chaining behaviour: Modelling issues and applications. *Transportation Research Part B: Methodological*, 26:45–59, 1992.

- [103] K. To, P. Y. Lai, and H. K. Pak. Jamming of granular flow in a two-dimensional hopper. *Physical Review Letters*, 86:71–74, 2001.
- [104] M. Treiber, A. Kesting, and D. Helbing. Three-phase traffic theory and two-phase models with a fundamental diagram in the light of empirical stylized facts. *Transportation Research Part B: Methodological*, 44:983–1000, 2010.
- [105] T. Vicsek, A. Czirók, E. Ben-Jacob, I. Cohen, and O. Shochet. Novel type of phase transition in a system of self-driven particles. *Physical Review Letters*, 75:1226–1229, 1995.
- [106] P. Wagner and K. Nagel. Comparing traffic flow models with different number of “phases”. *European Physical Journal B*, 63(3):315–320, 2008.
- [107] A. K. Wagoum, A. Tordeux, and W. Liao. Understanding human queuing behaviour at exits: An empirical study. *Royal Society Open Science*, 4:160896+, 2017.
- [108] C. D. Wickens and J. G. Hollands. *Engineering psychology and human performance*. Prentice Hall, third edition, 1999.
- [109] S. Xu and H. B. L. Duh. A simulation of bonding effects and their impacts on pedestrian dynamics. *IEEE Transactions on Intelligent Transportation Systems*, 11:153–161, 2010.
- [110] W. Yu and A. Johansson. Modeling crowd turbulence by many-particle simulations. *Physical Review E*, 76:046105+, 2007.
- [111] W. J. Yu, R. Chen, L. Y. Dong, and S. Q. Dai. Centrifugal force model for pedestrian dynamics. *Physical Review E*, 72:026112+, 2005.
- [112] F. Zanlungo, T. Ikeda, and T. Kanda. Social force model with explicit collision prediction. *Europhysics Letters*, 93:68005+, 2011.
- [113] F. Zanlungo, T. Ikeda, and T. Kanda. A microscopic “social norm” model to obtain realistic macroscopic velocity and density pedestrian distributions. *PLOS ONE*, 7:e50720+, 2012.
- [114] F. Zanlungo, T. Ikeda, and T. Kanda. Potential for the dynamics of pedestrians in a socially interacting group. *Physical Review E*, 89:012811+, 2014.

- [115] J. Zhang, W. Klingsch, A. Schadschneider, and A. Seyfried. Ordering in bidirectional pedestrian flows and its influence on the fundamental diagram. *Journal of Statistical Mechanics: Theory and Experiment*, 2012:P02002+, 2012.
- [116] Y. T. Zhang, H. K. Zhao, and J. Qian. High order fast sweeping methods for static Hamilton–Jacobi equations. *Journal of Scientific Computing*, 29:25–56, 2006.
- [117] H. Zhao. A fast sweeping method for eikonal equations. *Mathematics of Computation*, 74:603–627, 2005.
- [118] I. Zuriguel, A. Janda, A. Garcimartín, C. Lozano, R. Arévalo, and D. Maza. Silo clogging reduction by the presence of an obstacle. *Physical Review Letters*, 107:278001+, 2011.

Publication I

Kwak, J., Jo, H-H., Luttimen, T., and Kosonen, I. Collective dynamics of pedestrians interacting with attractions. *Physical Review E*, Volume 88, 6, 062810, December 2013.

© 2013 American Physical Society.

Reprinted with permission.

Collective dynamics of pedestrians interacting with attractions

Jaeyoung Kwak,^{1,*} Hang-Hyun Jo,² Tapio Luttinen,¹ and Iisakki Kosonen¹

¹*Department of Civil and Environmental Engineering,*

Aalto University School of Engineering, P.O. Box 12100, FI-00076, Finland

²*BECS, Aalto University School of Science, P.O. Box 12200, FI-00076, Finland*

(Dated: December 10, 2013)

In order to investigate collective effects of interactions between pedestrians and attractions, this study extends the social force model. Such interactions lead pedestrians to form stable clusters around attractions, or even to rush into attractions if the interaction becomes stronger. It is also found that for high pedestrian density and intermediate interaction strength, some pedestrians rush into attractions while others move to neighboring attractions. These collective patterns of pedestrian movements or phases and transitions between them are systematically presented in a phase diagram. The results suggest that safe and efficient use of pedestrian areas can be achieved by moderating the pedestrian density and the strength of attractive interaction, for example, in order to avoid situations involving extreme desire for limited resources.

PACS numbers: 89.40.-a, 89.65.-s, 05.65.+b

I. INTRODUCTION

Collective patterns of pedestrian movements have received increasing attention from various fields including physics [1], transportation engineering [2], and marketing [3]. In an attempt to understand mechanisms underlying collective patterns, different microscopic pedestrian behavior models have been proposed, such as cellular automata (CA) [4,5], social force models [68], and centrifugal force models [9,10]. Among these models, the social force model has produced promising results in that the model embodies behavioral elements and physical forces. The original model and its variants have successfully demonstrated various interesting phenomena such as lane formation [6], bottleneck oscillation [6], and turbulent movement [11]. Such self-organized patterns could be understood to some extent by considering mainly repulsive interactions among pedestrians.

Collective patterns of pedestrian movements have received increasing attention from various fields including physics [1], transportation engineering [2], and marketing [3]. In an attempt to understand mechanisms underlying collective patterns, different microscopic pedestrian behavior models have been proposed, such as cellular automata (CA) [4, 5], social force models [6–8], and centrifugal force models [9, 10]. Among these models, the social force model has produced promising results in that the model embodies behavioral elements and physical forces. The original model and its variants have successfully demonstrated various interesting phenomena such as lane formation [6], bottleneck oscillation [6], and turbulent movement [11]. Such self-organized patterns could be understood to some extent by considering mainly repulsive interactions among pedestrians.

In addition to the repulsive interactions, the effect of attractive interactions also has been investigated, which

was first introduced by Helbing and Molnár [6]. For example, Xu and Duh [12] simulated bonding effects of pedestrian groups and evaluated their impacts on pedestrian flows. In another study, Moussaïd *et al.* [13] analyzed attractive interactions among pedestrian group members and their spatial patterns.

Although several studies focused on attractive interactions among pedestrians, little attention has been paid to the attractive interactions between pedestrians and attractions. While walking to the destinations, pedestrians can be influenced by unexpected attractions such as window displays and street performances. If the attractive force between pedestrians and attractions is strong enough, pedestrians may stop walking to destinations and join attractions, namely impulse stops [14, 15]. For instance, museum managers have concerned with stop patterns of visitors because impulse stops in museums initiate contacts between visitors and museum displays [16]. Thus, architects have proposed various museum layouts in order to motivate visitors to have contact with more museum displays [17]. In the marketing area, since impulse stops in stores may result in unplanned purchases, marketing strategies have focused on exposing consumers to more merchandise and encouraging them to stop to buy [18]. Understanding such impulse stops can support effective design and management of pedestrian facilities.

In order to examine the collective effects of attractive interactions between pedestrians and attractions, this study extends the social force model by incorporating the attractive interactions. The extended social force model reproduces various collective patterns of pedestrian movements or phases, depending on the strength of attractive interaction and the pedestrian density. These phases are systematically presented in a phase diagram.

This paper is organized as follows. The extended social force model is described in Sec. II, and its numerical simulation results are presented in terms of a phase diagram in Sec. III. Finally, Sec. IV summarizes the results with concluding remarks.

* jaeyoung.kwak@aalto.fi

II. MODEL

The social force model [6] describes the pedestrian movements in terms of the superposition of driving, repulsive, and attractive force terms, analogously to self-propelled particle models [19–22]. Each pedestrian i is modeled as a circle with radius r_i in a two-dimensional space. The position and velocity of each pedestrian i at time t , denoted by $\vec{x}_i(t)$ and $\vec{v}_i(t)$, evolve according to the following equations:

$$\frac{d\vec{x}_i(t)}{dt} = \vec{v}_i(t) \quad (1)$$

and

$$\frac{d\vec{v}_i(t)}{dt} = \vec{f}_{i,d} + \sum_{j \neq i} \vec{f}_{ij} + \sum_B \vec{f}_{iB} + \sum_A \vec{f}_{iA}. \quad (2)$$

Here the driving force $\vec{f}_{i,d}$ describes the pedestrian i accelerating to reach its destination. The repulsive force between pedestrians i and j , \vec{f}_{ij} , denotes the tendency of pedestrians to keep a certain distance from each other. The repulsive force from boundaries \vec{f}_{iB} shows the interaction between pedestrians and boundaries, e.g., wall and obstacles. The attractive force \vec{f}_{iA} indicates pedestrian movements toward attractive stimuli, e.g., window displays and museum exhibits.

The driving force $\vec{f}_{i,d}$ is given as

$$\vec{f}_{i,d} = \frac{v_d \vec{e}_i - \vec{v}_i(t)}{\tau}, \quad (3)$$

where v_d is the desired speed and \vec{e}_i is a unit vector for the desired direction, independent of the position of the pedestrian i . The relaxation time τ controls how fast the pedestrian i adapts its velocity to the desired velocity. The repulsive force between pedestrians i and j , denoted by \vec{f}_{ij} , is the sum of the gradient of repulsive potential with respect to $\vec{d}_{ij} \equiv \vec{x}_j - \vec{x}_i$, and the friction force, \vec{g}_{ij} :

$$\vec{f}_{ij} = -\nabla_{\vec{d}_{ij}} V(b_{ij}) + \vec{g}_{ij}. \quad (4)$$

The repulsive potential is given as

$$V(b_{ij}) = C_p l_p \exp\left(-\frac{b_{ij}}{l_p}\right) \quad (5)$$

$$b_{ij} = \frac{1}{2} \sqrt{(\|\vec{d}_{ij}\| + \|\vec{d}_{ij} - \vec{y}_{ij}\|)^2 - \|\vec{y}_{ij}\|^2}, \quad (6)$$

where C_p and l_p denote the strength and the range of repulsive interaction between pedestrians. b_{ij} denotes the effective distance between pedestrians i and j by considering their relative displacement $\vec{y}_{ij} \equiv (\vec{v}_j - \vec{v}_i)\Delta t$ with the stride time Δt [23]. The interpersonal friction \vec{g}_{ij} becomes effective when the distance $d_{ij} = \|\vec{d}_{ij}\|$ is smaller than the sum $r_{ij} = r_i + r_j$ of their radii r_i and r_j :

$$\vec{g}_{ij} = h(r_{ij} - d_{ij}) \{k_n \vec{e}_{ij} + k_t [(\vec{v}_j - \vec{v}_i) \cdot \vec{t}_{ij}] \vec{t}_{ij}\}, \quad (7)$$

where k_n and k_t are the normal and tangential elastic constants. \vec{e}_{ij} is a unit vector pointing from pedestrian j to i and \vec{t}_{ij} is a unit vector perpendicular to \vec{e}_{ij} . The function $h(x)$ yields x if $x > 0$, while it gives 0 if $x \leq 0$. The repulsive force from boundaries is

$$\vec{f}_{iB} = C_b \exp\left(-\frac{d_{iB}}{l_b}\right) \vec{e}_{iB}, \quad (8)$$

where d_{iB} is the perpendicular distance between pedestrian i and wall, and \vec{e}_{iB} is the unit vector pointing from the wall B to the pedestrian i . C_b and l_b denote the strength and the range of repulsive interaction from boundaries.

The attractive force toward attractions is modeled similarly to the interaction between pedestrians and the wall, but in terms of both attractive and repulsive interactions. The repulsive effect of attractions is necessary so that pedestrians can keep certain distance from attractions. The strength and range of attractive force are modeled as [20, 21]

$$\vec{f}_{iA} = \left[C_r \exp\left(\frac{r_i - d_{iA}}{l_r}\right) - C_a \exp\left(\frac{r_i - d_{iA}}{l_a}\right) \right] \vec{e}_{iA} \quad (9)$$

Here C_a and l_a denote the strength and the range of attractive interaction toward attractions, respectively. Similarly, C_r and l_r denote the strength and the range of repulsive interaction from attractions. d_{iA} is the distance between pedestrian i and attraction A . \vec{e}_{iA} is the unit vector pointing from attraction A to pedestrian i . This study considers short-range strong repulsive and long-range weak attractive interactions, i.e., $C_r > C_a$ and $l_a > l_r$. By these conditions, the attractions attract distant pedestrians but not too close to the attractions.

The interaction between pedestrians and attractions is qualitatively different from others, in that a pedestrian can make decisions between moving in a desired direction and dropping by the attraction, or among multiple attractions. This behavior can be called switching. Such switching behavior can be effectively considered in our setup with plausible values of model parameters, instead of explicitly switching on/off related forces in Eq. (2).

III. RESULTS AND DISCUSSION

A. Numerical simulation setup

In order to investigate the decisive role of attractive interactions toward attractions, numerical simulations are performed. Each pedestrian is modeled by a circle with radius $r_i = 0.2$ m. N pedestrians move in a corridor of length 25 m, along the x -axis, and width 4 m, along the y -axis, with periodic boundary condition in the direction of x -axis. They move with desired speed $v_d = 1.2$ m/s and with relaxation time $\tau = 0.5$ s, and their speed is limited to $v_{\max} = 2.0$ m/s. The desired direction is set to $\vec{e}_i = (1, 0)$ for one half of population and $\vec{e}_i = (-1, 0)$

TABLE I. Model parameters

Model parameter	symbol	value
strength of interpersonal repulsion	C_p	3.0
range of interpersonal repulsion	l_p	0.2
normal elastic constants	k_n	25.0
tangential elastic constants	k_t	12.5
strength of boundary repulsion	C_b	10.0
range of boundary repulsion	l_b	0.2
strength of repulsive interaction from attraction	C_r	10.0
range of repulsive interaction from attraction	l_r	0.2
range of attractive interaction toward attraction	l_a	1.0
pedestrian stride time	Δt	0.5

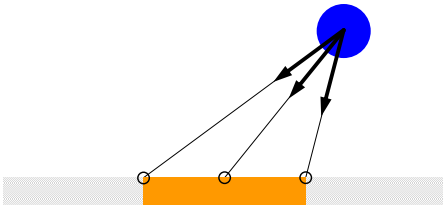


FIG. 1. (Color online) Each attraction, represented by an orange rectangle, is modeled as three point masses acting on a pedestrian, represented by a blue circle.

for the other half. On both the upper and lower walls of corridor, five attractions are evenly spaced, meaning that the distance between attractions is 5 m. To consider the dimension of attractions, each attraction is modeled as three point masses: one point at the center, the other two points at the distance of 0.5 m from the center (See Fig. 1).

To implement the social force model described in Sec. II, the parameter values in Table I are selected based on the previous works [6, 7, 23, 26]. Here the values of C_r and l_r are set to be the same as C_b and l_b . In particular, the values of C_a and l_a are chosen such that $l_a > l_r$ and $C_a < C_r$. The effect of attractive interaction toward attractions can be studied by controlling the ratio of C_a to C_r , defining the relative attraction strength $C = C_a/C_r$ with $C_r = 10.0$. For the corridor area, $A = 100 \text{ m}^2$, this study also controls the pedestrian density defined by $\rho = N/A$. At the initial time $t = 0$, pedestrians are randomly distributed in the corridor without overlapping.

B. Phase diagram

The simulation results show various collective patterns of pedestrian movements depending on relative attraction strength C and pedestrian density ρ . When the density is low, three different phases are observed depending on the relative attraction strength: (i) When the attractive interaction C is small, pedestrians walk in their desired directions, which enables to define the

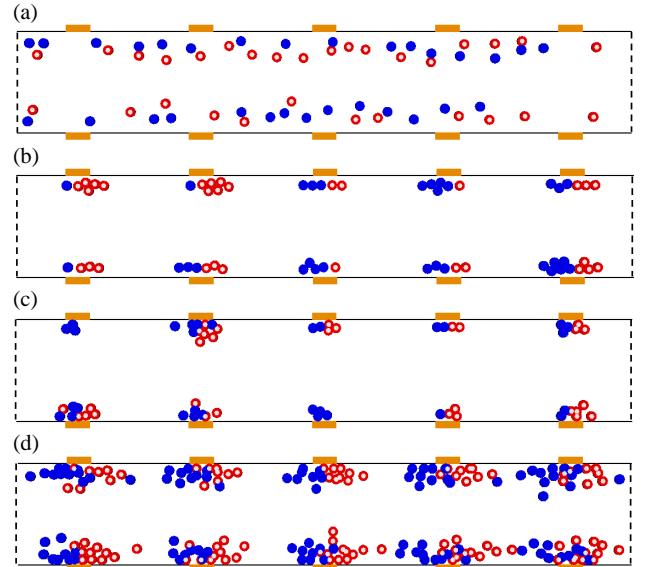


FIG. 2. (Color online) Snapshots of numerical simulations for various collective patterns, depending on the relative attraction strength C and the pedestrian density ρ . The attractions, depicted by rectangles, are located on the walls of the corridor with periodic boundary conditions in the horizontal direction. Filled blue and hollow red circles depict the pedestrians with desired directions to the left and to the right, respectively. The different phases are observed: (a) Free moving phase in the case of $C = 0.2$ and $\rho = 0.6$, in which pedestrians walk in their desired directions. (b) Agglomerate phase in the case of $C = 0.45$ and $\rho = 0.6$, in which pedestrians reach a standstill by forming clusters around attractions. (c) Competitive phase in the case of $C = 0.7$ and $\rho = 0.6$, in which pedestrians rush into attractions and tend to push others. (d) Coexistence subphase in the case of $C = 0.55$ and $\rho = 2.0$, in which the free moving and the competitive phases coexist.

free moving phase, see Fig. 2(a). (ii) For the intermediate range of C , one can observe an agglomerate phase, where pedestrians reach a standstill by forming clusters around attractions, although they intended to walk with their desired velocity [See Fig. 2(b)]. (iii) The competitive phase appears when C is large. Since increasing the relative attraction strength leads to extreme desire for attractions, pedestrians rush into attractions and tend to push others as shown in Fig. 2(c). On the other hand, if the density is high, the agglomerate phase is not observed any more, while the free moving and competitive phases coexist only for the intermediate range of C as shown in Fig. 2(d).

In order to quantitatively distinguish different pedestrian flow patterns, this study employs the efficiency of motion E and the normalized kinetic energy K [24] as follows:

$$E = \left\langle \frac{1}{N} \sum_{i=1}^N \frac{\vec{v}_i \cdot \vec{e}_i}{v_d} \right\rangle \quad (10)$$

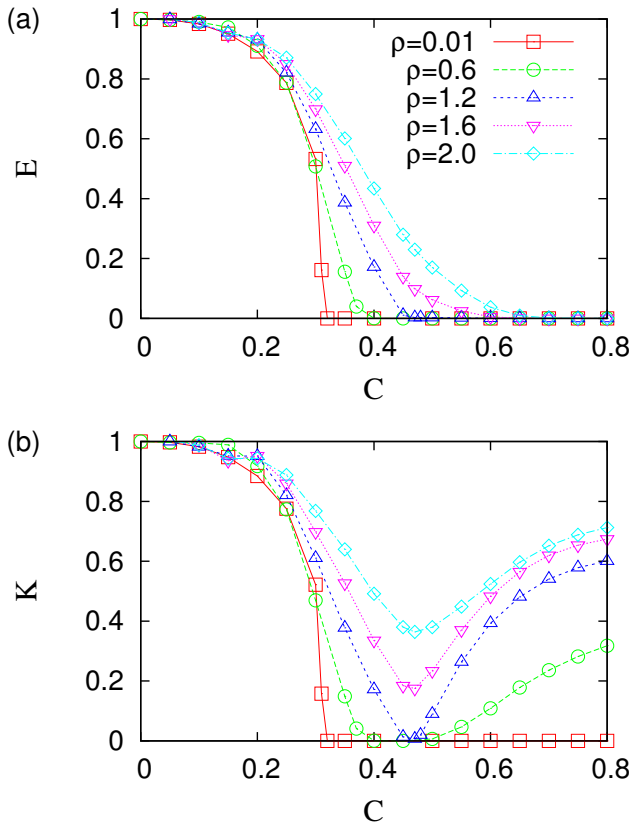


FIG. 3. (Color online) Numerical results of the efficiency of motion $E(C, \rho)$ (a) and the normalized kinetic energy $K(C, \rho)$ (b). Different symbols represent the different values of ρ . For each given ρ , $E(C)$ monotonically decreases according to C , while $K(C)$ decreases and then increases except for small ρ . Different phases and transitions among them can be characterized in terms of the behaviors of E and K .

and

$$K = \left\langle \frac{1}{N} \sum_{i=1}^N \frac{\|\vec{v}_i\|^2}{v_d^2} \right\rangle. \quad (11)$$

Here $\langle \cdot \rangle$ represents an average over 60 independent simulation runs after reaching the stationary state. The efficiency reflects the contribution of the driving force in the pedestrian motion. If all pedestrians walk with their desired velocity, the efficiency becomes 1. On the other hand, the zero efficiency can be obtained if pedestrians do not move in their desired directions and form clusters at attractions. The normalized kinetic energy has the value of 0 if all pedestrians do not move, otherwise it has a positive value.

Figure 3 shows how the efficiency $E(C, \rho)$ and the normalized kinetic energy $K(C, \rho)$ depend on the pedestrian density ρ and the relative attraction strength C . For a given ρ , E decreases according to C , meaning that pedestrians are more distracted from their desired velocity due to the larger strength of attractions. Interestingly, E becomes 0 at a finite value of $C = C_0(\rho)$, indicating the

transition from the free moving phase to the agglomerate phase for low ρ or to the competitive phase for high ρ . In case with $N = 1$, $\rho = 0.01$, the pedestrian movements end up with either moving or stopping the movement, depending on C . That is, the transition for $N = 1$ is discontinuous, depicted as an abrupt change in the curve of $\rho = 0.01$ in Fig. 3(a). The same behavior is observed up to $\rho = 0.1$, i.e., one pedestrian per attraction on average.

For the region of $\rho > 0.1$, the decreasing behavior of E becomes continuous mainly due to the collective effect of interpersonal repulsion. In addition, the larger E is observed with higher ρ , which can be explained by the interpersonal repulsion effect. The pedestrians moving far from the walls become less distracted by the attractions because of the repulsion by pedestrians close to the attractions. This interpersonal repulsion also explains why the transition point of $C_0(\rho)$ is larger for the higher ρ . The stronger attraction is needed to attract distant pedestrians.

Although the efficiency enables to identify the boundary of the free moving phase, the properties of agglomerate and competitive phases can be better understood in terms of the normalized kinetic energy. The decreasing behavior of K is overall similar to that of E up to $C \approx 0.45$. It also turns out that K begins to increase for larger values of C except for $\rho < 0.1$. In the case of $\rho < 0.1$, since pedestrians do not occupy the same attraction on average, the further increasing strength of attractions do not change pedestrian movements, keeping $K = 0$. The increasing behavior of K is of two kinds, depending on the range of ρ . First, the case with low values of ρ is considered. As C increases, K turns out to be 0 at the same critical point of $C = C_0$, and then gradually increases from 0 at $C = C_+(\rho)$ with $C_+ \geq C_0$ (see Fig. 3). The boundaries among different phases can be identified in terms of C_0 and C_+ . The free moving phase for $C < C_0$ is characterized by

$$E > 0 \text{ and } K > 0, \quad (12)$$

and the agglomerate phase for $C_0 < C < C_+$ by

$$E = K = 0. \quad (13)$$

When $C > C_+$,

$$E = 0 \text{ and } K > 0 \quad (14)$$

characterizes the competitive phase, in which pedestrians rush into attractions and jostle each other in order to get closer to attractions. This also explains the observation of $\partial K / \partial C > 0$. Even though the stronger attractions intensify jostling behavior of pedestrians, pedestrians do not jump to the neighboring attractions. Moreover, due to the competition, they stay near attractions and frequently move in the opposite direction of the desired velocity, leading to $E = 0$. It is found that $C_0(\rho)$ increases and $C_+(\rho)$ decreases according to the increasing ρ . They finally coincide at the crossover density $\rho_\times \approx 1.22$, in which the agglomerate phase vanishes. The value of ρ_\times

indicates the maximum number of pedestrians that can stay near attractions without jostling and can be interpreted as a total capacity of attractions. In this simulation setup, each attraction can accommodate about up to 12 pedestrians on average.

Secondly, for the high values of $\rho > \rho_\times$, K decreases and then increases according to C but without becoming zero. The striking difference from the case with low ρ is the existence of parameter region characterized by both

$$E > 0 \text{ and } \frac{\partial K}{\partial C} > 0. \quad (15)$$

This implies that some pedestrians rush into attractions as in the competitive phase ($\partial K/\partial C > 0$), while other pedestrians move in their desired directions as in the free moving phase ($E > 0$). The moving pedestrians are also attracted to attractions but cannot stay around them because of interpersonal repulsion effect by other pedestrians closer to attractions. Thus, this parameter region can be called coexistence subphase. The coexistence subphase belongs to the free moving phase in the sense that the coexistence subphase is also characterized by $E > 0$ and $K > 0$. However, one can identify the lower boundary of coexistence subphase by determining C_{\min} that minimizes K . At C_{\min} , the number of pedestrians accommodated by attractions is also maximized. C_{\min} seems to be independent of ρ . It is because the excessive pedestrians proportional to $\rho - \rho_\times$ cannot be accommodated by attractions, hence move between attractions, which elevates the curve of K at least around C_{\min} . The upper boundary to the competitive phase is determined by the critical point C_0 . It is found that $C_0(\rho)$ is an increasing function of ρ because stronger attractions are needed to entice more pedestrians. Different phases characterizing different collective patterns of pedestrians and transitions among them are summarized in the phase diagram of Fig. 4.

C. Spatiotemporal patterns

In addition to the global quantities characterizing the collective patterns, such as efficiency of motion and normalized kinetic energy, one can better describe the patterns by means of local quantities. As in [25, 26], the local speed and the local density are adopted to describe the spatiotemporal patterns of pedestrian movements. The local speed at a location \vec{z} and time t is measured as

$$V(\vec{z}, t) = \frac{\sum_i \|\vec{v}_i\| f(d_{iz})}{\sum_i f(d_{iz})}, \quad (16)$$

where d_{iz} is the distance between location \vec{z} and pedestrian i 's position. $f(d)$ is a Gaussian distance-dependent weight function

$$f(d) = \frac{1}{\pi R^2} \exp\left(-\frac{d^2}{R^2}\right) \quad (17)$$

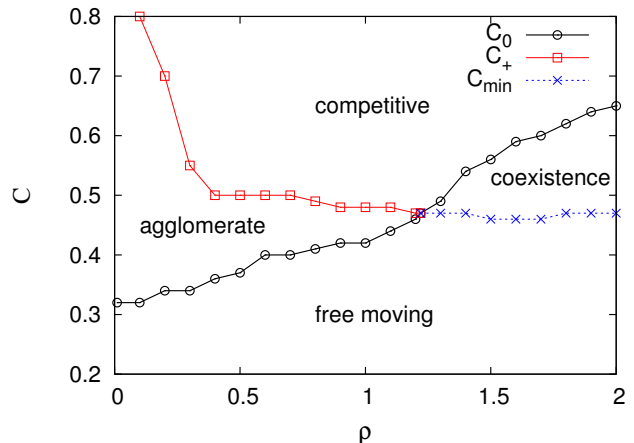


FIG. 4. (Color online) Phase diagram summarizing the numerical results. The parameter space of the pedestrian density ρ and the relative attraction strength C is divided into four regions by means of C_0 (\circ), C_+ (\square), and C_{\min} (\times).

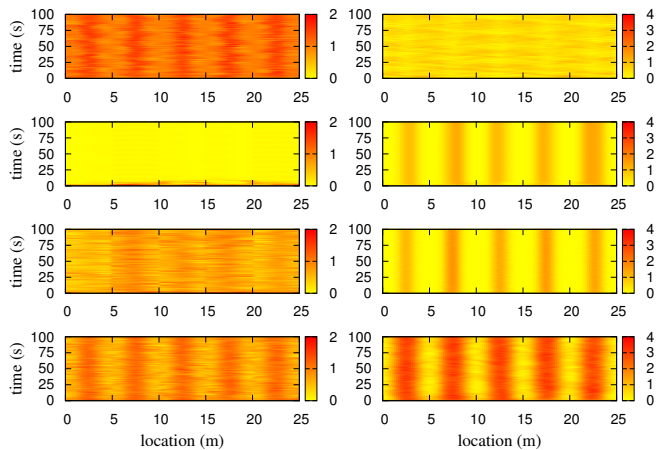


FIG. 5. (Color online) Local speed maps (left) and local density maps (right) for various collective patterns of pedestrian movements: free moving, agglomerate, and competitive phases, and coexistence subphase (from top to bottom). Yellow (light) and red (dark) colors indicate lower and higher values, respectively.

with a measurement parameter $R = 0.7$. The local density is similarly defined as

$$\rho(\vec{z}, t) = \sum_i f(d_{iz}). \quad (18)$$

Figure 5 shows for different phases the local speed maps $V(x, t)$ and the local density maps $\rho(x, t)$ that have been averaged along the y -axis. For the free moving phase, pedestrians speed up when they approach the attractions, and then slow down when moving away from them. The fast moving pedestrians around attractions lead to the low density, while slowly moving pedestrians between at-

tractions is related to the high density. In the agglomerate phase, pedestrians form clusters around attractions, resulting in the high local density around attractions and zero local speed in the entire corridor. In the competitive phase, the local density shows tighter clustering formation around attractions than that of the agglomerate phase. One can observe fluctuations in the local speed in that frenzied pedestrians rush into attractions. The coexistence subphase shows a similar pattern to the free moving phase in the local speed map and to the competitive phase in the local density map.

IV. CONCLUSION

This study has numerically investigated collective effects of attractive interactions between pedestrians and attractions by extending the social force model. A phase diagram with various collective patterns of pedestrian movements is presented. The phases are identified by means of the efficiency of motion E and the normalized kinetic energy K as functions of the pedestrian density ρ and the relative attraction strength C . For low density, as C increases, the transition occurs from the free moving phase ($E, K > 0$) to the agglomerate phase ($E = K = 0$) and finally to the competitive phase ($E = 0$ and $K > 0$). For high density, the agglomerate phase disappears and a coexistence subphase emerges where the properties of free moving and competitive phases are observed simultaneously for the intermediate range of C . The crossover density separating low and high densities can be understood as the total capacity of attractions. It is noted that these results are robust with respect to the choice of relevant parameter values for attractive interactions, i.e., l_a and C_r .

The findings from this study can provide insight into customer behavior in stores. The driving force and the attractive force can be interpreted as the initial plan and the influence of unexpected attractions, respectively. Accordingly, the appearance of the agglomerate phase might be analogous to consumer impulse purchase without an initial plan [27–29]. The competitive phase can be relevant to understanding the pedestrian incidents involving extreme desire for limited resources. This study also suggests that safe and efficient use of pedestrian facilities can be achieved by moderating the density and the strength of attractive interaction.

A very simple scenario has been focused in order to study the fundamental role of attractive interactions. Assuming superposition of various interaction terms in the social force model could yield switching behavior in effect by choosing plausible parameter values. However, switching behavior can be explicitly formulated for more realistic models, and should be verified against experimental data. Indeed, it is widely known that people have limited amount of attention, so they tend to focus on few stimuli rather than consider every stimulus around them [30, 31]. In addition, one can take into account heterogeneous properties of pedestrians and attractions, such as different strength of attractive interactions between pedestrians and attractions.

ACKNOWLEDGMENTS

This work is funded by Aalto University 4D-Space MIDE project (JK) and by Aalto University postdoctoral program (HJ).

-
- [1] D. Helbing, *Reviews of Modern Physics* **73**, 1067 (2001).
 - [2] W. Daamen and S. Hoogendoorn, *Transportation Research Record: Journal of the Transportation Research Board* **1828**, 20 (2003).
 - [3] S. K. Hui, P. S. Fader, and E. T. Bradlow, *Marketing Science* **28**, 320 (2009).
 - [4] V. J. Blue and J. L. Adler, *Transportation Research Part B: Methodological* **35**, 293 (2001).
 - [5] C. Burstedde, K. Klauck, A. Schadschneider, and J. Zittartz, *Physica A: Statistical Mechanics and its Applications* **295**, 507 (2001).
 - [6] D. Helbing and P. Molnár, *Physical Review E* **51**, 4282 (1995).
 - [7] D. Helbing, L. Buzna, A. Johansson, and T. Werner, *Transportation Science* **39**, 1 (2005).
 - [8] G. Köster, F. Tremel, and M. Gödel, *Physical Review E* **87**, 063305 (2013).
 - [9] W. J. Yu, R. Chen, L. Y. Dong, and S. Q. Dai, *Physical Review E* **72**, 026112 (2005).
 - [10] M. Chraïbi, A. Seyfried, and A. Schadschneider, *Physical Review E* **82** 046111 (2010).
 - [11] W. Yu and A. Johansson, *Physical Review E* **76**, 046105 (2007).
 - [12] S. Xu and H. B. L. Duh, *IEEE Transactions on Intelligent Transportation Systems* **11**, 153 (2010).
 - [13] M. Moussaïd, N. Perozo, S. Garnier, D. Helbing, and G. Theraulaz, *PLoS ONE* **5**, e10047 (2010).
 - [14] A. Borgers and H. Timmermans, *Geographical Analysis* **18**, 115 (1986).
 - [15] H. Timmermans, X. van der Hagen, and A. Borgers, *Transportation Research Part B: Methodological* **26**, 45 (1992).
 - [16] B. Serrell, *Curator: The Museum Journal* **40**, 108 (1997).
 - [17] I. K. Rohloff, Ph.D. thesis, The University of Michigan (2009).
 - [18] S. K. Hui, J. J. Inman, Y. Huang, and J. A. Suher, *Journal of Marketing Research* **77** (2013).
 - [19] T. Vicsek, A. Czirók, E. Ben-Jacob, I. Cohen, and O. Shochet, *Physical Review Letters* **75**, 1226 (1995).
 - [20] A. Mogilner, L. Edelstein-Keshet, L. Bent, and A. Spiros, *Journal of Mathematical Biology* **47**, 353 (2003).
 - [21] M. R. D’Orsogna, Y. L. Chuang, A. L. Bertozzi, and L. S.

- Chayes, Physical Review Letters **96**, 104302 (2006).
- [22] J. L. Silverberg, M. Bierbaum, J. P. Sethna, and I. Cohen, Physical Review Letters **110**, 228701 (2013).
- [23] A. Johansson, D. Helbing, and P. Shukla, Advances in Complex Systems **10** (2008).
- [24] D. Helbing, I. J. Farkas, and T. Vicsek, Physical Review Letters **84**, 1240 (2000).
- [25] D. Helbing, A. Johansson, and H. Z. Al-Abideen, Physical Review E **75**, 046109 (2007).
- [26] M. Moussaïd, D. Helbing, and G. Theraulaz, Proceedings of the National Academy of Sciences **108**, 6884 (2011).
- [27] D. W. Rook, Journal of Consumer Research **14**, 189 (1987).
- [28] D. W. Rook and R. J. Fisher, Journal of Consumer Research **22**, 305 (1995).
- [29] R. F. Baumeister, Journal of Consumer Research **28**, 670 (2002).
- [30] C. D. Wickens and J. G. Hollands, *Engineering Psychology and human Performance* (Prentice Hall, 1999), 3rd ed.
- [31] E. B. Goldstein, *Sensation and Perception* (Thomson Wadsworth, 2007), 7th ed.

Publication II

Kwak, J., Jo, H-H., Luttinen, T., and Kosonen, I. Effects of switching behavior for the attraction on pedestrian dynamics. *PLOS ONE*, Volume 10, 7, e0133668, July 2015.

© 2015 Authors.

Reprinted with permission.

RESEARCH ARTICLE

Effects of Switching Behavior for the Attraction on Pedestrian Dynamics

Jaeyoung Kwak^{1*}, Hang-Hyun Jo^{2,3}, Tapio Luttinen¹, Iisakki Kosonen¹

1 Department of Civil and Environmental Engineering, Aalto University, Espoo, Finland, **2** BK21plus Physics Division and Department of Physics, Pohang University of Science and Technology, Pohang, Republic of Korea, **3** Department of Computer Science, Aalto University, Espoo, Finland

* jaeyoung.kwak@aalto.fi



 OPEN ACCESS

Citation: Kwak J, Jo H-H, Luttinen T, Kosonen I (2015) Effects of Switching Behavior for the Attraction on Pedestrian Dynamics. PLoS ONE 10(7): e0133668. doi:10.1371/journal.pone.0133668

Editor: Frederic Amblard, University Toulouse 1 Capitole, FRANCE

Received: October 9, 2014

Accepted: June 30, 2015

Published: July 28, 2015

Copyright: © 2015 Kwak et al. This is an open access article distributed under the terms of the [Creative Commons Attribution License](https://creativecommons.org/licenses/by/4.0/), which permits unrestricted use, distribution, and reproduction in any medium, provided the original author and source are credited.

Data Availability Statement: All relevant data are within the paper.

Funding: JK was supported by Aalto University School of Engineering Doctoral Program. HJ was supported by Aalto University postdoctoral program and by Mid-career Researcher Program through the National Research Foundation of Korea (NRF) grant funded by the Ministry of Science, ICT and Future Planning (2014030018), and Basic Science Research Program through the National Research Foundation of Korea (NRF) grant funded by the Ministry of Science, ICT and Future Planning (2014046922). The funders had no role in study design, data collection

Abstract

Walking is a fundamental activity of our daily life not only for moving to other places but also for interacting with surrounding environment. While walking on the streets, pedestrians can be aware of attractions like shopping windows. They can be influenced by the attractions and some of them might shift their attention towards the attractions, namely switching behavior. As a first step to incorporate the switching behavior, this study investigates collective effects of switching behavior for an attraction by developing a behavioral model. Numerical simulations exhibit different patterns of pedestrian behavior depending on the strength of the social influence and the average length of stay. When the social influence is strong along with a long length of stay, a saturated phase can be defined at which all the pedestrians have visited the attraction. If the social influence is not strong enough, an unsaturated phase appears where one can observe that some pedestrians head for the attraction while others walk in their desired direction. These collective patterns of pedestrian behavior are summarized in a phase diagram by comparing the number of pedestrians who visited the attraction to the number of passersby near the attraction. Measuring the marginal benefits with respect to the strength of the social influence and the average length of stay enables us to identify under what conditions enhancing these variables would be more effective. The findings from this study can be understood in the context of the pedestrian facility management, for instance, for retail stores.

Introduction

Collective dynamics of interactions among individuals is one of the current central topics in the field of interdisciplinary physics. In an attempt to quantify self-organized phenomena in the real world, various topics have been studied such as opinion formation [1, 2], spread of disease [3], and pedestrian dynamics [4]. The study of pedestrian dynamics has generated considerable research interests in the physics community and various models have been proposed in order to describe fascinating collective phenomena, such as cellular automata (CA) approaches [5, 6], force-based models [7, 8], and heuristic-based models [9, 10]. The CA approaches discretize walking space into two dimensional lattices where each cell can have at most one agent.

and analysis, decision to publish, or preparation of the manuscript.

Competing Interests: The authors have declared that no competing interests exist.

Agents move between cells according to the probability of movement. The CA approaches offer simple and efficient computation, but yield limited accuracy on describing pedestrian movements due to the nature of discretized time and space. Force-based models present internal motivation and external stimuli as force terms and describe the movement of pedestrians by summing these force terms in continuous space. Although force-based models can describe pedestrian behaviors in detail, they are computationally expensive. Heuristic-based models predict pedestrian movements based on a set of rules defined for different situations. The heuristic-based models can intuitively simulate pedestrian movements for specific situations, but at the same time they might be able to mimic only a limited number of situations. Among these models, force-based models have been remarkably extended by improving behavioral aspects of pedestrian movements including repulsive interactions [11–13], collision prediction [14], pedestrian group behavior [15–17], and attractive interactions between pedestrians and attractions [18].

Numerical studies in Ref. [18] examined attractive interactions between pedestrians and attractions by appending the attractive force toward the attractions. Although their extended social force model exhibited various collective patterns of pedestrian movements, their study did not explicitly take into account selective attention. The selective attention is a widely recognized behavioral mechanism by which people can focus on tempting stimuli and disregard uninteresting ones [19, 20]. While walking on the streets, pedestrians can be aware of attractions like shopping windows and street performances. When such attractions come into sight, individuals can make decisions between moving in their initially planned directions and stopping by the attractions. This behavior can be called switching behavior, meaning that the individuals can shift their attention towards the attractions [18].

In reality, such switching behavior is likely to be influenced by the behavior of others. For instance, Milgram *et al.* [21] and Gallup *et al.* [22] reported that passersby on the streets were more likely to pay attention to stimulus crowds as the size of the crowd was increased. They noted that the size of the crowd was associated with the individual time spent looking at the stimulus crowd and social context. In the marketing area, it is widely believed that longer store visit duration and stronger social interactions are likely to attract more shoppers to stores. Having more visitors in the stores can affect one's information processing by raising awareness of merchandise displays in stores, and consequently the individual becomes prone to make more purchases [23, 24]. Therefore, marketing strategies have focused on increasing the length of store visit duration and the strength of social interactions [25].

In order to incorporate the switching behavior, this study constructs a simple probability model in which the preference for the attraction depends on the number of people who have already joined the attraction. By means of numerical simulations, the effects of the social influence and the average length of stay at the attraction are examined, and illustrated with a phase diagram.

The remainder of this paper is organized as follows. We first describe the proposed switching behavior model in the next section. Then we present its numerical simulation results with a phase diagram in the results section. Finally, we discuss the findings of this study in the section following the results.

Methods

Switching behavior

By the analogy with sigmoidal choice rule [21, 22, 26], the probability that a pedestrian joins an attraction point P_a can be formulated based on the number of pedestrians who have already

joined N_a and the number of pedestrians not stopping by the attraction N_0 :

$$P_a = \frac{sN_a}{N_0 + sN_a}. \tag{1}$$

This indicates that the joining probability increases as N_a grows. Here $s > 0$ is the strength of the social influence that can be also understood as pedestrians' awareness of the attraction. When s is small, individuals pay little attention to others' choice. For large s , the joining probability is more likely to be influenced by the number of people who have already joined the attraction rather than the number of people not joining the attraction. However, note that the joining probability cannot be determined when there is nobody within the range of perception, i.e., $N_a = N_0 = 0$. In order to avoid such indeterminate case, we introduce positive constants K_a for joining the attraction and K_0 for not stopping by the attraction as baseline values of N_a and N_0 , respectively, as follows:

$$P_a = \frac{s(N_a + K_a)}{(N_0 + K_0) + s(N_a + K_a)}. \tag{2}$$

According to previous studies [21, 22, 25], here we postulated that the strength of social influence can be different for different situations and can be controlled in the presented model. After joining the attraction, the individual will then stay near the attraction for an exponentially distributed time with an average of t_d , similar to previous works [7, 22, 27].

Pedestrian movement

According to the social force model [7], the velocity $\vec{v}_i(t)$ of pedestrian i at time t is given by the following equation:

$$\frac{d\vec{v}_i(t)}{dt} = \frac{v_d \vec{e}_i - \vec{v}_i(t)}{\tau} + \sum_{j \neq i} \vec{f}_{ij} + \sum_B \vec{f}_{iB}. \tag{3}$$

Here the first term on the right-hand side indicates the driving force describing the tendency of pedestrian i moving toward his destination with the desired speed v_d and an unit vector \vec{e}_i pointing to the desired direction. The relaxation time τ controls how fast pedestrian i adapts its velocity to the desired velocity. The repulsive force terms \vec{f}_{ij} and \vec{f}_{iB} reflect his tendency to keep certain distance from other pedestrian j and the boundary B , e.g., wall and obstacles. Based on previous studies [7, 12, 18], the repulsive force between pedestrians i and j is specified by summing the gradient of repulsive potential with respect to $\vec{d}_{ij} \equiv \vec{x}_j - \vec{x}_i$, and the friction force, \vec{g}_{ij} :

$$\vec{f}_{ij} = -\nabla_{\vec{d}_{ij}} \left[C_p l_p \exp\left(-\frac{b_{ij}}{l_p}\right) \right] + \vec{g}_{ij}. \tag{4}$$

C_p and l_p are the strength and the range of repulsive interaction between pedestrians i and j . Here $b_{ij} = \frac{1}{2} \sqrt{(\|\vec{d}_{ij}\| + \|\vec{d}_{ij} - \vec{y}_{ij}\|)^2 - \|\vec{y}_{ij}\|^2}$ is the effective distance between pedestrians i and j by assuming their relative displacement $\vec{y}_{ij} \equiv (\vec{v}_j - \vec{v}_i)\Delta t$ with the stride time Δt [12]. The interpersonal friction $\vec{g}_{ij} = kh(r_{ij} - d_{ij})\vec{e}_{ij}$ becomes effective when the distance $d_{ij} = \|\vec{d}_{ij}\|$ is smaller than the sum $r_{ij} = r_i + r_j$ of their radii r_i and r_j , where k is the normal elastic constant and \vec{e}_{ij} is an unit vector pointing from pedestrian j to i . The function $h(x)$ yields x if $x > 0$, while it gives 0 if $x \leq 0$. The repulsive force from boundaries is denoted as $\vec{f}_{iB} = C_b \exp(-d_{iB}/l_b)\vec{e}_{iB}$, where d_{iB} is the perpendicular distance between pedestrian i and wall, and \vec{e}_{iB} is the unit vector

pointing from the wall B to the pedestrian i . C_b and l_b denote the strength and the range of repulsive interaction from boundaries.

Numerical simulation setup

Each pedestrian is modeled by a circle with radius $r_i = 0.25$ m. $N = 100$ pedestrians move in a corridor of length 30 m and width 6 m with periodic boundary condition in the horizontal direction. They move with desired speed $v_d = 1.2$ m/s and with relaxation time $\tau = 0.5$ s, and their speed cannot exceed $v_{\max} = 2.0$ m/s. The desired direction points from the left to the right boundary of the corridor for one half of population and the opposite direction for the other half. The parameters of the repulsive force terms are given based on previous works: $C_p = 3$, $l_p = 0.2$, $k = 62.5$, $C_b = 10$, and $l_b = 0.2$ [7, 10, 12, 18].

The joining probability (Eq (2)) is updated with the social force model (Eq (3)) for each simulation time step of 0.05 s. The individual can decide whether he will join the attraction when the attraction comes into his perception range $R_i = 10$ m. Once the individual decides to join the attraction, then he shifts his desired direction vector \vec{e}_i toward the attraction. The attraction is placed at the center of lower wall, i.e., at the distance of 15 m from the left boundary of the corridor. For the sake of simplicity, K_a and K_0 are set to be 1, meaning that both options are equally attractive when the individual would see nobody within his perception range. An individual is counted as an attending pedestrian if his efficiency of motion $E_i = (\vec{v}_i \cdot \vec{e}_i)/v_d$ is lower than 0.05 within a range of 3 m from the center of the attraction after he decided to join there. Here the efficiency of motion indicates how much the driving force contributes to the pedestrian motion with a range from 0 to 1 [18, 28]. $E_i = 1$ implies that the individual is walking towards his destination with the desired velocity while lower E_i indicates that an individual is distracted from his initial destination because of the attraction.

Results and Discussion

Feasibility zone

The simulation results show different patterns of pedestrian movements depending on the strength of the social influence s and the average length of stay t_d . If the social influence is weak, one can define an unsaturated phase where some pedestrians move towards the attraction while others walk in their desired directions (see Fig 1(a)). For large values of s , a saturated phase can be defined, in which every pedestrian near the attraction heads for the attraction (see Fig 1(b)).

We focus on the behavior of the number of pedestrians who visited the attraction N_v , out of pedestrians within a range of $R_a = 10$ m from the center of the attraction, denoted by N_p . Then the number of pedestrians not visiting the attraction is $N_p - N_v$. Quantifying the behavior of N_v is useful because it reflects the level of crowding and helps facility managers to estimate the cost of making the accommodation necessary for visitors. Fig 2 shows how N_v depends on the strength of social influence s and the average length of stay t_d . For a given t_d , N_v increases according to s , indicating that more pedestrians are distracted from their initial desired velocity due to others' choice on the attraction, see the left panel of Fig 2. Furthermore, N_v curves rapidly increase as t_d grows, meaning that the larger t_d , the smaller s is needed to attract the majority of pedestrians (see the right panel of Fig 2). The increasing behavior of N_v in the right panel of Fig 2 shows a similar pattern to that in the left panel.

Although N_v enables us to evaluate the attraction influence on pedestrians, quantifying marginal benefits of facility improvements can indicate the effective ways of enhancing the attraction influence on pedestrians. The increase of N_v can be understood as the benefit of the facility improvements in the sense that the attraction is likely to have more potential customers with

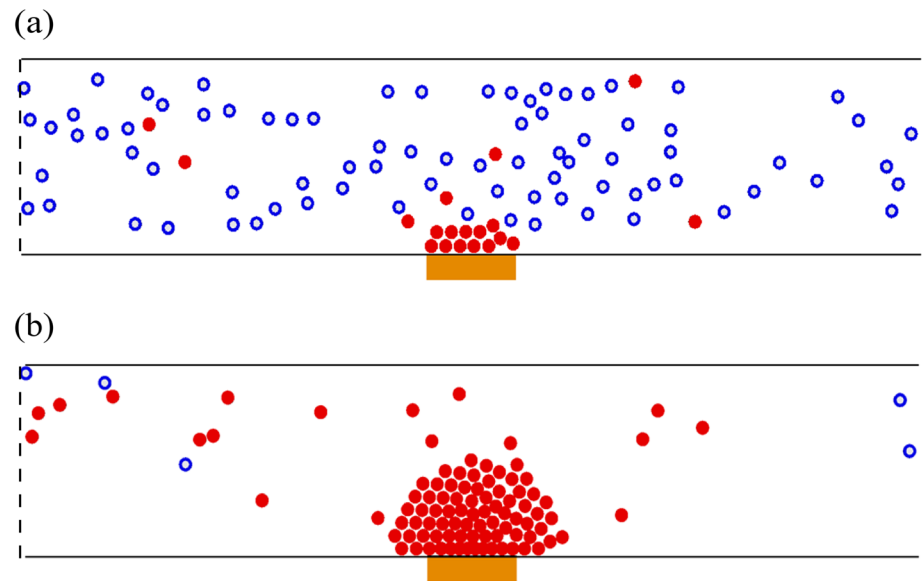


Fig 1. Representative snapshots of numerical simulations with various values of the social influence s and the average length of stay t_d . The attraction, depicted by an orange rectangle, is located at the center of the lower wall. Filled red and hollow blue circles depict the pedestrians who have and have not visited the attraction, respectively. Two phases are observed: (a) Unsaturated phase in the case of $s = 0.4$ and $t_d = 30$ s, in which some pedestrians have visited the attraction while others walk in their desired directions. (b) Saturated phase in the case of $s = 1.5$ and $t_d = 60$ s, where all the pedestrians around the attraction, within a range of $R_a = 10$ m, have visited the attraction.

doi:10.1371/journal.pone.0133668.g001

higher N_v . Firstly, $\Delta N_v / \Delta s$ defines the marginal benefit with respect to the change of s , which can be calculated as the first derivative of N_v curves in the left panel of Fig 2. In a similar way, we can also evaluate $\Delta N_v / \Delta t_d$ from the first derivative of N_v curve in the right panel of Fig 2, which defines the marginal benefit with respect to the average length of stay t_d . As indicated in Fig 3(a) and 3(b), each marginal benefit curve increases up to a certain level and then decreases. For higher t_d and s , the values of the marginal benefits are sensitive to the variations of s and t_d for low values of s and t_d , respectively. Thus, one can find certain ranges or windows of s and t_d , where the effective improvements of N_v can be achieved. The variations of s and t_d are considered as effective if $\Delta N_v / \Delta s$ is larger than 30 and if $\Delta N_v / \Delta t_d$ is larger than 0.3. Feasible conditions of the effective improvements can be further illustrated in the parameter space of s and t_d by means of $\Delta N_v / \Delta s$ and $\Delta N_v / \Delta t_d$, as shown in Fig 4. The parameter region can be called a feasibility zone of the effective improvements, indicating that higher increase of N_v is expected with smaller increase of s and t_d . Other than the feasibility zone, the impact of changing those variables are insignificant.

Phase diagram

The parameter space of s and t_d is divided into two regions according to the value of N_v . For each value of $t_d > 43$ s, N_v increases as s increases, and then finally reaches N_p at a critical value of s , i.e., s_c . This indicates the transition from the unsaturated phase to the saturated phase (see Fig 4). For the region of $t_d < 43$ s, N_v increases as s grows but does not reach to its maximum allowed value even for the large values of s , as can be seen from Fig 2(a) and 2(c). The average length of stay t_d is not long enough, so it fails to obtain sufficient amount of visitors. One can

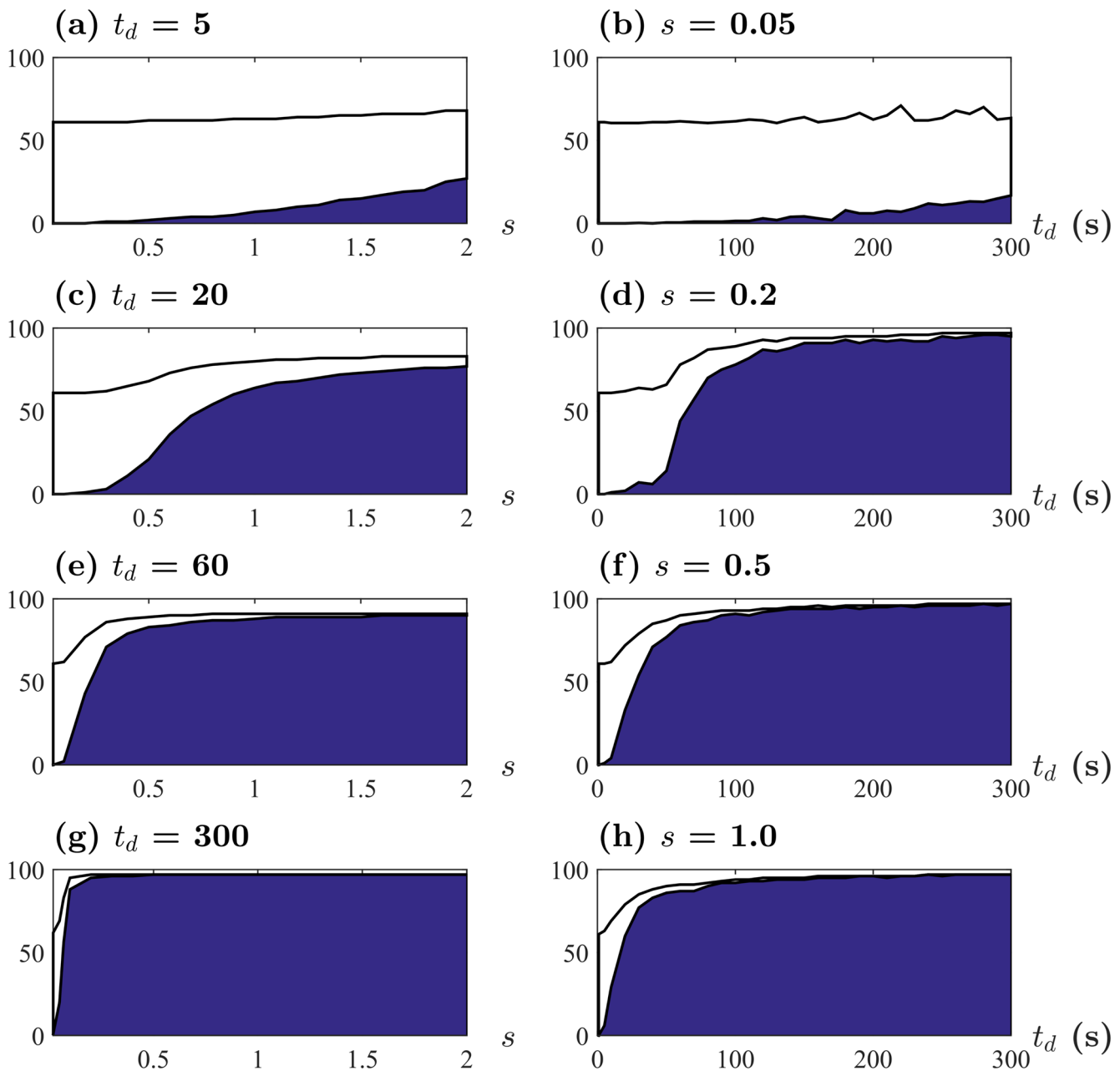


Fig 2. Numerical results of N_v and N_p . Filled blue area indicates the number of pedestrians who visited the attraction N_v , and hollow area bounded by solid lines corresponds to the number of pedestrians not visiting the attraction $N_p - N_v$. Top subplots present the cases of small s (a) and small t_d (b) while bottom subplots for large s (g) and large t_d (h). It is observed that higher values of t_d and s appear to yield rapid growth of N_v for smaller intervals as s and t_d increase, respectively.

doi:10.1371/journal.pone.0133668.g002

also observe that s_c substantially decreases for $t_d \leq 120$ s and appears to stay around 0.2 when t_d is larger than 180 s. It is reasonable to suppose that the departure rate of attending pedestrians is positively associated with the reciprocal of t_d while the arrival rate of joining pedestrians is linked to s . Accordingly, we can infer that the impact of the departure rate on N_v is dominated by that of the arrival rate when t_d is large, so the marginal impact of increasing t_d becomes less notable for larger t_d .

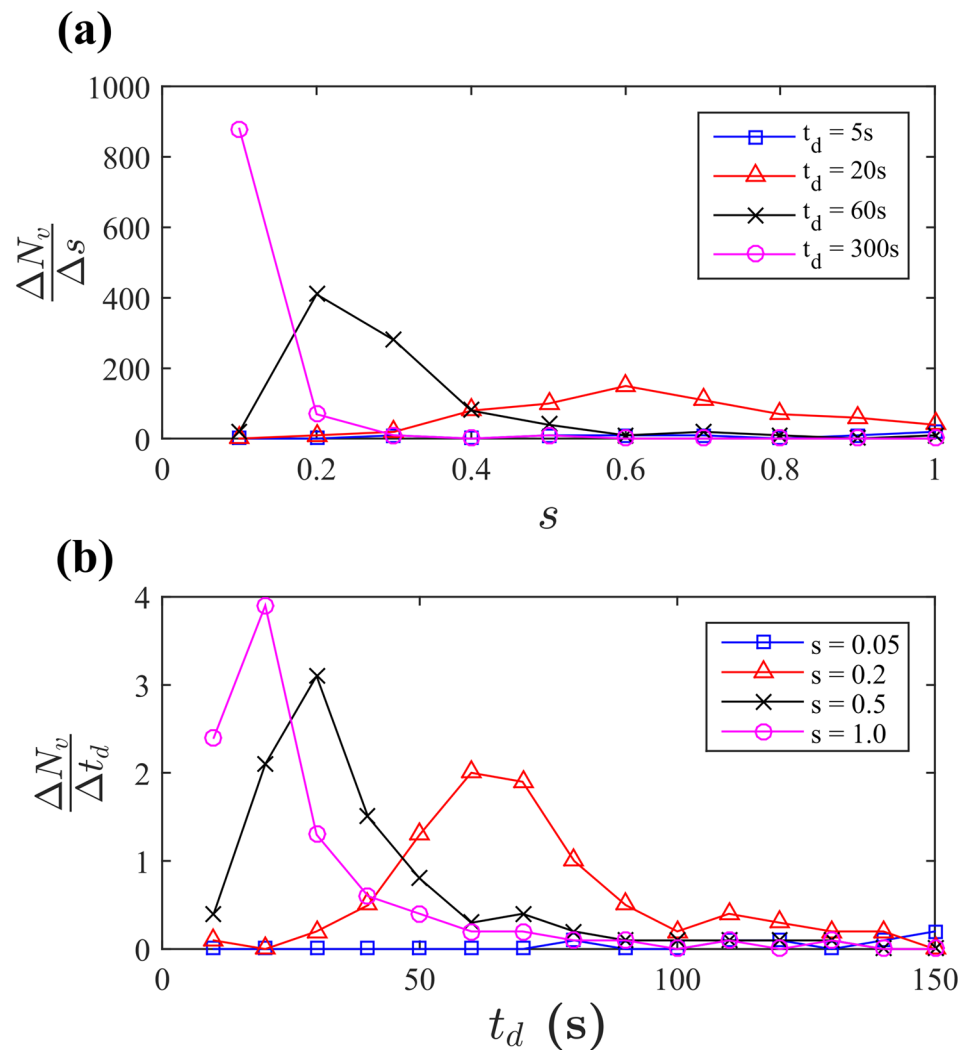


Fig 3. Numerical results of the marginal benefits, $\Delta N_v/\Delta s$ (a) and $\Delta N_v/\Delta t_d$ (b). The marginal benefits increase up to a certain level and then decrease for given t_d and s , respectively. Interestingly, the marginal benefits are sensitive to the variations of s and t_d within the bounded intervals, showing that effective improvements of these variables can be achieved. Different symbols represent the different values of t_d and s .

doi:10.1371/journal.pone.0133668.g003

Conclusion

In order to examine the collective effects of the switching behavior, this study has developed a behavioral model of pedestrians' joining an attraction. A phase diagram with different collective patterns of pedestrian behavior is presented. The phases are identified by comparing the number of pedestrians who visited the attraction N_v to the number of passersby near the attraction N_p . For strong social influence, the saturated phase appears where all pedestrians were enticed by the attraction, so all of them have visited the attraction. When the social influence is weak, the unsaturated phase is observed where the attraction is not captivating enough to entice all the pedestrians. Based on the numerical simulation results, feasible conditions of the effective improvements have been identified in terms of the marginal benefits. It is noted that

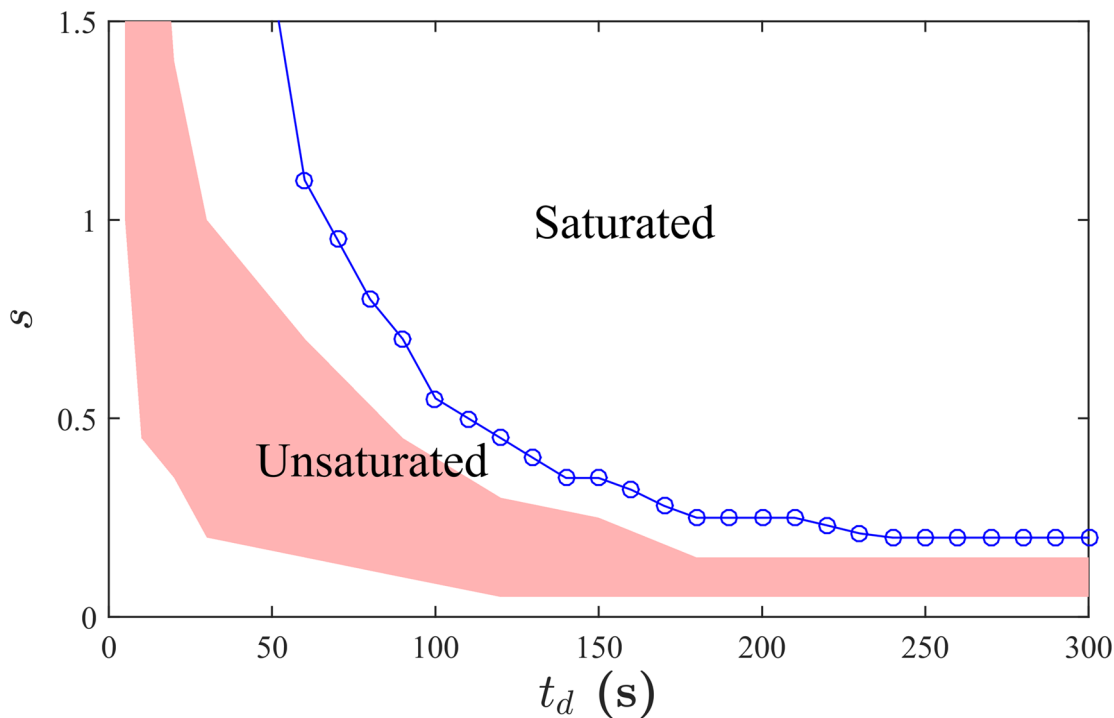


Fig 4. A feasibility zone of effective improvements and an envelope of the saturated phase. The red shade area depicts a feasibility zone of the effective improvements characterized in terms of the marginal benefits $\Delta N_v/\Delta s$ and $\Delta N_v/\Delta t_d$. The blue solid line with circle symbols represents the envelope of the saturated phase at which $N_v = N_p$. The saturated phase indicates that all the pedestrians have visited the attraction, while the unsaturated phase represents that not all pedestrians are enticed by the attraction.

doi:10.1371/journal.pone.0133668.g004

the results are qualitatively similar to the cases of other K_a and K_0 values. When K_0 is set to larger than K_a , the individual will have a higher probability of walking towards the initial destination than the case of joining the attraction. On the other hand, if K_a is larger than K_0 , the choice probability is increased. This study therefore presents a new approach to quantifying the collective effects of switching individuals' attention to the attraction depending on the strength of the social influence s and the average length of stay t_d .

The findings from this study can be contextualized in the domain of pedestrian facility management. The number of pedestrians who visited the attraction N_v is relevant to store traffic which makes it possible to assess the attractiveness of the facility and predict the number of potential customers [29, 30]. The appearance of the saturated phase can be interpreted as a thorough dissemination of important information to the visitors, indicating that all the visitors are informed of events, for instance conferences and campaigns. The social influence s can be understood as pedestrians' awareness of the attraction. For instance, an attraction in a busy train station tends to have a low s value so a few number of pedestrians might gather around the attraction. If there is an artwork produced by a famous artist in a museum (i.e., moderate s) and the value of t_d is large, the artwork is likely to attract a large group of passersby around the artwork. On the other hand, when t_d value of the artwork is small, it might fail to attract many people. In practice, for pedestrian facilities such as stores and museums, there are likely to exist costs associated with increasing the strength of social influence s and the average length of stay t_d . Facility managers can think of increasing t_d by making the pedestrian attractions more

comfortable, so they might expect that visitors would stay longer. Although the strength of the social influence seems to be given for specific situations such as different time of day or locations, the managers can attempt to increase s by changing the layouts of the facilities or changing pedestrian traffic density near the attractions. With the feasibility zone of effective investments, one can identify under what conditions facility improvements would be more effective.

As a first step to study the collective effects of switching behavior, a simple scenario has been considered. Based on the findings from this study, the following recommendations can be made for future research. First, a future study is recommended for the case with multiple attractions in order to consider more realistic situations such as a shopping street having several stores. An important question for the future study is to understand the spatio-temporal dynamics of pedestrians near the attractions. The future study will specifically examine the effects of increasing the number of attractions and the size of pedestrian clusters at the attractions. Second, one can take into account heterogeneous properties of attractions and pedestrians such as the strength of social influence and the average length of stay. In addition, different pedestrians reveal diverse characteristics in terms of desired speed, destinations, and preference on attractions. While this paper only considers homogeneous properties of pedestrians and attractions for the purpose of understandability, considering those heterogeneous properties are needed for immediate applications of this study. Finally, the presented model can be extended by incorporating various aspects of pedestrian behavior. For instance, we can postulate that pedestrians have time budget, so they evaluate the attractiveness and the cost of time due to joining the attractions.

Acknowledgments

Jaeyoung Kwak would like to thank Aalto University School of Engineering Doctoral Program for financial support. He is grateful to CSC–IT Center for Science, Finland for providing computational resources. Hang-Hyun Jo gratefully acknowledges financial support by Aalto University postdoctoral program and by Mid-career Researcher Program through the National Research Foundation of Korea (NRF) grant funded by the Ministry of Science, ICT and Future Planning (2014030018), and Basic Science Research Program through the National Research Foundation of Korea (NRF) grant funded by the Ministry of Science, ICT and Future Planning (2014046922).

Author Contributions

Conceived and designed the experiments: JK HJ. Performed the experiments: JK. Analyzed the data: JK HJ. Wrote the paper: JK HJ TL IK.

References

1. Sznajd-Weron K, Sznajd J. Opinion evolution in closed community. *International Journal of Modern Physics C*. 2000; 11(6):1157–1165. Available from: <http://dx.doi.org/10.1142/S0129183100000936>
2. Galam S. Minority opinion spreading in random geometry. *European Physical Journal B*. 2002; 25(4):403–406. Available from: <http://dx.doi.org/10.1140/epjb/e20020045>
3. Johansson A, Batty M, Hayashi K, Al Bar O, Marcozzi D, Memish ZA. Crowd and environmental management during mass gatherings. *The Lancet Infectious Diseases*. 2012 Feb; 12(2):150–156. Available from: [http://dx.doi.org/10.1016/s1473-3099\(11\)70287-0](http://dx.doi.org/10.1016/s1473-3099(11)70287-0) PMID: 22252150
4. Helbing D, Buzna L, Johansson A, Werner T. Self-organized pedestrian crowd dynamics: Experiments, simulations, and design solutions. *Transportation Science*. 2005 Feb; 39(1):1–24. Available from: <http://dx.doi.org/10.1287/trsc.1040.0108>

5. Blue VJ, Adler JL. Cellular automata microsimulation for modeling bi-directional pedestrian walkways. *Transportation Research Part B: Methodological*. 2001 Mar; 35(3):293–312. Available from: [http://dx.doi.org/10.1016/s0191-2615\(99\)00052-1](http://dx.doi.org/10.1016/s0191-2615(99)00052-1)
6. Burstedde C, Klauck K, Schadschneider A, Zittartz J. Simulation of pedestrian dynamics using a two-dimensional cellular automaton. *Physica A: Statistical Mechanics and its Applications*. 2001 Jun; 295(3-4):507–525. Available from: [http://dx.doi.org/10.1016/s0378-4371\(01\)00141-8](http://dx.doi.org/10.1016/s0378-4371(01)00141-8)
7. Helbing D, Molnár P. Social force model for pedestrian dynamics. *Physical Review E*. 1995 May; 51(5):4282–4286. Available from: <http://dx.doi.org/10.1103/physreve.51.4282>
8. Yu WJ, Chen R, Dong LY, Dai SQ. Centrifugal force model for pedestrian dynamics. *Physical Review E*. 2005 Aug; 72(2):026112+. Available from: <http://dx.doi.org/10.1103/physreve.72.026112>
9. Lamarche F, Donikian S. Crowd of virtual humans: a New approach for real time navigation in complex and structured environments. *Computer Graphics Forum*. 2004 Sep; 23(3):509–518. Available from: <http://dx.doi.org/10.1111/j.1467-8659.2004.00782.x>
10. Moussaïd M, Helbing D, Theraulaz G. How simple rules determine pedestrian behavior and crowd disasters. *Proceedings of the National Academy of Sciences*. 2011 Apr; 108(17):6884–6888. Available from: <http://dx.doi.org/10.1073/pnas.1016507108>
11. Seyfried A, Steffen B, Lippert T. Basics of modelling the pedestrian flow. *Physica A: Statistical Mechanics and its Applications*. 2006 Aug; 368(1):232–238. Available from: <http://dx.doi.org/10.1016/j.physa.2005.11.052>
12. Johansson A, Helbing D, Shukla P. Specification of the social force pedestrian model by evolutionary adjustment to video tracking data. *Advances in Complex Systems*. 2007 Oct; 10:271–288. Available from: <http://dx.doi.org/10.1142/S0219525907001355>
13. Yu W, Johansson A. Modeling crowd turbulence by many-particle simulations. *Physical Review E*. 2007 Oct; 76(4):046105+. Available from: <http://dx.doi.org/10.1103/physreve.76.046105>
14. Zanlungo F, Ikeda T, Kanda T. Social force model with explicit collision prediction. *Europhysics Letters*. 2011; 93(6):68005+. Available from: <http://dx.doi.org/10.1209/0295-5075/93/68005>
15. Moussaïd M, Perozo N, Garnier S, Helbing D, Theraulaz G. The walking behaviour of pedestrian social groups and its impact on crowd dynamics. *PLoS ONE*. 2010 Apr; 5(4):e10047+. Available from: <http://dx.doi.org/10.1371/journal.pone.0010047> PMID: 20383280
16. Xu S, Duh HBL. A simulation of bonding effects and their impacts on pedestrian dynamics. *IEEE Transactions on Intelligent Transportation Systems*. 2010 Mar; 11(1):153–161. Available from: <http://dx.doi.org/10.1109/tits.2009.2036152>
17. Zanlungo F, Ikeda T, Kanda T. Potential for the dynamics of pedestrians in a socially interacting group. *Physical Review E*. 2014; 89:012811+. Available from: <http://dx.doi.org/10.1103/PhysRevE.89.012811>
18. Kwak J, Jo HH, Luttinen T, Kosonen I. Collective dynamics of pedestrians interacting with attractions. *Physical Review E*. 2013 Dec; 88(6):062810+. Available from: <http://dx.doi.org/10.1103/PhysRevE.88.062810>
19. Wickens CD, Hollands JG. *Engineering psychology and human performance*. 3rd ed. Prentice Hall; 1999.
20. Goldstein EB. *Sensation and perception*. 7th ed. Thomson Wadsworth; 2007.
21. Milgram S, Bickman L, Berkowitz L. Note on the drawing power of crowds of different size. *Journal of Personality and Social Psychology*. 1969 Oct; 13(2):79–82. Available from: <http://dx.doi.org/10.1037/h0028070>
22. Gallup AC, Hale JJ, Sumpter DJT, Garnier S, Kacelnik A, Krebs JR, et al. Visual attention and the acquisition of information in human crowds. *Proceedings of the National Academy of Sciences*. 2012 May; 109(19):7245–7250. Available from: <http://dx.doi.org/10.1073/pnas.1116141109>
23. Bearden WO, Netemeyer RG, Teel JE. Measurement of consumer susceptibility to interpersonal influence. *Journal of Consumer Research*. 1989; 15(4):473–481. Available from: <http://dx.doi.org/10.1086/209186>
24. Childers TL, Rao AR. The influence of familial and peer-based reference groups on consumer decisions. *Journal of Consumer Research*. 1992; 19(2):198–211. Available from: <http://dx.doi.org/10.1086/209296>
25. Kaltcheva VD, Weitz BA. When should a retailer create an exciting store environment? *Journal of Marketing*. 2006 Jan; 70:107–118. Available from: <http://dx.doi.org/10.1509/jmkg.2006.70.1.107>
26. Nicolis S, Fernández J, Pérez-Penichet C, Noda C, Tejera F, Ramos O, et al. Foraging at the edge of chaos: Internal clock versus external forcing. *Physical Review Letters*. 2013; 110:268104+. Available from: <http://dx.doi.org/10.1103/PhysRevLett.110.268104> PMID: 23848927

27. Wu F, Huberman BA. Novelty and collective attention. *Proceedings of the National Academy of Sciences*. 2007 Nov; 104(45):17599–17601. Available from: <http://dx.doi.org/10.1073/pnas.0704916104>
28. Helbing D, Farkas IJ, Vicsek T. Freezing by heating in a driven mesoscopic system. *Physical Review Letters*. 2000 Feb; 84(6):1240–1243. Available from: <http://dx.doi.org/10.1103/physrevlett.84.1240> PMID: [11017488](https://pubmed.ncbi.nlm.nih.gov/11017488/)
29. Lam SY, Vandenbosch M, Hlland J, Pearce M. Evaluating promotions in shopping environments: Decomposing sales response into attraction, conversion, and spending effects. *Marketing Science*. 2001; 20(2):194–215. Available from: <http://dx.doi.org/10.1287/mksc.20.2.194.10192>
30. Perdikaki O, Kesavan S, Swaminathan JM. Effect of traffic on sales and conversion rates of retail stores. *Manufacturing & Service Operations Management*. 2012; 14(1):145–162. Available from: <http://dx.doi.org/10.1287/msom.1110.0356>

Publication III

Kwak, J., Jo, H-H., Luttimen, T., and Kosonen, I. Jamming transitions induced by an attraction in pedestrian flow. *Physical Review E*, Volume 96, 2, 022319, August 2017.

© 2017 American Physical Society.

Reprinted with permission.

Jamming transitions induced by an attraction in pedestrian flow

Jaeyoung Kwak,^{1,*} Hang-Hyun Jo,^{2,3,4} Tapio Luttinen,¹ and Iisakki Kosonen¹

¹*Department of Built Environment, Aalto University, Espoo, Finland*

²*Asia Pacific Center for Theoretical Physics, Pohang, Republic of Korea*

³*Department of Physics, Pohang University of Science and Technology, Pohang, Republic of Korea*

⁴*Department of Computer Science, Aalto University, Espoo, Finland*

(Dated: August 24, 2017)

We numerically study jamming transitions in pedestrian flow interacting with an attraction, mostly based on the social force model for pedestrians who can join the attraction. We formulate the joining probability as a function of social influence from others, reflecting that individual choice behavior is likely influenced by others. By controlling pedestrian influx and the social influence parameter, we identify various pedestrian flow patterns. For the bidirectional flow scenario, we observe a transition from the free flow phase to the freezing phase, in which oppositely walking pedestrians reach a complete stop and block each other. On the other hand, a different transition behavior appears in the unidirectional flow scenario, i.e., from the free flow phase to the localized jam phase and then to the extended jam phase. It is also observed that the extended jam phase can end up in freezing phenomena with a certain probability when pedestrian flux is high with strong social influence. This study highlights that attractive interactions between pedestrians and an attraction can trigger jamming transitions by increasing the number of conflicts among pedestrians near the attraction. In order to avoid excessive pedestrian jams, we suggest suppressing the number of conflicts under a certain level by moderating pedestrian influx especially when the social influence is strong.

PACS numbers: 89.40.-a, 89.65.-s, 05.65.+b

I. INTRODUCTION

Collective dynamics of many-body systems has attracted much attention in the fields of statistical physics and its neighboring disciplines. As for the examples, one finds the collective motions of particles [1], vehicles [2], pedestrians [3], and animals [4]. This subject has been studied by modeling a set of individual behavioral rules in order to quantify emergent collective patterns from interactions among individuals. Based on this approach, various interesting collective behaviors have been identified such as the coherent state in highway traffic [5] and lane formation in pedestrian flow [3]. These collective behaviors are interesting not only because they arise without any external controls but also because they improve the efficiency of traffic flow. However, for the density of particles above a certain level, the interactions among individuals may cause jamming transitions that reduce the traffic flow efficiency [6–8]. Jamming transitions have generated considerable research interest, not only because of their relevance to collective dynamics including the clogging effect in granular flow [9] and the faster-is-slower effect in pedestrian evacuations [10], but also for practical applications such as monitoring congestion on freeways [11, 12] and developing adaptive cruise control strategies [13].

In order to understand jamming transitions and related phenomena in pedestrian flow, experimental studies have been performed for unidirectional [14, 15] and bidi-

rectional flow scenarios [16–18]. Seyfried *et al.* [14] and Zhang *et al.* [15, 18] studied the shape of fundamental diagrams based on various pedestrian flow experiments. For different sizes of two oppositely walking pedestrian groups, Kretz *et al.* [16] examined the characteristics of bidirectional flow by looking into passing times, walking speeds, fluxes, and lane formation. Feliciani and Nishinari [17] investigated the lane formation process based on experiment data of different directional split in bidirectional flow. Pedestrian flow through bottlenecks has been also actively studied [19–21]. Those bottleneck studies analyzed the influence of bottleneck width on pedestrian flow including bottleneck capacity, time headways, and total times to flee all the pedestrians from the bottleneck. Up to now, most of pedestrian bottleneck studies have been performed for static bottlenecks, meaning that the bottlenecks are at fixed locations and their size does not change over time.

Jamming transitions in pedestrian flow have also been investigated for various situations based on numerical simulations. With the lattice gas model, Muramatsu *et al.* [22] studied jamming transitions as a function of pedestrian density in bidirectional flow and observed a freezing transition for high pedestrian density in a straight corridor. Later, Tajima *et al.* [23] identified a jamming transition from free flow to saturated flow at a critical density. Above the critical density, the pedestrian flow rate stays constant against increasing density, defining the saturated flow rate. They also presented the scaling behavior of the saturated flow rate and critical density depending on the width of the bottleneck and corridor. For an evacuation scenario, Helbing *et al.* [10] found that an arch-like blocking appears in front of an

* jaeyoung.kwak@aalto.fi

exit which significantly increases the evacuation time. In another study, they reported that a noise term in the equation of pedestrian motion can reproduce a freezing phenomenon in which pedestrian flow reaches a complete stop [24]. Recently, Yanagisawa investigated the influence of memory effect on bidirectional flow in a narrow corridor. When the memory-loss rate is above a certain value, oppositely walking pedestrians fail to avoid encountering each other, leading to clogging [25].

A considerable amount of literature has reported jamming transitions in the flow of pedestrians walking from one point to another. In addition, previous studies provided narrative descriptions of the case interacting with attractions such as shop displays and public events. For instance, Goffman [26] described that window shoppers act like obstructions to passersby on streets when they stop to check store displays. Those shoppers can further interfere with other pedestrians when the shoppers enter and leave the stores. In another study, Gipps and Marksjö [27] stated that an attraction in a pedestrian facility can attract nearby pedestrians, and such an attraction may impede pedestrian traffic especially during peak periods.

Although it has been well recognized that an attraction can trigger pedestrian jams, little attention has been paid to characterize the dynamics of their jamming transitions. In pedestrian facilities, pedestrians can see the attractions and might shift their attention towards the attractions. If the attractions are tempting enough, a fair number of pedestrians gather around the attractions, forming attendee clusters. In our previous studies [28, 29], we characterized collective patterns of attendee clusters, and investigated how such various patterns can emerge from attractive interactions between pedestrians and attractions. Nevertheless, little is known about how an attendee cluster can contribute to jamming transitions in pedestrian flow. It is apparent that if a large attendee cluster exists near an attraction, passersby are forced to walk through the reduced available space. Consequently, the attendee cluster is acting as a pedestrian bottleneck for passersby. The flow through the bottleneck can show transitions from free flow to jamming states and may end in gridlock. The jamming transitions near an attraction will be the subject of this paper. In the following, we investigate jamming patterns induced by the attraction and understand the transitions at a microscopic level.

By means of numerical simulations, we characterize jamming transitions in pedestrian flow interacting with an attraction. The simulation model and its setup are explained in Sec. II. Then we analyze the spatio-temporal patterns of jamming transitions induced by an attraction and summarize the results with phase diagrams, as shown in Sec. III. We provide microscopic understanding of the jamming transitions by mainly looking into conflicts among pedestrians. Finally, we discuss the findings of this study in Sec. IV.

II. MODEL

Following the work of Helbing and Molnár [3], we describe the motion of pedestrian i with the following equation:

$$\frac{d\vec{v}_i(t)}{dt} = \frac{v_d\vec{e}_i - \vec{v}_i}{\tau} + \sum_{j \neq i} \vec{f}_{ij} + \sum_B \vec{f}_{iB}. \quad (1)$$

The first term on the right hand-side is the driving force term indicating that pedestrian i adjusts walking velocity \vec{v}_i in order to achieve a desired walking speed v_d along with the desired walking direction vector \vec{e}_i . Here \vec{e}_i is a unit vector pointing to the direction in which pedestrian i wants to move. The relaxation time τ controls how quickly the pedestrian adapts one's velocity to the desired velocity. The repulsive force terms \vec{f}_{ij} and \vec{f}_{iB} reflect the pedestrian's collision avoidance behavior against another pedestrian j and the boundary B , respectively. In this section, the details of Eq. (1) and the numerical simulation setup are explained.

A. Desired walking speed

Previous studies have reported that preventing excessive overlaps among pedestrians is important to provide better representation of pedestrian stopping behavior, which often triggers jams. Parisi *et al.* [30] introduced the respect area, which reserves a space on the order of pedestrian radius, in order to suppress overlapping among pedestrians. Later, Chraïbi *et al.* [31] proposed an interpersonal repulsion model that can prevent overlapping in one dimensional pedestrian flow. In their models, the driving force term becomes inactive when a pedestrian does not have enough room for stride. Inspired by those studies, we postulate that the desired speed v_d is an attainable speed of pedestrian i depending on the available walking space in front of the pedestrian,

$$v_d = \min\{v_0, d_{ij}/T_c\}, \quad (2)$$

where v_0 is a comfortable walking speed and d_{ij} is the distance between pedestrian i and the first pedestrian j encountering with pedestrian i in the course of \vec{v}_i . Time-to-collision T_c represents how much time remains for a collision of two pedestrians i and j . Further details of T_c are given in Appendix B.

B. Collision avoidance behavior

The collision avoidance behavior is modeled with \vec{f}_{ij} and \vec{f}_{iB} . Previous studies [3, 28, 29, 32] specified the interpersonal repulsion term \vec{f}_{ij} as a derivative of repulsive potential with respect to $\vec{d}_{ij} \equiv \vec{x}_i - \vec{x}_j$. It is given as

$$\vec{f}_{ij} = -\nabla_{\vec{d}_{ij}} \left[C_p l_p \exp\left(-\frac{b_{ij}}{l_p}\right) \right] \omega_{ij}. \quad (3)$$

Here, C_p and l_p are the strength and range of the interpersonal repulsion, and $b_{ij} = \frac{1}{2}\sqrt{(\|\vec{d}_{ij}\| + \|\vec{d}_{ij} - \vec{y}_{ij}\|)^2 - \|\vec{y}_{ij}\|^2}$ is the effective distance between pedestrians i and j by assuming their relative displacement $\vec{y}_{ij} \equiv (\vec{v}_j - \vec{v}_i)\Delta t_s$ with the stride time Δt_s [32]. The anisotropic function ω_{ij} represents the directional sensitivity to pedestrian j ,

$$\omega_{ij} = \lambda_{ij} + (1 - \lambda_{ij})\frac{1 + \cos \phi_{ij}}{2}, \quad (4)$$

where $0 \leq \lambda_{ij} \leq 1$ is pedestrian i 's minimum anisotropic strength against pedestrian j . In addition, the angle ϕ_{ij} is measured between the velocity vector of the pedestrian i , \vec{v}_i , and relative location of pedestrian j with respect to pedestrian i , $\vec{d}_{ji} = \vec{x}_j - \vec{x}_i$.

The boundary repulsion is given as $\vec{f}_{iB} = C_b \exp[(r_i - d_{iB})/l_b]\vec{e}_{iB}$, where d_{iB} is the perpendicular distance between pedestrian i and wall B , and \vec{e}_{iB} is the unit vector pointing from the wall B to the pedestrian i . The strength and the range of repulsive interaction from boundaries are denoted by C_b and l_b , respectively.

C. Joining behavior

It has been widely believed that individual choice behavior can be influenced by the choice of other individuals. For instance, previous studies on stimulus crowd effects reported that a pedestrian is more likely to shift his attention towards the crowd as its size grows [33, 34]. This belief is also generally accepted in the marketing area, which can be interpreted that having more visitors in a store can attract more pedestrians to the store [35, 36]. It is also suggested that the sensitivity to others' choice is different for different places, time-of-day, and visitors' motivation [34, 37]. Based on those studies [33–37], we assume that an individual decides whether to visit an attraction based on the number of pedestrians attending the attraction. The sensitivity to others' choice can be represented as the social influence parameter s . As suggested by Ref. [29], we formulate the probability of joining an attraction P_a by the analogy with sigmoidal choice rule [33, 34, 38],

$$P_a = \frac{s(N_a + K_a)}{(N_0 + K_0) + s(N_a + K_a)}. \quad (5)$$

Here, N_a and N_0 are the number of pedestrians who have already joined and that of the pedestrians not stopping by the attraction, respectively. In order to prevent the indeterminate case of Eq. (5), we set K_a and K_0 as baseline values for N_a and N_0 . The social influence parameter $s > 0$ can be also understood as pedestrians' awareness of the attraction. According to previous studies [33, 34, 37], we assume that the strength of social influence can be different for different situations and can be controlled in the presented model. Once an individual has joined an

attraction, the individual will then stay near the attraction for an exponentially distributed time with an average of t_d [3, 29, 34]. After the duration of visit, one leaves the attraction and continues walking towards one's initial destination, not visiting the attraction again.

D. Steering behavior of passersby

While attracted pedestrians are joining the attraction according to Eq. (5), passersby are the pedestrians who are not interested in the attraction, thus they do not visit the attraction. In this study, we assume passersby aim at smoothly bypassing an attendee cluster near the attraction while walking towards their destination.

Various approaches are available for modeling pedestrian steering behavior, including the pedestrian stream model [39], the Voronoi diagram based approach [40], and dynamic floor field models [41–44]. Among these approaches, the dynamic floor field models have been widely applied to model pedestrian steering behavior. Similar to cellular automata based pedestrian models [45, 46], the dynamic floor field models discretize the pedestrian walking space into grids on the order of pedestrian size. In line with the eikonal equation, the walking speed at each grid point is assumed to be inversely proportional to the derivative of the expected travel time function. That is, a pedestrian standing at the grid point is going to walk in a direction minimizing the expected travel time to a destination. The expected travel time is updated based on the local pedestrian density at every time step. Analogously to wave propagation in fluids, the expected travel time is calculated along a pathway from the destination to the grid point, inferring that pedestrians can plan ahead to take a pathway offering the shortest travel time. That is, the dynamic floor field models consider that pedestrians walk along the fastest way to the destination. Previous studies demonstrated that using the models can significantly improve pedestrian steering behavior in numerical simulations [41–43]. However, the approach is computationally expensive mainly due to the calculation of the local density for almost every time step.

For computational efficiency, we employ streamline approach to steer passersby between boundaries of the corridor. Similar to the potential flow in fluid dynamics [47, 48] and the pedestrian stream model [39], streamlines are used to represent plausible trajectories of particles smoothly bypassing obstacles. For a location $z = (x, y)$, the pedestrian velocity components in the x - and y -directions are expressed as partial derivatives of a streamline function. In this study, the streamline function is formulated as a function of attendee cluster size, so that passersby can detour around an attendee cluster near the attraction. The attendee cluster size is measured at every time step. See Appendix A for more details. According to the streamline approach, pedestrians decide their walking direction in response to immediate changes around them rather than based on a prediction of travel

time to the destination. In contrast to the dynamic floor field models, the streamline approach is computationally efficient because it does not require one to compute the local density at every time step.

E. Numerical simulation setup

Each pedestrian is modeled by a circle with radius $r_i = 0.2$ m. Pedestrians move in a corridor of length $L = 60$ m and width $W = 4$ m in the horizontal direction. An attraction is placed at the center of the lower wall. Pedestrians move with comfortable walking speed $v_0 = 1.2$ m/s and with relaxation time $\tau = 0.5$ s, and their speed cannot exceed $v_{\max} = 2.0$ m/s. The parameters of the repulsive force terms are given based on previous works: $C_p = 3$, $l_p = 0.3$, $\Delta t_s = 2.5$, $C_b = 6$, and $l_b = 0.3$ [3, 28, 29, 32, 49]. The minimum anisotropic strength λ_{ij} is set to 0.25 for attendees near the attraction and 0.5 for others, yielding that the attendees exert smaller repulsive force on others than passersby do. Consequently, the attendees can stay closer to the attraction while being less disturbed by the passersby.

The social force model in Eq. (1) is updated for each simulation time step $\Delta t = 0.05$ s. Following previous studies [50–52], we employ the first-order Euler method for numerical integration of Eq. (1). We refer the readers to Appendix C for further details. We note that $\Delta t = 0.05$ s yields good results in our numerical simulations without excessive overlaps among pedestrians. This is possible because pedestrians reduce their desired walking speed when they encounter other pedestrians in a course of collision. Smaller values of Δt can be selected for better resolution of pedestrian trajectories [53]. Based on Eq. (5), the joining probability is updated for every 0.05 s. For convenience, the evaluation time of Eq. (5) is the same value as Δt . As pointed out by Ref [54], there is no established value for update frequency of pedestrian decision. An individual evaluates the joining probability when one can perceive the attraction 10 m ahead. If the individual decides to join the attraction, then the desired direction vector \vec{e}_i is changed from $\vec{e}_{i,0}$ into \vec{e}_{Ai} . Here, $\vec{e}_{i,0}$ and \vec{e}_{Ai} are unit vectors indicating the initial desired walking direction of pedestrian i and pointing from pedestrian i to the attraction, respectively. For simplicity, K_a and K_0 are set to be 1, meaning that both options are equally attractive when the individual would see nobody within 10 m from the center of the attraction. An individual i is counted as an attending pedestrian if pedestrian i 's efficiency of motion $E_i \equiv (\vec{v}_i \cdot \vec{e}_{i,0})/v_0$ is lower than 0.05 within a range of 1 m from the boundary of the attendee cluster. The individual efficiency of motion E_i indicates how much the driving force contributes to pedestrian i 's progress towards the destination with a range from 0 to 1 [24, 28]. We assumed that $E_i = 0.05$ is tolerant enough to distinguish a weak motion of attendees near an attraction from actively walking pedestrians not visiting the attraction. The average duration of visiting

an attraction t_d is set to be 30 s.

For our numerical simulations, a straight corridor will be considered to study pedestrian jams induced by an attraction. In the straight corridor, one can consider two possible patterns of flow, i.e., bidirectional and unidirectional flows. In the bidirectional flow, one half of the population is walking towards the right boundary of the corridor from the left, and the opposite direction for the other half. In the unidirectional flow, all pedestrians are entering the corridor through the left boundary and walking towards the right.

An open boundary condition is employed in order to continuously supply pedestrians to the corridor. By doing so, pedestrians can enter the corridor regardless of the number of leaving pedestrians. Pedestrians are inserted at random places on either side of the corridor without overlapping with other nearby pedestrians and boundaries. The number of pedestrians in the corridor is associated with the pedestrian influx Q , i.e., the arrival rate of pedestrians entering the corridor. The unit of Q is indicated by P/s, which stands for pedestrians per second. Based on previous studies [55, 56], the pedestrian interarrival time is assumed to follow a shifted exponential distribution. That is, pedestrians are entering the corridor independently and their arrival pattern is not influenced by that of others. The minimum headway is set to 0.4 s between successive pedestrians entering the corridor, which is large enough to prevent overlaps between arriving pedestrians.

III. RESULTS AND DISCUSSION

A. Jam patterns in bidirectional flow

Our simulation results show different patterns of pedestrian motion depending on influx Q and social influence parameter s . The free flow phase appears when both Q and s are small. From Fig. 1(a), one can observe that passersby walk towards their destinations without being interrupted by the cluster of attracted pedestrians. Passersby walking to the right form lanes in lower part of the corridor while the upper part of the corridor is occupied by passersby walking to the left. This spatial segregation appears as a result of the lane formation process which has been reported in previous studies [3, 16–18]. Simultaneously, the attracted pedestrians form a stable cluster near the attraction. If both Q and s are large, we can see freezing phase, in which oppositely walking pedestrians reach a complete stop because they block each other, as shown in Fig. 1(b).

To quantify spatio-temporal patterns of pedestrian flow, we measure the local efficiency $E(x, t)$ for a given time t and segment x in the horizontal direction:

$$E(x, t) = \frac{1}{|N(x, t)|} \sum_{i \in N(x, t)} E_i. \quad (6)$$

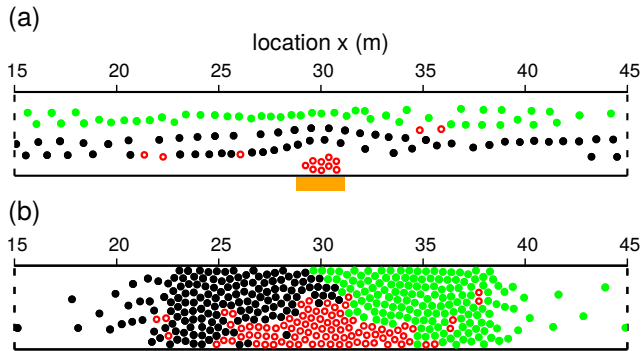


FIG. 1. (Color online) Representative snapshots of different passerby flow patterns, showing a section of 30 m in the center of the corridor, i.e., $15 \text{ m} \leq x \leq 45 \text{ m}$. The attraction, depicted by an orange rectangle, is located at the center of the lower wall with open boundary conditions in the horizontal direction. Closed black and green circles indicate passersby walking to the right and to the left, respectively. Open red circles depict pedestrians attracted by the attraction. In bidirectional flow, we can observe (a) the free flow phase in the case of $Q = 4 \text{ P/s}$ and $s = 0.5$, in which passersby can walk towards their destinations without being interrupted by the cluster of attracted pedestrians, and (b) the freezing phase in the case of $Q = 4 \text{ P/s}$ and $s = 1$, where oppositely walking pedestrians stopped because they block each other. Note that P/s stands for pedestrians per second, being the unit of pedestrian flux Q .

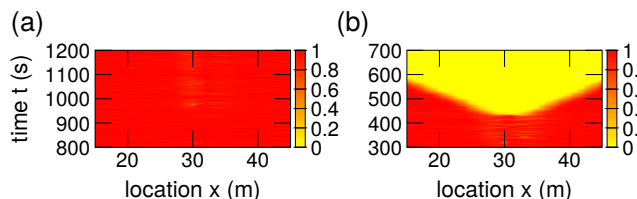


FIG. 2. (Color online) Local efficiency for a given time t and location x , $E(x, t)$, for different pedestrian flow patterns in bidirectional flow. The attraction is located at $x = 30 \text{ m}$, at the center of the corridor. Light yellow and dark red colors indicate lower and higher values, respectively. (a) Free flow phase with $Q = 4 \text{ P/s}$ and $s = 0.5$, and (b) Freezing phase with $Q = 4 \text{ P/s}$ and $s = 1$. Note that the spatio-temporal representation of local efficiency is dark red for (a) $t < 800 \text{ s}$ and $t > 1200 \text{ s}$ and (b) $t < 300 \text{ s}$.

Here $N(x, t)$ is the set of passersby in a 1 m long segment x at time t . The individual efficiency of motion $E_i = (\vec{v}_i \cdot \vec{e}_{i,0})/v_0$ can be understood as a normalized speed of pedestrian i in the horizontal direction. The local efficiency $E(x, t)$ indicates how fast passersby in segment x progress towards their destination at time t . If $|N(x, t)| = 0$, we set to $E(x, t) = 1$ inferring that the passersby can walk with their comfortable speed v_0 if they are in the segment x at time t . Thus, $E(x, t) = 1$ indicates that the passersby can freely walk without reducing their speed, while $E(x, t) = 0$ implies that the passersby have reached a standstill.

Figure 2 shows the corresponding spatio-temporal rep-

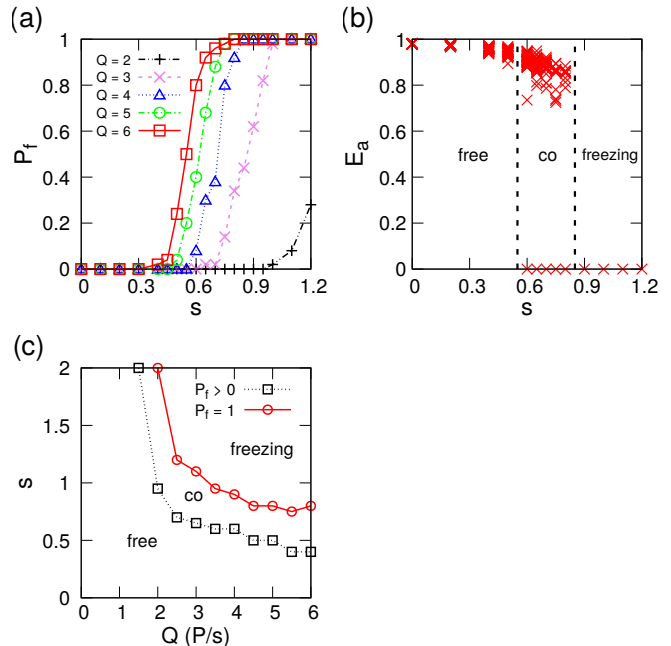


FIG. 3. (Color online) (a) Freezing probability P_f as a function of influx Q and social influence parameter s in bidirectional flow. Different symbols represent different values of Q . (b) Stationary state average of local efficiency near the attraction E_a against s in bidirectional flow with $Q = 4 \text{ P/s}$. Each point depicts a value of E_a obtained from one simulation run. Here, free, freezing, and co indicate free flow phase, freezing phase, and coexisting phase, respectively. In coexisting phase, one can observe freezing phenomena with a certain probability P_f . (c) Phase diagram summarizing the numerical results of bidirectional flow. The parameter space of pedestrian influx Q and social influence parameter s is divided into different phases by means of P_f for bidirectional flow.

resentation of different pedestrian flow patterns. As shown in Fig. 2(a), in the free flow phase, the local efficiency $E(x, t)$ is almost 1 over the stationary state period, meaning that all the passersby walk with their comfort speed. In the freezing phase, the local efficiency $E(x, t)$ suddenly becomes zero near the attraction around at $t = 450 \text{ s}$, and then the low efficiency area expands to the left and right boundaries of the corridor in the course of time [see Fig. 2(b)].

Next, we identify the freezing phase by means of cumulative throughput at $x = 30 \text{ m}$, according to Ref. [57]. If the cumulative throughput does not change for 120 s , it infers the appearance of the freezing phenomenon. We obtain the freezing probability P_f by counting the occurrence of freezing phenomena over 50 independent simulation runs for each parameter combination (Q, s) . The freezing probability P_f tends to increase as Q and s increase, see Fig. 3(a). For small value of $Q \leq 1.4 \text{ P/s}$, P_f is zero up to $s = 2$, indicating that the freezing phenomenon is not observable. We classify parameter combinations of (Q, s) yielding $P_f = 0$ as the free flow phase and $P_f = 1$ for the freezing phase. We call the parameter space between the envelopes of $P_f = 0$ and $P_f = 1$ as

the coexisting phase, noting that both phases can appear depending on random seeds in the numerical simulations.

In order to further quantify different phases, we calculate stationary state average of local efficiency, $E(x)$, in the vicinity of the attraction. Here, $E(x)$ is given as

$$E(x) = \langle E(x, t) \rangle, \quad (7)$$

where $\langle \cdot \rangle$ represents the average obtained from a simulation run after reaching the stationary state. We select a section of $27 \text{ m} \leq x \leq 33 \text{ m}$ to evaluate the stationary state average value in the vicinity of the attraction, and the minimum value of $E(x)$ is denoted by E_a . Note that E_a is selected in a way to reflect the largest possible efficiency drop in the section. Figure 3(b) presents E_a against s in the case of $Q = 4 \text{ P/s}$. One can observe that E_a is almost 1 for $s < 0.6$, depicting the free flow phase. For $0.6 \leq s \leq 0.8$, some data points of E_a are positive while others are zero. That is, two distinct pedestrian flow patterns can be observed for the same value of s depending on random seeds. For $s > 0.8$, E_a is always zero, corresponding to the freezing phase.

Figure 3(c) summarizes numerical results of phase characterizations. The parameter space of pedestrian influx Q and social influence parameter s is divided into different phases by means of P_f . In the coexisting phase, one can observe freezing phenomena with a certain probability P_f .

B. Jam patterns in unidirectional flow

In unidirectional flow, we can also define the free flow phase if Q and s are small [see Fig. 4(a)]. The localized jam phase appears in the vicinity of the attraction for medium and high Q with the intermediate range of s , as can be seen from Fig. 4(b). Passersby walk slow near the attraction because of reduced walking area, and then they recover their speed after walking away from the attraction. One can observe that pedestrians walking away from the attraction tend to form lanes. This is possible because the standard deviation of speed among the walking away pedestrians is not significant after the pedestrians recover their speed. According to the study of Moussaïd *et al.* [58], the formation of pedestrian lanes is stable when pedestrians are walking at nearly the same speed. Once the walking away pedestrians form lanes, the lanes are not likely to collapse. An extended jam phase can be observed when both Q and s are large, in which the pedestrian queue is growing towards the left boundary and then the queue is persisting for a long period of time [see Fig. 4(c)]. In the extended jam phase, the attendee cluster does not maintain its semi-circular shape any more in that passersby seize up the attracted pedestrians. Meanwhile, pedestrians in the queue still can slowly walk towards the right side of the corridor as they initially intended. When Q and s are very large, the extended jam phase can end up in freezing phenomena

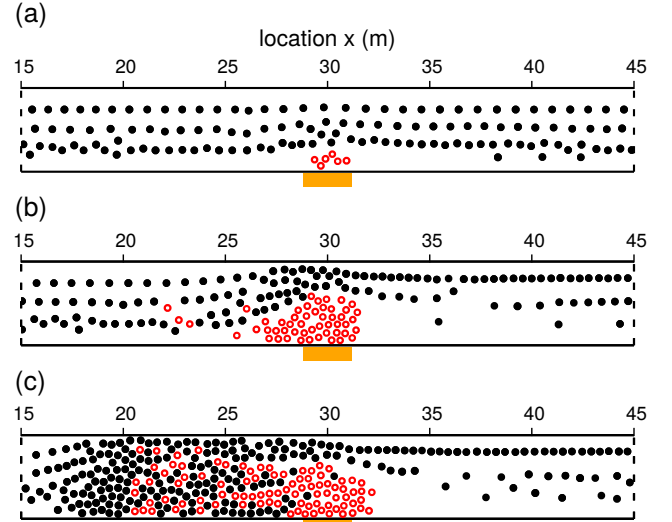


FIG. 4. (Color online) Same as Fig. 1, but for unidirectional flow. Passersby are walking from the left to the right. We can observe (a) free flow phase in case of $Q = 5 \text{ P/s}$ and $s = 0.5$, which is similar to the case of bidirectional flow, (b) localized jam phase in case of $Q = 5 \text{ P/s}$ and $s = 1$, in which passersby walk slow near the attraction before they pass the area, and (c) extended jam phase in case of $Q = 5 \text{ P/s}$ and $s = 1.8$, in which the passersby queue is growing towards the left boundary. Sometimes the extended jam phase ends up in freezing phenomena if Q and s are very large.

with a certain probability, indicating that passersby cannot proceed beyond the attraction due to the clogging effect. Some passersby are pushed out towards the attraction by the attracted pedestrians and inevitably they prevent attracted pedestrians from joining the attraction. Consequently, the attracted pedestrians cannot approach the boundary of the attendee cluster although they keep their walking direction towards the attraction. Simultaneously, the passersby near the attraction attempt to walk away from the attraction, but they cannot because they are blocked by the attracted pedestrians. Eventually, the pedestrian movements near the attraction come to a halt.

In order to reflect speed variation among passersby for a given time t and segment x , we introduce the local standard deviation $\sigma(x, t)$, which is given as

$$\sigma(x, t) = \sqrt{\frac{1}{|N(x, t)|} \sum_{i \in N(x, t)} [E_i - E(x, t)]^2}. \quad (8)$$

If $\sigma(x, t)$ is 0, the speed of passersby is homogeneous in segment x for a given time t . On the other hand, large $\sigma(x, t)$ indicates significant speed difference among passersby, and possibly suggests the existence of stop-and-go motions in passerby flow with low local efficiency [31, 59, 60].

As can be seen from Fig. 5(a), in the localized jam phase, one can observe a low-efficiency area in the vicinity of the attraction. In the low-efficiency area, passersby are

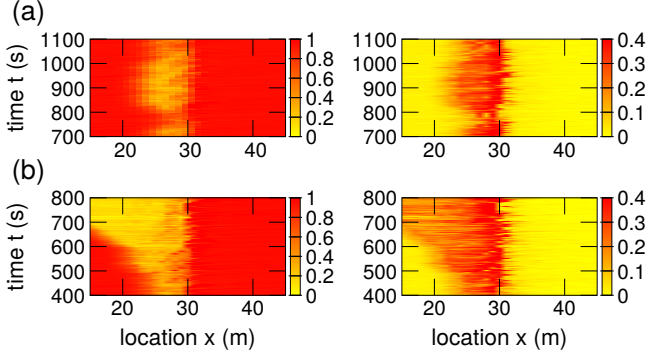


FIG. 5. (Color online) Plots of $E(x,t)$ (left column) and $\sigma(x,t)$ (right column) for different pedestrian jam patterns for unidirectional flow with $Q = 5$ P/s and $s = 1$, in which passersby are likely to reduce their speed near the attraction and then speed up when they walk away from the attraction. The local standard deviation $\sigma(x,t)$ is notable in the low efficiency area, reflecting that some passersby walk with high speed while others walk slowly. (b) Extended jam phase in unidirectional flow with $Q = 5$ P/s and $s = 1.8$. The low efficiency area begins to expand towards the left at near $t = 500$ s, and then the local efficiency remains low for a long period of time over a spatially extended area.

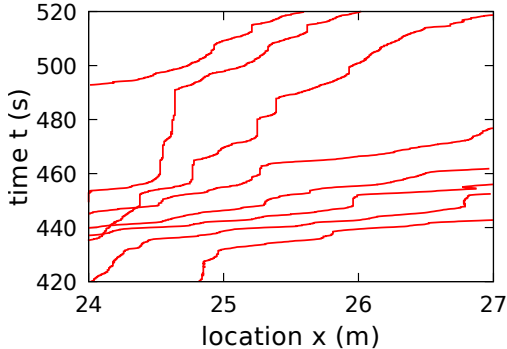


FIG. 6. (Color online) Representative trajectories of passersby in the extended jam phase ($Q = 5$ P/s and $s = 1.8$). One can observe that the progress of the passersby is interrupted several times, indicating stop-and-go motions near the attraction.

likely to reduce their speed near the attraction and then speed up when they walk away from the attraction. In the extended jam phase, the low-efficiency area appears near the attraction as in the localized jam [see Fig. 5(b)]. In contrast to the case of localized jam, the low efficiency area begins to extend towards the left boundary and then the local efficiency remains low for a long period of time over a spatially extended area. In the low-efficiency area, some passersby move while others are at near standstill, and consequently stop-and-go motions can be observed as reported in previous studies [31, 59, 60]. Figure 6 shows the presence of stop-and-go motions near the at-

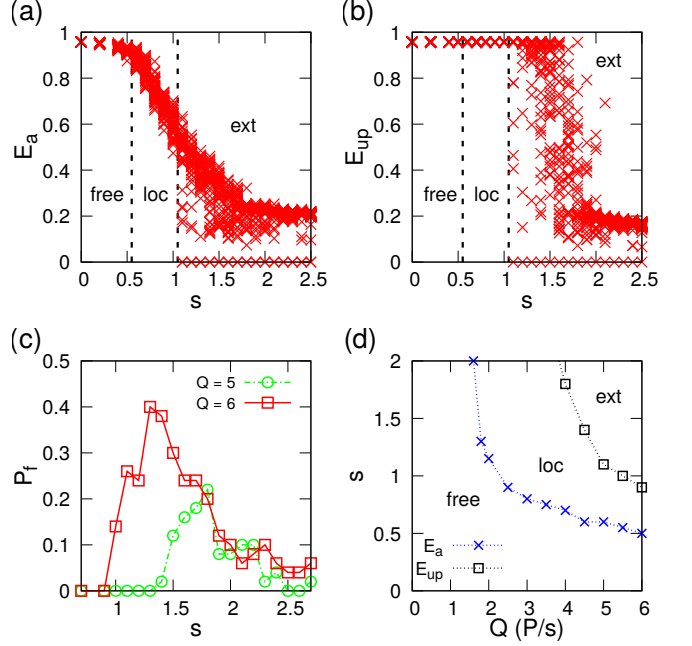


FIG. 7. (Color online) (a) Stationary state average of local efficiency near the attraction E_a against s in bidirectional flow with $Q = 5$ P/s. Each point depicts a value obtained from one simulation run. Here, free, loc, and ext indicate the free flow phase, the localized jam phase, and the extended jam phase, respectively. In the extended jam phase, one can observe freezing phenomena with a certain probability P_f . (b) Same as (a), but for E_{up} , measured upstream of the attraction. (c) Freezing probability P_f as a function of influx Q and social influence parameter s in unidirectional flow. (d) Phase diagram summarizing the numerical results of unidirectional flow. The parameter space of pedestrian influx Q and social influence parameter s is divided into different phases by means of local efficiency measures.

traction. Therefore, the local standard deviation $\sigma(x,t)$ becomes notable in the low-efficiency area. Due to the passersby flowing out from the low efficiency area, a high local standard deviation $\sigma(x,t)$ is observed near the attraction. Although the average speed of passersby is significantly decreased in the left part of the corridor, the local standard deviation $\sigma(x,t)$ is not zero, indicating that the speed variation among passersby is still observable.

Based on observations presented in Figs. 4 and 5, we characterize the localized jam and extended jam phases in terms of $E(x)$ as in Eq. (7). Similarly to the bidirectional flow scenario, we select a section of $27 \text{ m} \leq x \leq 33 \text{ m}$ to calculate E_a . Likewise, a section of $12 \text{ m} \leq x \leq 18 \text{ m}$ is selected for upstream of the attraction, and E_{up} denotes the minimum value of $E(x)$ in the section. Figures 7(a) and 7(b) provide plots of local efficiency measures in the stationary state, E_a and E_{up} , produced with $Q = 5$ P/s. For small values of s , free flow phase can be characterized by

$$E_a \approx 1 \text{ and } E_{up} \approx 1. \quad (9)$$

For $0.6 \leq s \leq 1.05$, data points of E_a show a clear decreasing trend against s . As can be seen from Fig. 7(b), data points of E_{up} are still near 1 up to $s = 1.05$. Thus, the localized jam phase can be characterized by

$$0 < E_a < 1 \text{ and } E_{up} \approx 1. \quad (10)$$

When s is larger than 1.05, some data points of E_a and E_{up} become zero, indicating that freezing phenomena can be observed. In contrast, positive E_a and E_{up} values show a decreasing trend against s for a section of $1.05 \leq s \leq 2$; then they become nearly constant if s is larger than 2. Consequently, the extended jam phase can be characterized by

$$0 \leq E_a < 1 \text{ and } 0 \leq E_{up} < 1. \quad (11)$$

In contrast to the bidirectional flow scenario, P_f is always smaller than 1 in unidirectional flow, indicating that the freezing phase does not exist [see Fig. 7(c)]. However, there exists parameter space producing $P_f > 0$, inferring that freezing phenomena can be observed depending on random seeds. Interestingly, in unidirectional flow, P_f is increasing and then decreasing against s for large Q . It can be understood that the proportion of passersby decreases considerably as s increases above a certain value, so the attracted pedestrians are less likely blocked by the passersby.

Figure 7(d) summarizes numerical results of phase characterizations. We divide the parameter space of Q and s into different phases by means of local efficiency measures, E_a and E_{up} . Note that, in the extended jam phase, one can observe freezing phenomena with a certain probability P_f .

C. Microscopic understanding of jamming transitions

In previous subsections, we have observed various jam patterns. In bidirectional flow, the free flow phase can turn into a freezing phase if Q and s are large. Jamming transitions in unidirectional flow are different from those of bidirectional flow: from free flow to localized jam, and then to extended jam phases. In addition, it is possible that the extended jam phase ends up in freezing phenomena for large Q and s .

While previous sections focused on describing collective patterns of various jam patterns, this section presents the appearance of such different patterns at the individual level in a unified way. This inspired us to take a closer look at the conflicts among pedestrians. Similar to previous studies [61, 62], we employ a conflict index to measure the average number of conflicts per passerby. When two pedestrians are in contact and hinder each other, we call this situation a conflict. The number of conflicts $N_{c,i}(t)$ is evaluated by counting the number of pedestrians who hinder the progress of passerby i at time t . In our simulations, most conflicts appear near the attraction; therefore, we calculate the conflict index for

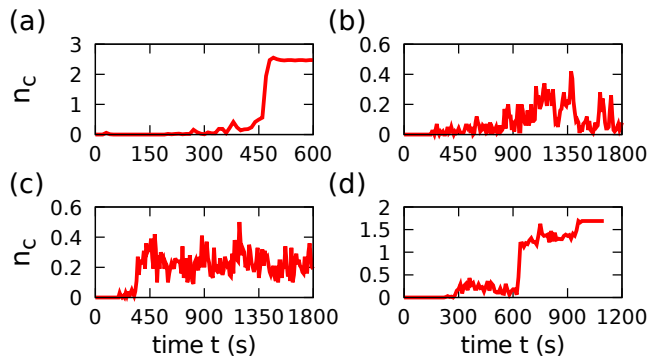


FIG. 8. (Color online) Representative time series of conflict index $n_c(t)$. (a) In the beginning, the $n_c(t)$ curve of the freezing phase in bidirectional flow with $Q = 4$ P/s and $s = 1$ is virtually zero, indicating that the pedestrian flow is initially free flow. However, the curve shows a sharp increase at near $t = 460$ s, signaling the onset of freezing phenomenon. (b) The $n_c(t)$ curve of the localized jam phase in unidirectional flow with $Q = 5$ P/s and $s = 1$ exhibits an upward trend until $t = 1350$ s, and then it shows a downward trend leading to zero. (c) For the extended jam phase in unidirectional flow with $Q = 5$ P/s and $s = 1.8$, one can see that the $n_c(t)$ curve sharply increases at near $t = 320$ s, and thereafter it oscillates around $n_c(t) = 0.25$. (d) Same parameter combination (Q, s) as (c), but with a different set of random seeds. The behavior of the $n_c(t)$ curve is similar to that of the extended jam phase until $t = 600$ s. However, the curve abruptly increases at near $t = 600$ s, indicating the appearance of the freezing phenomenon.

pedestrians in location x such that $25 \text{ m} \leq x \leq 35 \text{ m}$. The conflict index is measured as

$$n_c(t) = \frac{1}{|N_p|} \sum_{i \in N_p} N_{c,i}(t), \quad (12)$$

where N_p is the set of passersby near the attraction.

The representative time series of conflict index $n_c(t)$ are presented in Fig. 8. As can be seen from Fig. 8(a), a sharp increase of the conflict index indicates the appearance of the freezing phenomenon, which leads pedestrian flow into the freezing phase. In Fig. 8(b), the conflict index increases and then decreases in the course of time. We can observe a localized jam phase in which the jam near the attraction does not further grow upstream. Figures 8(c) and 8(d) are generated with the same parameter combination $(Q, s) = (5, 1.8)$ in unidirectional flow but with different sets of random seeds. As shown in Fig. 8(c), in the extended jam phase, the conflict index $n_c(t)$ is maintained near a certain level after reaching the stationary state, indicating the persistent jam in the corridor. In Fig. 8(d), the behavior of the $n_c(t)$ curve is similar to that of the extended jam phase in the beginning, but the curve abruptly increases at near $t = 600$ s. That is, the pedestrian flow eventually ends up in a freezing phenomenon in that conflicting pedestrians fail to coordinate their movements.

Apart from the conflict index $n_c(t)$, we have also ob-

served that increasing s for a given value of Q likely increases the size of the attendee cluster and consequently reduces the available walking space near the attraction. The narrower walking space tends to yield higher freezing probability in that pedestrians tend to have less space for resolving conflicts among them. Therefore, we suggest that an attendee cluster can trigger jamming transitions not only by reducing the available walking space but also by increasing the number of conflicts among pedestrians near the attraction. See Appendix D for further discussion of this issue.

Furthermore, changing other simulation parameters can affect the jamming transitions. For instance, increasing t_d often results in a larger attendee cluster near the attraction, activating jamming transitions for lower values of s . Larger corridor width W possibly reduces the freezing probability for a given value of s by providing additional space for resolving pedestrian conflicts. However, increasing W does not effectively reduce the freezing probability when W is large enough in that an attendee cluster can grow further as W grows. In Appendix E, we show the influence of t_d and W on jamming transitions.

D. Fundamental diagram

In addition to the phase diagram presented in Figs. 3(c) and 7(d), one can further describe the dynamics of passerby flow by means of a fundamental diagram. The fundamental diagram depicts the relationship between flow and density, which has been widely applied to analyze traffic dynamics to represent various phenomena including hysteresis [63] and capacity drop [64]. We calculate pedestrian flow quantities including density ρ , speed u , and flow J over two 6-m-long segments in length for every 5 seconds. Note that pedestrian flow quantities J , ρ , and u are calculated for passersby, not including attracted pedestrians. The details are explained in Appendix F. The first section of $27 \text{ m} \leq x \leq 33 \text{ m}$ is selected for passerby traffic near the attraction and $12 \text{ m} \leq x \leq 18 \text{ m}$ for upstream traffic.

To explore the dynamics of passerby traffic, we plot fundamental diagrams for different phases in bidirectional flow near the attraction. As shown in Fig. 9(a), in the free flow phase, a linear relationship between ρ and J is observed. The corresponding local speed u stays near comfortable walking speed $v_0 = 1.2 \text{ m/s}$. In Fig. 9(b), an inverse- λ shape is observed, reflecting that capacity drop occurs near $\rho = 1.2 \text{ P/m}^2$ and then the pedestrian traffic turns into the freezing phase as depicted in Fig. 2(b). The corresponding local speed u curve begins to sharply decrease at near $t = 460 \text{ s}$, relevant to the appearance of the congestion branch. This is similar to the metastable state induced by conflicts among pedestrians [65].

Likewise, we also plot fundamental diagrams and corresponding local speed curves for various jam patterns in unidirectional flow. Figure 9(c) shows that in the localized jam phase, (ρ, J) begins to scatter after the density

level reaches around $\rho = 1.2 \text{ P/m}^2$. The cluster of scattered data points reflects that speed fluctuation begins to appear, in agreement with Fig. 5(b). In contrast, the fundamental diagram upstream of the attraction only shows a linear relationship between ρ and J , similar to arrow 1 in Fig. 9(c). That is, upstream traffic is not influenced by the speed reduction near the attraction, thus speed fluctuation is invisible.

In the extended jam phase, a μ shape is observed in the fundamental diagram as depicted in Fig. 9(d). As indicated by arrow 2, one can see a cluster of (ρ, J) slightly off from the free flow branch, which corresponds to a moderate speed drop from near $t = 320 \text{ s}$ to near $t = 510 \text{ s}$. Simultaneously, the maximum flow rate J is lower than that in the free flow branch. This can be understood as a transition period in which local speed u is gradually decreasing. After the transition period, one can see data points of (ρ, J) widely spread over in the fundamental diagram while the local speed u slightly oscillates around $u = 0.5 \text{ m/s}$.

Figure 9(e) shows fundamental diagrams obtained from the same parameter combination (Q, s) of Fig. 9(d) but from a different set of random seeds. Similar to the case of the extended jam phase, a free flow branch appears, and then one can observe scattered data points of (ρ, J) indicating that the local speed u near the attraction gradually decreases. However, after showing such scattered data points, congestion branches are observed as indicated by the arrow in Fig. 9(e). Interestingly, the behavior of congestion branches observed from Figs. 9(e) and 9(b) is different. In Fig. 9(b), the flow J is decreasing as density ρ increases, because there are no outflowing passersby near the attraction while additional pedestrians arrive behind the stopped passersby. On the other hand, the congestion branch in Fig. 9(e) indicate that the flow J is decreasing as density ρ decreases due to passersby flowing out from the attraction.

IV. CONCLUSION

This study has numerically investigated jamming transitions in pedestrian flow interacting with an attraction. Our simulation model is mainly based on the social force model for pedestrian motions and joining probability reflecting the social influence from other pedestrians. For different values of pedestrian influx Q and the social influence parameter s , we characterized various pedestrian flow patterns for bidirectional and unidirectional flows. In the bidirectional flow scenario, we observed a transition from the free flow phase to the freezing phase in which oppositely walking pedestrians reach a complete stop and block each other. However, a different transition behavior appeared in unidirectional flow scenario: from the free flow phase to the localized jam phase, and then to the extended jam phase. One can also see that the extended jam phase end up in freezing phenomena with a certain probability when pedestrian flux is high with

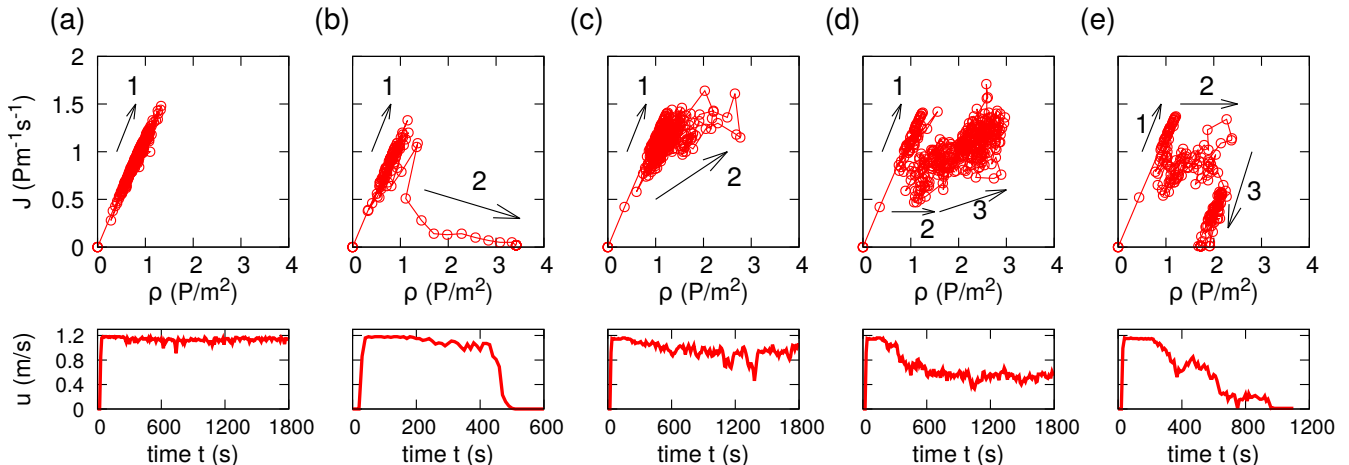


FIG. 9. (Color online) Fundamental diagram of passerby traffic near the attraction. For each panel, the upper part shows the fundamental diagram and the lower part shows the corresponding local speed u . Note that pedestrian flow quantities J , ρ , and u are calculated for passersby, not including attracted pedestrians. Arrows are guide for the eyes, indicating the evolution of fundamental diagram in the course of time. (a) Free flow phase in bidirectional flow with $Q = 4$ P/s and $s = 0.5$. (b) Freezing phase in bidirectional flow with $Q = 4$ P/s and $s = 1$. (c) Localized jam phase in unidirectional flow with $Q = 5$ P/s and $s = 1$. (d) Extended jam phase in unidirectional flow with $Q = 5$ P/s and $s = 1.8$. (e) Generated from the same parameter combination (Q, s) of as (d), but from a different set of random seeds. The passerby flow turns from an extended jam into the freezing phenomenon.

strong social influence. It is noted that these results are qualitatively the same for values of simulation time step smaller than 0.05 s, seemingly due to the introduction of an attainable walking speed in Eq. (2).

The findings of this study can be interpreted in line with the freezing-by-heating phenomenon observed in particle systems [24]. Helbing *et al.* [24] demonstrated that increasing noise intensity in particle motions leads to the freezing phenomenon, in which particles tend to block each other in a straight corridor. We observed the same phenomenon from pedestrians flow interacting with an attraction. However, it should be noted that Ref. [24] did not state possible sources of the noise, since that study presented the noise as an abstract concept. Our study suggests that existence of an attraction in pedestrian flow can be a source of such noise.

Our study highlights that attractive interactions between pedestrians and an attraction can lead to jamming transitions. From the results of numerical simulations, we observed that an attendee cluster can trigger jamming transitions not only by reducing the available walking space but also by increasing the number of conflicts among pedestrians near the attraction. The conflicts arose mainly because attracted pedestrians interfered with passersby who were not interested in the attraction. If the average number of conflicts per passerby is maintained under a certain level, the appearance of freezing phenomena can be prevented. However, when the pedestrian flux is high with strong social influence, the conflicting pedestrians may not be able to have enough time to resolve the conflicts. Therefore, we note that moderating pedestrian flux is important in order to avoid excessive pedestrian jams in pedestrian facilities when the social

influence is strong.

In order to focus on essential features of jamming transitions, this study has considered simple scenarios of pedestrian flow in a straight corridor. Further studies need to be carried out in order to improve the presented models. To mimic pedestrian stopping behavior, pedestrians are represented as non elastic solid disks, indicating that compression among pedestrians is not modeled. The interpersonal friction effect [66, 67] needs to be included in the equation of motion for crowd pressure predictions. The joining behavior model in Eq. (5) can be further improved and extended by adding additional behavioral features. For instance, explicit representation of group behavior [52] and an interest function [68] can be added to the joining behavior model. A natural progression of this work is to analyze the numerical simulation results from the perspective of capacity estimation. Capacity estimation can be performed to calculate the optimal capacity, balancing the mobility needs for passersby and the activity needs for attracted pedestrians. The concept of stochastic capacity [69–71] can also be studied as an extension of this study. In this study, for some parameter values, speed breakdown is observed depending on random seeds, inferring that capacity might follow a probability distribution. Future studies can be planned from the perspective of pedestrian flow experiments. Although the joining behavior presented in this study might not be controlled in experimental studies, the experiments can be performed for different levels of pedestrian flux and joining probability. For various experiment configurations, the number of conflicts among pedestrians can be measured and the influence of the conflicts on pedestrian jams can be analyzed.

ACKNOWLEDGEMENTS

J.K., T.L., and I.K. would like to thank Aalto Energy Efficiency research program (Light Energy-Efficient and Safe Traffic Environments project) for financial support. J.K. is grateful to CSC-IT Center for Science, Finland for providing computational resources. H.-H.J. acknowledges financial support from Basic Science Research Program through the National Research Foundation of Korea grant funded by the Ministry of Education (Grant No. 2015R1D1A1A01058958).

Appendix A: Streamline approach for passerby steering behavior

For passerby traffic moving near an attraction, an attendee cluster can act like an obstacle. We assume that passersby set their initial desired walking direction $\vec{e}_{i,0}$ along the streamlines. As reported in a previous study [29], the shape of an attendee cluster near an attraction can be approximated as a semicircle. By doing so, we can set the streamline function ψ for passerby traffic similar to the case of fluid flow around a circular cylinder in a two dimensional space [47, 48]:

$$\psi = v_0 d_{zA} \sin(\theta_z) \left(1 - \frac{r_c}{d_{zA}} \right), \quad (\text{A1})$$

where v_0 is the comfortable walking speed and d_{zA} is the distance between the center of the semicircle A and location $z = (x, y)$. The angle θ_z is measured between $y = 0$ m and \vec{d}_{zA} . The attendee cluster size at time t is denoted by $r_c = r_c(t)$. To measure r_c , we slice the walking area near the attraction into thin layers with the width of a pedestrian size (i.e., $2r_i = 0.4$ m) in the horizontal direction. From the bottom layer to the top one, we count the number of layers consecutively occupied by attendees. The attendee cluster size r_c can then be obtained by multiplying the number of consecutive layers by the layer width 0.4 m. The initial desired walking direction $\vec{e}_{i,0}$ can be obtained as

$$\vec{e}_{i,0} = \left(\frac{\partial \psi}{\partial y}, -\frac{\partial \psi}{\partial x} \right). \quad (\text{A2})$$

Note that passersby pursue their initial destination, thus their desired walking direction \vec{e}_i is identical to $\vec{e}_{i,0}$ given in Eq. (A2), i.e., $\vec{e}_i = \vec{e}_{i,0}$.

Appendix B: Time-to-collision T_c

In line with Refs. [72, 73], we assume that pedestrian i predicts time-to-collision T_c with pedestrian j by extending current velocities of pedestrians i and j , v_i and v_j , from their current positions, x_i and x_j :

$$T_c = \frac{\beta - \sqrt{\beta^2 - \alpha\gamma}}{\alpha}, \quad (\text{B1})$$

where $\alpha = \|\vec{v}_i - \vec{v}_j\|^2$, $\beta = (\vec{x}_i - \vec{x}_j) \cdot (\vec{v}_i - \vec{v}_j)$, and $\gamma = \|\vec{x}_i - \vec{x}_j\|^2 - (r_i + r_j)^2$. Note that T_c is valid for $T_c > 0$, meaning that pedestrians i and j are in a course of collision, whereas $T_c < 0$ implies the opposite case. If $T_c = 0$, the disks of pedestrians i and j are in contact.

Appendix C: Numerical integration of Eq. (1)

Based on the first-order Euler method, the numerical integration of Eq. (1) is discretized as

$$\begin{aligned} \vec{v}_i(t + \Delta t) &= \vec{v}_i(t) + \vec{a}_i(t)\Delta t, \\ \vec{x}_i(t + \Delta t) &= \vec{x}_i(t) + \vec{v}_i(t + \Delta t)\Delta t. \end{aligned} \quad (\text{C1})$$

Here, $\vec{a}_i(t)$ is the acceleration of pedestrian i at time t and the velocity of pedestrian i at time t is given as $\vec{v}_i(t)$. The position of pedestrian i at time t is denoted by $\vec{x}_i(t)$.

Appendix D: Discussion of jamming mechanisms

In Sec. III C, we discussed the dynamics of jamming transitions mainly based on the conflict index [see Eq. (12)]. This appendix provides further details of jamming mechanisms.

In both bidirectional and unidirectional flows, attracted pedestrians often trigger conflicts among pedestrians. When the attracted pedestrians are walking towards the attraction, sometimes they cross the paths of passersby and hinder their walking. Furthermore, such crossing behavior of attracted pedestrians makes others change their walking directions due to the interpersonal repulsion, possibly giving rise to conflicts among the others. Once a couple of pedestrians hinder each other, they need some time and space to resolve the conflict by adjusting their walking directions. If there is not enough space for the movement, the conflict situation cannot be resolved and turns into a blockage in pedestrian flow. Higher pedestrian flux Q can be interpreted as the conflicting pedestrians likely have less time for resolving the conflict, in that additional pedestrians arrive behind the blockage. Once the arriving pedestrians stand behind the blockage, the number of conflicts among pedestrians is rapidly increasing as indicated in Figs. 8(a) and 8(d). In the case of bidirectional flow, this freezing phenomenon is similar to the freezing-by-heating phenomenon [24]. We note, however, that the freezing phenomenon in our simulations is caused by attracted pedestrians without noise terms in the equation of motion.

The onset of freezing phenomena in bidirectional flow can be further understood by looking at streamwise velocity profiles. Figure 10 visualizes streamwise velocity profiles of passerby traffic in the corridor at $x = 30$ m where the attraction is placed. In the beginning (i.e., $t = 120$ s), one can observe that the velocity vectors of two passerby streams show distinct spatial separation, indicating that passerby lane formation appears to be

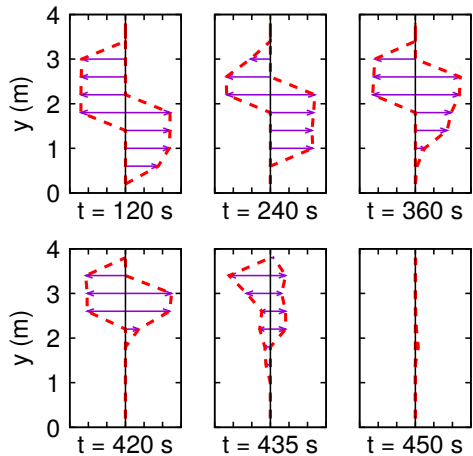


FIG. 10. (Color online) Streamwise velocity profiles of passerby traffic in the corridor at $x = 30$ m with $Q = 4$ P/s and $s = 1$ in bidirectional flow. Based on Eq. (F3), the velocity vectors are presented for eastbound and westbound passerby traffic in the right and left parts of each panel, respectively. In the course time, the velocity profile curves are gradually shifting upward while their magnitude decreases.

well maintained. We notice that the velocity magnitude near the bottom of the corridor is virtually zero when the attendee cluster becomes active. In the course of time, the velocity distribution curves shrink while the curves are gradually shifting upward. This implies that two passerby streams moving in opposite directions confront each other, leading to a freezing phenomenon.

Furthermore, the attendee cluster also contributes to jamming transitions by reducing the available space in the corridor. To understand the influence of attendee cluster size on jamming transitions, we perform numerical simulations with a static bottleneck instead of an attraction, in which all the pedestrians are passersby. In doing so, we can exclude the interactions among passersby and attendees, thereby focusing on the influence of reduced available space. For the comparison, we use a stationary state average of cluster size $\langle r_c \rangle$ because the attendee cluster size changes in the course of time but the size of the static bottleneck is constant. In the case of a static bottleneck, we also use the notation of $\langle r_c \rangle$ for convenience. A semicircle with radius $\langle r_c \rangle$ is placed at the center of the lower corridor boundary, acting as a static bottleneck. By changing $\langle r_c \rangle$, we observe the behavior of various measures including P_f , E_a , and E_{up} [see Fig. 11].

It is obvious that larger $\langle r_c \rangle$ leads to higher freezing probability P_f for bidirectional flow, as shown in Fig. 11(a). However, P_f of the attendee cluster case is higher than that of a static bottleneck for a given value of $\langle r_c \rangle$. While the E_a and E_{up} curves obtained from the static bottleneck case show a clear dependence on $\langle r_c \rangle$, those from attendee cluster do not show clear tendency when $\langle r_c \rangle > 1.5$ m [see Figs. 11(b) and 11(c)]. Although increasing $\langle r_c \rangle$ evidently leads to a localized jam transi-

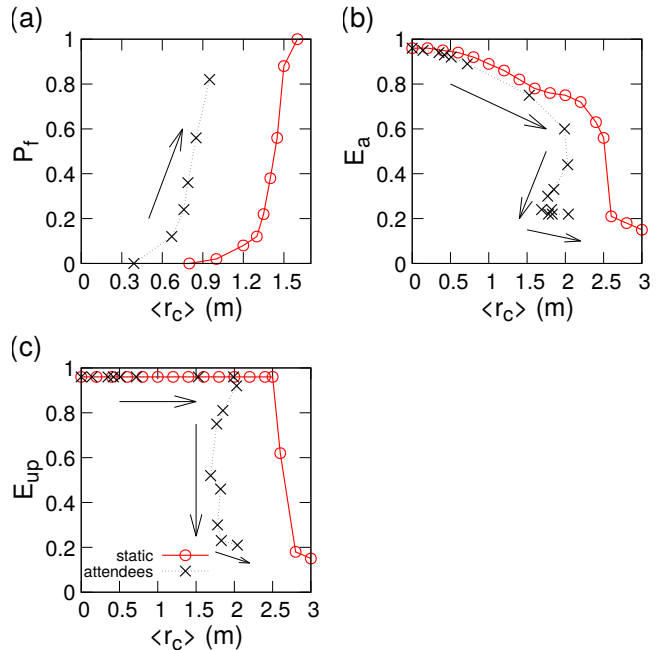


FIG. 11. (Color online) Dependence of various measures on the stationary state average of cluster size $\langle r_c \rangle$ for pedestrian influx $Q = 5$ P/s. The results of the static bottleneck and attendee cluster are denoted by \circ and \times , respectively. Arrows indicate the direction of increasing s , for the results of the attendee cluster. (a) Freezing probability P_f for bidirectional flow indicating the appearance of the freezing phase (b) Local efficiency near the attraction E_a for unidirectional flow reflecting the onset of localized jam phase, and (c) local efficiency upstream E_{up} for unidirectional flow, which is relevant to the extended jam phase.

tion, it can be suggested that conflicts among pedestrians play an important role in jamming transitions if $\langle r_c \rangle$ is large enough.

Appendix E: Sensitivity analysis

Since the presented results are sensitive to the numerical simulation setup, so we briefly discuss the influence of different simulation parameters especially for the average length of stay t_d and the corridor width W . As can be seen from Figs. 12(a), 12(c), and 12(e) the freezing probability reaches $P_f = 1$ quicker, and local efficiency measures E_a and E_{up} tend to decrease faster as t_d grows. One can infer that larger t_d likely leads to having more attendees near attractions, resulting in higher freezing probability and smaller local efficiency measures. Therefore, it can be suggested that increasing t_d activates jamming transitions for lower values of s .

In Figs. 12(b), 12(d), and 12(f), increasing W apparently changes the behavior of P_f in bidirectional flow in that conflicting pedestrians seem to have enough space for resolving the conflicts. Although increasing the corridor width from $W = 4$ m to $W = 6$ m produces notable

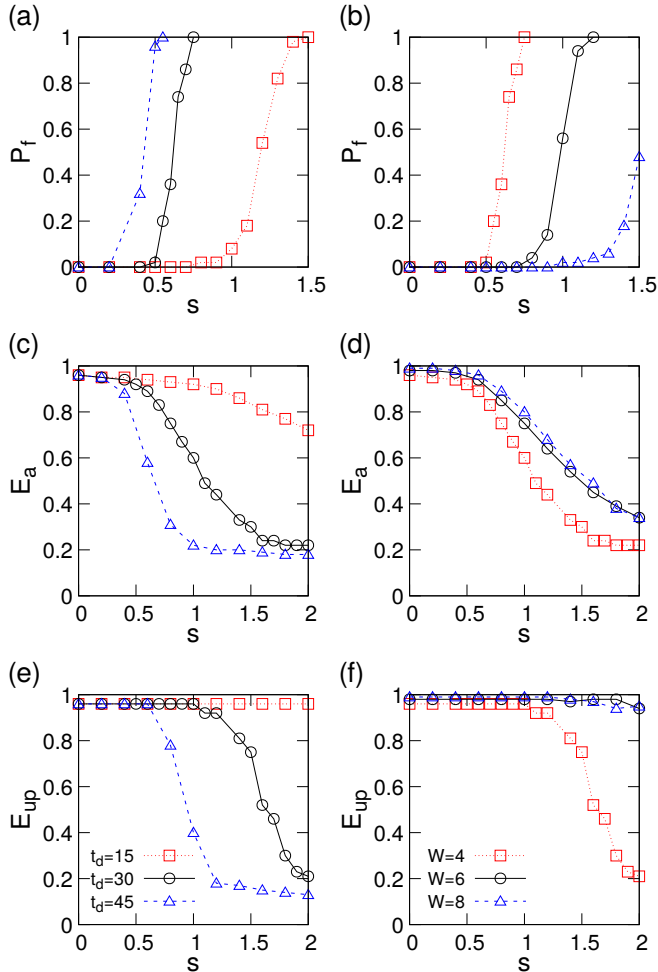


FIG. 12. (Color online) Dependence of various measures on social influence parameter s for t_d (left column) and W (right column) with pedestrian influx $Q = 5$ P/s. From top to bottom, (a) and (b) Freezing probability P_f for bidirectional flow, (c) and (d) local efficiency near the attraction E_a for unidirectional flow, and (e) and (f) local efficiency upstream E_{up} for unidirectional flow. Note that $t_d = 30$ s and $W = 4$ m are the simulation parameter values that we are mainly using in this study.

differences in the E_a and E_{up} curves, increasing W further does not seem to yield any significant changes. It is reasonable to suppose that the impact of increasing W becomes less notable for large W , in that increased W allows conflicting pedestrians to have more space for resolving the conflicts but also the attendee cluster to grow larger.

Appendix F: Pedestrian flow quantities

We evaluated pedestrian flow quantities such as local density, local speed, and local flow. Following the idea of the particle-in-cell method [74–77], we convert the discrete number of pedestrians into continuous density field values by using a bilinear weight function w_{iz} for each

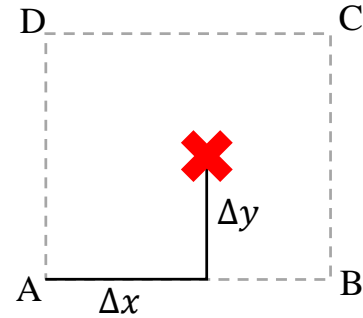


FIG. 13. (Color online) Schematic representation of the grid structure. Points A, B, C, and D indicate the neighboring grid points of pedestrian i . The location of pedestrian i is denoted by \times . The relative coordinates of pedestrian i with respect to point A in the horizontal and vertical directions are indicated by Δx and Δy , respectively.

neighboring grid point $z \in \{A, B, C, D\}$,

$$\begin{aligned} w_{iA} &= (l - \Delta x)(l - \Delta y)/l^2, \\ w_{iB} &= \Delta x(l - \Delta y)/l^2, \\ w_{iC} &= \Delta x\Delta y/l^2, \\ w_{iD} &= (l - \Delta x)\Delta y/l^2, \end{aligned} \quad (\text{F1})$$

where Δx and Δy indicate the relative coordinates from the left bottom cell center A to the location of pedestrian i (see Fig. 13). Although the use of a Gaussian function is a well-established approach in quantifying the local flow characteristics [28, 66, 72], it tends to overestimate the local quantities. This is because it takes into account distant pedestrians. Notice that $\sum w_{iz} = 1$ indicating that the weight function w_{iz} reflects the density contribution from pedestrian i . We choose grid spacing $l = 2r_i$ on the order of pedestrian size. With the weight function w_{iz} , the local density $\rho(\vec{z}, t)$ is defined as

$$\rho(\vec{z}, t) = \sum_i \frac{w_{iz}}{l^2}. \quad (\text{F2})$$

Likewise, the local speed $u(\vec{z}, t)$ is given as

$$u(\vec{z}, t) = \frac{\sum_i \|\vec{v}_i\| w_{iz}}{\sum_i w_{iz}}. \quad (\text{F3})$$

We can calculate the local pedestrian flow $J(\vec{z}, t)$ as a product of local density and local speed,

$$J(\vec{z}, t) = \rho(\vec{z}, t)u(\vec{z}, t). \quad (\text{F4})$$

-
- [1] T. Vicsek, A. Czirók, E. Ben-Jacob, I. Cohen, and O. Shochet, "Novel type of phase transition in a system of self-driven particles," *Physical Review Letters* **75**, 1226–1229 (1995).
- [2] D. Helbing, "Traffic and related self-driven many-particle systems," *Reviews of Modern Physics* **73**, 1067–1141 (2001).
- [3] D. Helbing and P. Molnár, "Social force model for pedestrian dynamics," *Physical Review E* **51**, 4282–4286 (1995).
- [4] I. D. Couzin and N. R. Franks, "Self-organized lane formation and optimized traffic flow in army ants," *Proceedings of the Royal Society of London B: Biological Sciences* **270**, 139–146 (2002).
- [5] D. Helbing and B. A. Huberman, "Coherent moving states in highway traffic," *Nature* **396** (1998).
- [6] Y. Sugiyama, M. Fukui, M. Kikuchi, K. Hasebe, A. Nakayama, K. Nishinari, S. I. Tadaki, and S. Yukawa, "Traffic jams without bottlenecks – experimental evidence for the physical mechanism of the formation of a jam," *New Journal of Physics* **10**, 033001+ (2008).
- [7] A. Nakayama, M. Fukui, M. Kikuchi, K. Hasebe, K. Nishinari, Y. Sugiyama, S. I. Tadaki, and S. Yukawa, "Metastability in the formation of an experimental traffic jam," *New Journal of Physics* **11**, 083025+ (2009).
- [8] S. I. Tadaki, M. Kikuchi, M. Fukui, A. Nakayama, K. Nishinari, A. Shibata, Y. Sugiyama, T. Yosida, and S. Yukawa, "Phase transition in traffic jam experiment on a circuit," *New Journal of Physics* **15**, 103034+ (2013).
- [9] I. Zuriguel, A. Janda, A. Garcimartín, C. Lozano, R. Arévalo, and D. Maza, "Silo clogging reduction by the presence of an obstacle," *Physical Review Letters* **107**, 278001+ (2011).
- [10] D. Helbing, I. Farkas, and T. Vicsek, "Simulating dynamical features of escape panic," *Nature* **407**, 487–490 (2000).
- [11] B. S. Kerner, H. Rehborn, M. Aleksic, and A. Haug, "Recognition and tracking of spatio-temporal congested traffic patterns on freeways," *Transportation Research Part C: Emerging Technologies* **12**, 369–400 (2004).
- [12] B. S. Kerner, *The physics of traffic: empirical freeway pattern features, engineering applications, and theory* (Springer, 2004).
- [13] A. Kesting, M. Treiber, M. Schönhof, and D. Helbing, "Adaptive cruise control design for active congestion avoidance," *Transportation Research Part C: Emerging Technologies* **16**, 668–683 (2008).
- [14] A. Seyfried, B. Steffen, W. Klingsch, and M. Boltes, "The fundamental diagram of pedestrian movement revisited," *Journal of Statistical Mechanics: Theory and Experiment* **2005**, P10002+ (2005).
- [15] J. Zhang, W. Klingsch, A. Schadschneider, and A. Seyfried, "Transitions in pedestrian fundamental diagrams of straight corridors and T-junctions," *Journal of Statistical Mechanics: Theory and Experiment* **2011**, P06004+ (2011).
- [16] T. Kretz, A. Grünebohm, M. Kaufman, F. Mazur, and M. Schreckenberg, "Experimental study of pedestrian counterflow in a corridor," *Journal of Statistical Mechanics: Theory and Experiment* **2006**, P10001+ (2006).
- [17] C. Feliciani and K. Nishinari, "Empirical analysis of the lane formation process in bidirectional pedestrian flow," *Physical Review E* **94**, 032304+ (2016).
- [18] J. Zhang, W. Klingsch, A. Schadschneider, and A. Seyfried, "Ordering in bidirectional pedestrian flows and its influence on the fundamental diagram," *Journal of Statistical Mechanics: Theory and Experiment* **2012**, P02002+ (2012).
- [19] T. Kretz, A. Grünebohm, and M. Schreckenberg, "Experimental study of pedestrian flow through a bottleneck," *Journal of Statistical Mechanics: Theory and Experiment* **2006**, P10014+ (2006).
- [20] S. P. Hoogendoorn and W. Daamen, "Pedestrian behavior at bottlenecks," *Transportation Science* **39**, 147–159 (2005).
- [21] A. Seyfried, O. Passon, B. Steffen, M. Boltes, T. Rupprecht, and W. Klingsch, "New insights into pedestrian flow through bottlenecks," *Transportation Science* **43**, 395–406 (2009).
- [22] M. Muramatsu, T. Irie, and T. Nagatani, "Jamming transition in pedestrian counter flow," *Physica A: Statistical Mechanics and its Applications* **267**, 487–498 (1999).
- [23] Y. Tajima, K. Takimoto, and T. Nagatani, "Scaling of pedestrian channel flow with a bottleneck," *Physica A: Statistical Mechanics and its Applications* **294**, 257–268 (2001).
- [24] D. Helbing, I. J. Farkas, and T. Vicsek, "Freezing by heating in a driven mesoscopic system," *Physical Review Letters* **84**, 1240–1243 (2000).
- [25] D. Yanagisawa, "Coordination game in bidirectional flow," *Collective Dynamics* **1**, A8+ (2016).
- [26] E. Goffman, *Relations in public: Microstudies of the public order* (Basic Books, New York, 1971).
- [27] P. G. Gipps and B. Marksjö, "A micro-simulation model for pedestrian flows," *Mathematics and Computers in Simulation* **27**, 95–105 (1985).
- [28] J. Kwak, H. H. Jo, T. Luttinen, and I. Kosonen, "Collective dynamics of pedestrians interacting with attractions," *Physical Review E* **88**, 062810+ (2013).
- [29] J. Kwak, H. H. Jo, T. Luttinen, and I. Kosonen, "Effects of switching behavior for the attraction on pedestrian dynamics," *PLoS ONE* **10**, e0133668+ (2015).
- [30] D. R. Parisi, M. Gilman, and H. Moldovan, "A modification of the Social Force Model can reproduce experimental data of pedestrian flows in normal conditions," *Physica A: Statistical Mechanics and its Applications* **388**, 3600–3608 (2009).
- [31] M. Chraïbi, T. Ezaki, A. Tordeux, K. Nishinari, A. Schadschneider, and A. Seyfried, "Jamming transitions in force-based models for pedestrian dynamics," *Physical Review E* **92**, 042809+ (2015).
- [32] A. Johansson, D. Helbing, and P. Shukla, "Specification of the social force pedestrian model by evolutionary adjustment to video tracking data," *Advances in Complex Systems* **10**, 271–288 (2007).
- [33] S. Milgram, L. Bickman, and L. Berkowitz, "Note on the drawing power of crowds of different size," *Journal of Personality and Social Psychology* **13**, 79–82 (1969).
- [34] A. C. Gallup, J. J. Hale, D. J. T. Sumpter, S. Garnier, A. Kacelnik, J. R. Krebs, and I. D. Couzin, "Visual

- attention and the acquisition of information in human crowds,” *Proceedings of the National Academy of Sciences* **109**, 7245–7250 (2012).
- [35] W. O. Bearden, R. G. Netemeyer, and J. E. Teel, “Measurement of consumer susceptibility to interpersonal influence,” *Journal of Consumer Research* **15**, 473–481 (1989).
- [36] T. L. Childers and A. R. Rao, “The influence of familial and peer-based reference groups on consumer decisions,” *Journal of Consumer Research* **19**, 198–211 (1992).
- [37] V. D. Kaltcheva and B. A. Weitz, “When should a retailer create an exciting store environment?” *Journal of Marketing* **70**, 107–118 (2006).
- [38] S. Nicolis, J. Fernández, C. Pérez-Penichet, C. Noda, F. Tejera, O. Ramos, D. J. T. Sumpter, and E. Alshuler, “Foraging at the edge of chaos: Internal clock versus external forcing,” *Physical Review Letters* **110**, 268104+ (2013).
- [39] R. Hughes, “A continuum theory for the flow of pedestrians,” *Transportation Research Part B: Methodological* **36**, 507–535 (2002).
- [40] Y. Xiao, Z. Gao, Y. Qu, and X. Li, “A pedestrian flow model considering the impact of local density: Voronoi diagram based heuristics approach,” *Transportation Research Part C: Emerging Technologies* **68**, 566–580 (2016).
- [41] T. Kretz, “Pedestrian traffic: on the quickest path,” *Journal of Statistical Mechanics: Theory and Experiment* **2009**, P03012+ (2009).
- [42] D. Hartmann, “Adaptive pedestrian dynamics based on geodesics,” *New Journal of Physics* **12**, 043032+ (2010).
- [43] A. Kneidl, D. Hartmann, and A. Borrmann, “A hybrid multi-scale approach for simulation of pedestrian dynamics,” *Transportation Research Part C: Emerging Technologies* **37**, 223–237 (2013).
- [44] D. Hartmann and P. Hasel, “Efficient dynamic floor field methods for microscopic pedestrian crowd simulations,” *Communications in Computational Physics* **16**, 264–286 (2014).
- [45] C. Burstedde, K. Klauck, A. Schadschneider, and J. Zittartz, “Simulation of pedestrian dynamics using a two-dimensional cellular automaton,” *Physica A: Statistical Mechanics and its Applications* **295**, 507–525 (2001).
- [46] A. Kirchner and A. Schadschneider, “Simulation of evacuation processes using a bionics-inspired cellular automaton model for pedestrian dynamics,” *Physica A: Statistical Mechanics and its Applications* **312**, 260–276 (2002).
- [47] G. K. Batchelor, *An introduction to fluid dynamics* (Cambridge University Press, Cambridge, UK, 2000).
- [48] J. D. Anderson, *Fundamentals of aerodynamics*, 5th ed. (McGraw-Hill Education, New York, NY, 2010).
- [49] F. Zanlungo, T. Ikeda, and T. Kanda, “A microscopic “social norm” model to obtain realistic macroscopic velocity and density pedestrian distributions,” *PLoS ONE* **7**, e50720+ (2012).
- [50] S. Xu and H. B. L. Duh, “A simulation of bonding effects and their impacts on pedestrian dynamics,” *IEEE Transactions on Intelligent Transportation Systems* **11**, 153–161 (2010).
- [51] F. Zanlungo, T. Ikeda, and T. Kanda, “Social force model with explicit collision prediction,” *Europhysics Letters* **93**, 68005+ (2011).
- [52] F. Zanlungo, T. Ikeda, and T. Kanda, “Potential for the dynamics of pedestrians in a socially interacting group,” *Physical Review E* **89**, 012811+ (2014).
- [53] G. Köster, F. Treml, and M. Gödel, “Avoiding numerical pitfalls in social force models,” *Physical Review E* **87**, 063305+ (2013).
- [54] S. Heliövaara, H. Ehtamo, D. Helbing, and T. Korhonen, “Patient and impatient pedestrians in a spatial game for egress congestion,” *Physical Review E* **87**, 012802+ (2013).
- [55] A. D. May, *Traffic flow fundamentals* (Prentice Hall, Englewood Cliffs, NJ, 1990).
- [56] T. Luttinen, “Properties of Cowan’s M3 headway distribution,” *Transportation Research Record: Journal of the Transportation Research Board* **1678**, 189–196 (1999).
- [57] C. F. Daganzo, *Fundamentals of transportation and traffic operations* (Pergamon, Oxford, UK, 1997).
- [58] M. Moussaïd, E. G. Guilloit, M. Moreau, J. Fehrenbach, O. Chabiron, S. Lemerrier, J. Pettré, C. Appert-Rolland, P. Degond, and G. Theraulaz, “Traffic instabilities in self-organized pedestrian crowds,” *PLOS Computational Biology* **8**, e1002442+ (2012).
- [59] F. Dietrich and G. Köster, “Gradient navigation model for pedestrian dynamics,” *Physical Review E* **89**, 062801+ (2014).
- [60] A. Tordeux and A. Schadschneider, “White and relaxed noises in optimal velocity models for pedestrian flow with stop-and-go waves,” *Journal of Physics A: Mathematical and Theoretical* **49**, 185101+ (2016).
- [61] A. Kirchner, K. Nishinari, and A. Schadschneider, “Friction effects and clogging in a cellular automaton model for pedestrian dynamics,” *Physical Review E* **67**, 056122+ (2003).
- [62] S. Nowak and A. Schadschneider, “Quantitative analysis of pedestrian counterflow in a cellular automaton model,” *Physical Review E* **85**, 066128+ (2012).
- [63] J. A. Laval, “Hysteresis in traffic flow revisited: An improved measurement method,” *Transportation Research Part B: Methodological* **45**, 385–391 (2011).
- [64] F. L. Hall and K. Agyemang-Duah, “Freeway capacity drop and the definition of capacity,” *Transportation Research Record* **1320**, 91–98 (1991).
- [65] T. Ezaki, D. Yanagisawa, and K. Nishinari, “Pedestrian flow through multiple bottlenecks,” *Physical Review E* **86**, 026118+ (2012).
- [66] D. Helbing, A. Johansson, and H. Z. Al-Abideen, “Dynamics of crowd disasters: An empirical study,” *Physical Review E* **75**, 046109+ (2007).
- [67] W. Yu and A. Johansson, “Modeling crowd turbulence by many-particle simulations,” *Physical Review E* **76**, 046105+ (2007).
- [68] P. M. Kielar and A. Borrmann, “Modeling pedestrians’ interest in locations: A concept to improve simulations of pedestrian destination choice,” *Simulation Modelling Practice and Theory* **61**, 47–62 (2016).
- [69] M. Minderhoud, H. Botma, and P. Bovy, “Assessment of roadway capacity estimation methods,” *Transportation Research Record: Journal of the Transportation Research Board* **1572**, 59–67 (1997).
- [70] J. Geistfeldt and W. Brilon, “A comparative assessment of stochastic capacity estimation methods,” in *Transportation and Traffic Theory 2009* (Springer, New York).
- [71] B. S. Kerner, S. L. Klenov, and M. Schreckenberg, “Probabilistic physical characteristics of phase transitions at highway bottlenecks: incommensurability of three-phase and two-phase traffic-flow theories,” *Physi-*

- cal Review E **89**, 052807+ (2014).
- [72] M. Moussaïd, D. Helbing, and G. Theraulaz, “How simple rules determine pedestrian behavior and crowd disasters,” *Proceedings of the National Academy of Sciences* **108**, 6884–6888 (2011).
- [73] I. Karamouzas, B. Skinner, and S. J. Guy, “Universal power law governing pedestrian interactions,” *Physical Review Letters* **113**, 238701+ (2014).
- [74] F. H. Harlow, *The Particle-in-cell method for numerical solution of problems in fluid dynamics*, Tech. Rep. (Los Alamos Scientific Laboratory, 1962).
- [75] J. M. Dawson, “Particle simulation of plasmas,” *Reviews of Modern Physics* **55**, 403–447 (1983).
- [76] A. Treuille, S. Cooper, and Z. Popović, “Continuum crowds,” *ACM Transactions on Graphics* **25**, 1160–1168 (2006).
- [77] R. Narain, A. Golas, S. Curtis, and M. C. Lin, “Aggregate dynamics for dense crowd simulation,” *ACM Transactions on Graphics* **28**, 122+ (2009).